

2015

Activity Based Profiling: New Insights into Metabolic Homeostasis

Keith Tan

Follow this and additional works at: http://digitalcommons.rockefeller.edu/student_theses_and_dissertations

 Part of the [Life Sciences Commons](#)

Recommended Citation

Tan, Keith, "Activity Based Profiling: New Insights into Metabolic Homeostasis" (2015). *Student Theses and Dissertations*. Paper 285.



**ACTIVITY BASED PROFILING: NEW
INSIGHTS INTO METABOLIC
HOMEOSTASIS**

A Thesis Presented to the Faculty of
The Rockefeller University
in Partial Fulfillment of the Requirements for
the degree of Doctor of Philosophy

by

Keith Tan

June 2015

ACTIVITY BASED PROFILING: NEW INSIGHTS INTO METABOLIC HOMEOSTASIS

Keith Tan, Ph.D.
The Rockefeller University 2015

There is mounting evidence that demonstrates that body weight and energy homeostasis is tightly regulated by a physiological system. This system consists of sensing and effector components that primarily reside in the central nervous system and disruption to these components can lead to obesity and metabolic disorders. Although many neural substrates have been identified in the past decades, there is reason to believe that there are numerous unidentified neural populations that play a role in energy balance. Besides regulating caloric consumption and energy expenditure, neural components that control energy homeostasis are also tightly intertwined with circadian rhythmicity but this aspect has received less attention.

In this dissertation, I will first describe a novel method to identify functionally activated neurons in the central nervous system using phosphorylated ribosome profiling. I will use this method to identify new neuronal populations that regulate energy balance as well as uncover new functions for well-studied neural populations. I will elaborate on key findings such as the role of prodynorphin, agouti-related protein and melanin concentrating hormone expressing neurons during scheduled feeding and the role of galanin neurons in maintaining body weight.

I dedicate this dissertation to my family for their unwavering belief in me and their unconditional love. To my mum, thank you for being such an inspiration to my life and for all the sacrifices you have made.

Acknowledgements

I would like to thank Jeffrey Friedman for all the advice, support and encouragement he has so generously given me throughout the years. To Zachary Knight, thank you for all your help and guidance and teaching me so much about science. I would also like to thank Cori Bargmann and Sidney Strickland for all their constructive suggestions to my thesis work. To members of the Friedman lab: Susan Korres, Kristina Hedbacker, Leah Kelly, Olof Dallner, Yi-Hsueh Lu, Zhiying Li, Wenwen Zeng, Wei Shen, Lisa Pomeranz, Sarah Stanley, Mats Ekstrand, Bianca Field, Kaamashri Latcha, Allyn Mark and Sarah Schmidt, thank you all for being such wonderful co-workers and helping in my greatest time of need. To my friends from Wesleyan: Ivy, Iwan and Carlo, thank you for being in the greater New York area all these years and all your support and encouragement.

Table of Contents

Dedication	iii
Acknowledgements	iv
Table of Contents	v
List of Figures	vi
Chapter 1: Introduction	1
Chapter 2: Materials and Methods	20
Chapter 3: Molecular Profiling of Activated Neurons by Phosphorylated Ribosome Capture	42
Chapter 4: Ablation of AgRP Neurons Impairs Adaptation to Scheduled Feeding ..	68
Chapter 5: Loss of MCH Neurons Enhances Adaption to Scheduled Feeding	87
Chapter 6: Loss of Galanin Neurons Leads to Leanness	94
Chapter 7: Summary and Conclusion	99
References	104

List of Figures

Figure 1: A graph of body mass index as a function of weight and height.....	2
Figure 2: Factors influencing obesity.....	4
Figure 3: Summary of parabiosis experiments.....	8
Figure 4: Fluorescence in situ hybridization of NPY and POMC in the arcuate nucleus.....	11
Figure 5: Role of arcuate neurons in adiposity signaling.....	12
Figure 6: Metabolism and circadian clocks.....	15
Figure 7: Circadian rhythms.....	17
Figure 8: Phosphorylated ribosome profiling.....	44
Figure 9: Colocalization of cfos and pS6 following diverse stimuli.....	45
Figure 10: Selective capture of phosphorylated ribosomes in vitro.....	46
Figure 11: Selective capture of phosphorylated ribosomes in vivo.....	48
Figure 12: pS6 activation in hypothalamic VIP neurons.....	50
Figure 13: Identification of neurons activated by salt challenge.....	53
Figure 14: Identification of neurons activated by fasting.....	56
Figure 15: Identification of neurons activated by ghrelin and scheduled feeding.....	59
Figure 16: KOR signaling restrains bouts of feeding during scheduled feeding.....	63
Figure 17: Expression of cfos in AgRP neurons during scheduled feeding.....	71
Figure 18: Ablation of AgRP neurons.....	73
Figure 19: Metabolic phenotype after loss of AgRP neurons.....	74
Figure 20: Response of AgRP DTR animals to overnight fast.....	75
Figure 21: Response of AgRP DTR animals to ghrelin.....	77
Figure 22: Response of AgRP DTR animals to scheduled feeding during the light phase.....	78
Figure 23: Response of AgRP DTR animals to scheduled feeding during the dark phase.....	80

Figure 24: Ablation of MCH neurons.....	88
Figure 25: Metabolic phenotype after loss of MCH neurons.....	89
Figure 26: Response of MCH DTR animals to scheduled feeding during the light phase.....	90
Figure 27: Response of MCH Vgat fl/fl animals to restricted feeding during the light phase.....	92
Figure 28: Ablation of galanin cells.....	95
Figure 29: Metabolic phenotype of Gal DTA animals.....	96
Figure 30: Metabolic phenotype of Gal Vgat fl/fl animals on high fat diet.....	97

Chapter 1:

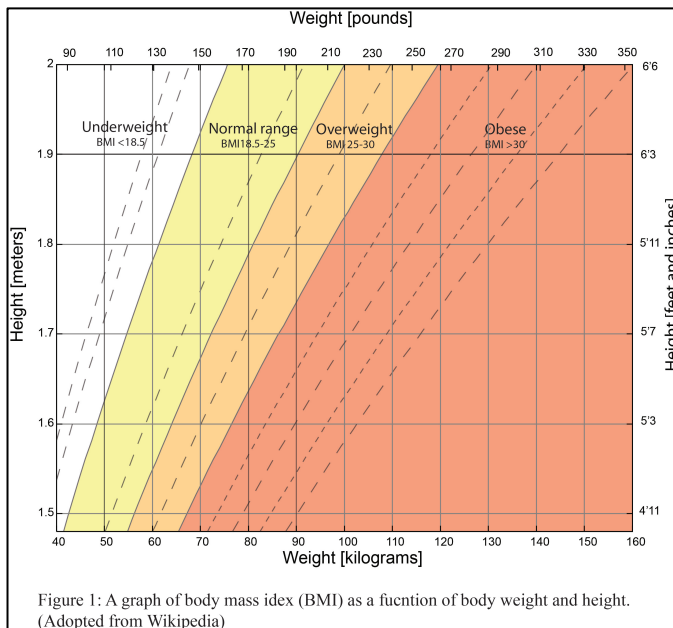
Introduction

Obesity as a public health problem

Worldwide prevalence of obesity has increased significantly in the past decades. Obesity causes or exacerbates many health problems and is associated with type 2 diabetes mellitus, hypertension, hyperlipidemia, coronary heart disease, osteoarthritis and increase incidence of certain forms of cancer(Flegal et al., 2010; Grundy, 2000). Actuarial tables and epidemiological studies confirm that life expectancy is reduced with increasing degrees of overweight and obesity(Lew, 1985). According to the World Health Organization, in 2008 more than 1.4 billion adults, age 20 and older, were overweight. Of these overweight adults, over 200 million men and nearly 300 million women were obese. Overweight and obesity, once considered a high-income country problem, are also on the rise in low and middle-income countries especially in urban settings. The causes of obesity are multi-factorial including genetic susceptibility, increase availability and access to high-energy foods and decreased requirement for physical activity due to increasingly sedentary nature of many forms of work, changing modes of transportation and increasing urbanization. Changes in dietary and physical activity patterns can be attributed to societal changes associated with lack of supportive policies in areas such as health care, agriculture, transport, urban planning, food processing, marketing and education. Estimates of the economic costs of obesity in developed countries are between 2-7% of total health costs, which is a significant proportion of national health care budgets(Seidell, 1995). This alarming increase in overweight and obesity threatens global well-being and adds more burden to public health spending worldwide.

Definition of overweight and obesity

Obesity is commonly defined as an excess of body adiposity. In practice, body fat is usually estimated by using a formula that takes into account weight and height. The underlying assumption of this metric is that most variation in weight for individuals of the same height is due to fat mass and the formula most frequently used is body mass index (BMI): weight in kilograms divided by the square of height in meters. A commonly



used cutoff for overweight adults is BMI 25-30 and obese individuals is BMI > 30 (Figure 1). Such a graded classification of overweight and obesity using BMI values allows for meaningful comparisons between and within populations and the identification of individuals and

groups for appropriate interventions. It is worth bearing in mind that due to differences in body proportions, BMI may not correspond to the same degree of fatness across different populations. There is a close correlation between BMI and the incidence of several chronic conditions caused by excess adiposity such as type 2 diabetes mellitus, hypertension and coronary heart disease (Willett et al., 1999; 1995). Other measures of body fat include waist circumference: measured at mid-point between lower border of ribs and upper border of pelvis, skinfold thickness: measurement of skinfold thickness with calipers and bioimpedance: based on the principle that lean mass conducts current

better than fat mass, measurement of resistance to a weak current applied across extremities provides an estimate of body fat using an empirically derived formula.

Causes of Obesity

A common perception of obesity espouses the view that individuals are obese due to a lack of discipline and affected individuals are the product of their own actions (or inactions). However, there is increasing evidence for the view that body weight is regulated by a physiological system and that changes in body weight in either direction evokes a counter-response that restores the change, maintaining body weight over the lifetime of many adults(Weigle, 1994). For instance, normal-weight individuals are protected against expansion of body fat stores resulting from overeating, demonstrating that biological mechanisms must regulate body weight (Leibel et al., 1995; Sims et al., 1973). The presence of a tightly regulated physiological system strongly suggests the role of genetics in obesity development.

The genetic basis for obesity is most clearly illustrated in twin studies. Pairs of twins were exposed to periods of positive and negative energy balance and the differences in their rate of weight gain, proportion of weight gained and site of fat deposition exhibited greater similarity within pairs than between pairs(Bouchard et al., 1990). Furthermore, when correlations of BMI were determined for monozygotic and dizygotic twin pairs, the weighted mean BMI correlation for monozygotic twins was 0.74 compared with 0.32 for dizygotic twin pairs. This corresponds to heritability of between 50-90%, a level exceeded only by height(Maes et al., 1997; Stunkard et al., 1990).

Studies of monogenic rodent models of obesity have led to the discovery of key components of body weight homeostasis. Positional cloning of the *ob* gene revealed that mice with a nonsense mutation in this gene are deficient in the gene product: leptin (derived from Greek leptos, meaning thin)(Zhang et al., 1994). Mice with homozygous mutations in the *ob* gene are hyperphagic, develop early onset obesity, hyperinsulinaemia and insulin resistance, all of which can be reversed with recombinant leptin treatment(Campfield et al., 1995; Halaas et al., 1995; Pelleymounter et al., 1995). Similarly, *db/db* mice have non-functional leptin receptor and manifests strikingly similar metabolic phenotypes as *ob/ob* mice, albeit with high levels of plasma leptin(Chen et al., 1996). While monogenic causes of obesity has provided insights into fundamental physiological pathways that regulate body weight and energy balance (which will be covered later), the low incidence of monogenic mutations causing obesity in the general population, despite increasing number of obese individuals, suggests that obesity is influenced by multiple gene loci. The susceptibility gene hypothesis postulates that several genes increase the risk of developing obesity but are not essential for its expression or by themselves sufficient to explain the development of obesity(Kopelman, 2000). Moreover, if body weight is determined by a homeostatic

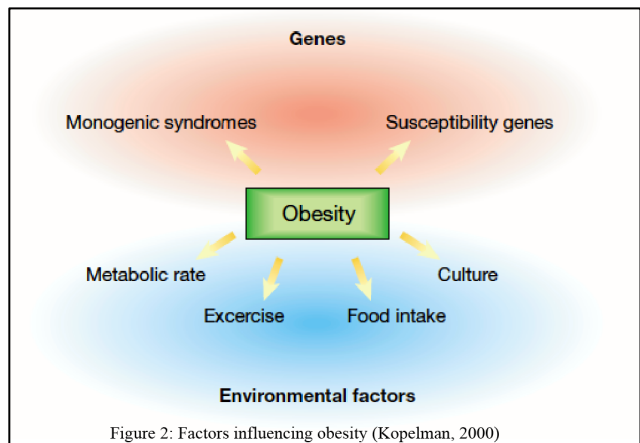


Figure 2: Factors influencing obesity (Kopelman, 2000)

physiological system encoded by the genome, it begs the question to why ever increasing numbers of individuals are failing to regulate their body weight within a healthy range?

Implicit in the susceptibility gene hypothesis is the role of environmental factors that unmask latent tendencies to pathogenesis of obesity. The thrifty gene hypothesis as proposed by Neel (NEEL, 1962; 1999a; 1999b), sets out to explain the increased incidence of obesity through the lens of evolution and a changing environment. Neel argues that a thrifty gene results in a phenotype that is 'exceptionally efficient in the intake and/or utilization of food'. It is suggested that throughout most of human evolutionary history, humans experienced alternate periods of famine and feast and that a thrifty gene is an advantageous adaptation that allows humans to store energy, in the form of fat deposits, in times of food abundance to successfully survive in reciprocal periods of famine. Individuals with the thrifty genotype would have a survival advantage since they relied on previously stored energy to tide over periods of scarce food availability while those without the thrifty genotype would less likely survive famine due to lack of 'emergency' energy stores. Another advantage of the thrifty genotype was sustained fecundity during famine. Therefore, in an environment where food availability was unpredictable, thrifty genes are positively selected for because of survival and fecundity advantages conferred by energy stores in fat deposits during times of abundance. However, in today's modern society where food is readily available, thrifty genes prepare individuals for famines that almost never occur, resulting in increased incidence of excess energy storage and obesity.

Fetal nutrition is also another environmental factor that has been implicated in the onset of obesity, hypertension and type 2 diabetes mellitus later on in life independent of genetic inheritance (Kopelman, 2000). Predisposition to adult obesity is an adaptation to malnutrition by the developing fetus. It is suggested that the developing fetus adapts its

growth and metabolism to the expectation of low food availability postnatally, thereby increasing its ability to store energy as fat to provide energy reserves for use when food is scarce. These adaptations can prove detrimental when food and nutrition becomes readily available. The study of babies born at the time of the Dutch famine during the winter of 1944-1945 provides evidence that early gestation is a critical period for the onset of obesity during adulthood(Ravelli et al., 1976). Obesity was more prevalent in adults whose fetal exposure to famine coincided with the first and second trimesters of pregnancy compared to a control group not exposed to famine during pregnancy.

More recently, gut microbome has also been implicated in obesity. Gut bacteria from pairs of human twins in which one was obese and the other lean was transferred into mice reared in a sterile environment and had no bacteria of their own(Ridaura et al., 2013). Over a 5-week period, mice with bacteria from fat twins developed more body fat than those that had bacteria from lean twins. Furthermore, when mice with gut bacteria from lean twins were housed together with mice with gut bacteria from obese twins, bacteria from lean twins took over in the mice that started out with bacteria from obese twins, resulting in weight loss. The causes of obesity are multifactorial with contributions from both genetic and extrinsic elements. Figure 2 summarizes the genetic and environmental factors that influence development of obesity.

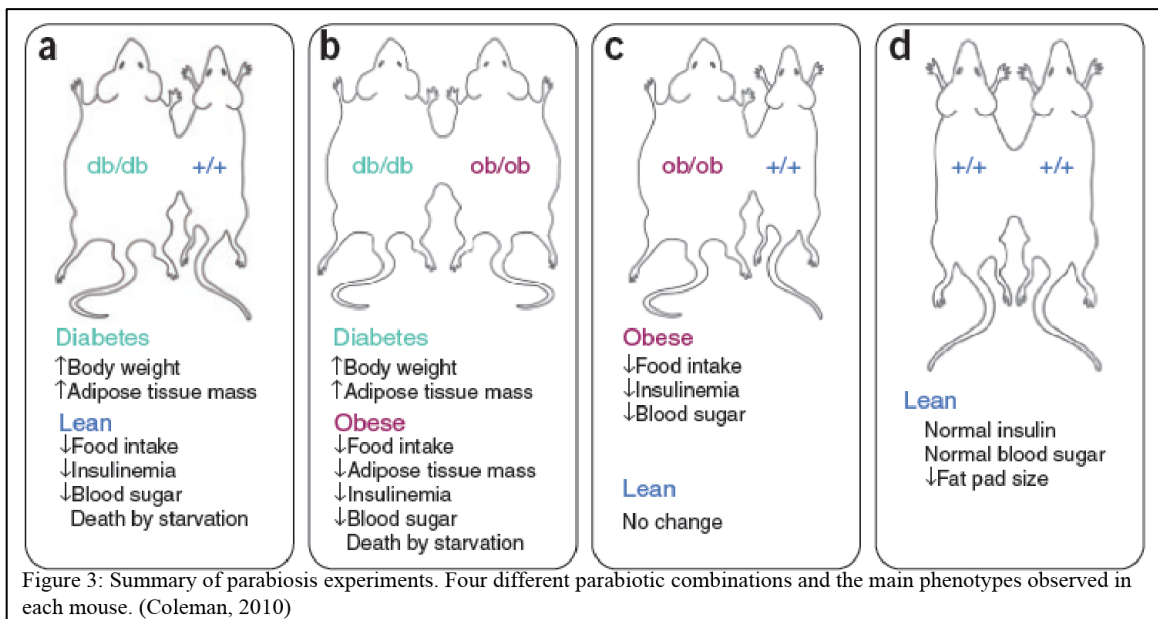
Physiological System for Energy Balance

Kennedy first proposed the idea that energy homeostasis is achieved whereby circulating factors inform the brain of available energy stores and the brain makes adjustments to food intake in response to changes in energy stores(KENNEDY, 1953).

This adiposity negative-feedback model of energy balance suggests the presence of a blood-borne factor that circulates at levels proportionate to fat mass and can cross the blood-brain barrier. This factor, if present, should also promote weight loss by acting on neural systems involved in energy homeostasis and inhibition of these neural systems should increase food intake and body weight.

Despite low incidence of obesity due to single gene disruptions in the general population, studies of monogenic causes of obesity especially in rodent models have provided great insight into the components of the physiological system that maintains body weight homeostasis. In the 1950s and 1960s, two independent obese mutant mice were discovered at Jackson Laboratory: *ob/ob* mouse with mutation on chromosome 6 and *db/db* with mutation on chromosome 4 (Coleman, 2010). Douglas Coleman at Jackson Laboratory set out to characterize the phenotype of these mutants. Both mutants exhibit remarkably identical phenotype of morbid obesity and Coleman reasoned that two genes on separate chromosomes manifesting identical phenotypes strongly suggested that these genes mediate a common metabolic pathway. Coleman performed a series of elegant parabiosis experiments where he linked the blood supplies of different mouse strains by surgical joining of two mice by skin to skin anastomosis from the shoulder to the pelvic girdle (Coleman, 1973; Coleman and Hummel, 1969). When the *db/db* mutant was parabiosed to a wildtype mouse, the wildtype mouse died of starvation while the mutant continued to gain weight and fat mass. When the *db/db* mutant was fused to an *ob/ob* mutant, the *ob/ob* mutant also died of starvation while the *db/db* animal continued to gain weight. When the *ob/ob* mutant was parabiosed to a wildtype mouse, the *ob/ob* mutant decreased body weight gain and food consumption while the wildtype animal was

not affected. Lastly, when two wildtype animals were fused, the pair remained healthy but did show smaller fat pads compared to unparabiosed mice. These experiments are summarized in Figure 3. With the observations from these experiments, Coleman concluded that the *db/db* mutant mouse overproduced a satiety factor but was unable to respond to it (possibly due to a defective receptor) whereas the *ob/ob* mutant recognized and responded to the factor but was deficient in it. Decades later in 1994, Jeffrey



Friedman definitively cloned and identified the satiety factor and named it leptin (Zhang et al., 1994). This groundbreaking discovery was followed by the discovery of the leptin receptor (Tartaglia et al., 1995). With these discoveries, the predictions of the parabiosis experiments were confirmed: *ob/ob* encodes a blood-borne hormone that acts in a negative feedback loop to regulate adipose tissue mass and appetite; while *db/db* gene encodes the leptin receptor.

Leptin is an approximately 16-kDa protein produced and secreted by adipocytes into the circulatory system. Plasma leptin levels increase proportionately with adipose tissue mass and decrease when adipose tissue is reduced (Halaas et al., 1995). As

expected, administration of recombinant leptin reduces body weight and food intake of wildtype mice and normalized weight and food consumption of *ob/ob* mice but had no effect on *db/db* mice(Campfield et al., 1995; Halaas et al., 1995; 1997; Pelleymounter et al., 1995).

The leptin receptor is a cytokine family receptor with 5 splice variants (ObRa-ObRe)(Fei et al., 1997; Lee et al., 1996; Tartaglia et al., 1995), of which only ObRb is capable of activating the Janus kinase signal transducer and activator of transcription (JAK-STAT) signaling pathway(Morton et al., 2006). Binding of leptin to ObRb stimulates tyrosine kinase Jak2 to phosphorylate STAT3 at tyrosine residues(Bjørbaek et al., 1997). Phospho-STAT3 dimerizes and enters the nucleus to regulate transcription of target genes. It was later determined that the *db/db* mouse is only mutant for ObRb(Chen et al., 1996; Lee et al., 1996). While other receptor isoforms are found broadly, ObRb is highly expressed in the hypothalamus(Fei et al., 1997; Lee et al., 1996). Furthermore, *in vivo* activation of leptin receptor results in stimulation of STAT3 tyrosine phosphorylation in the rodent hypothalamus, demonstrating the presence of functionally active ObRb there(McCowen et al., 1998; Vaisse et al., 1996). Brain-specific knockout of the leptin receptor results in obesity similar to that of the *db/db* mutant while brain-specific expression of leptin receptor can suppress obesity of *db/db* mice(de Luca et al., 2005; Kowalski et al., 2001; McMinn et al., 2005). Taken together, these data strongly demonstrate that the primary site of leptin's action is the central nervous system and that leptin maintains energy balance by modulating activity of food intake, energy expenditure and metabolism.

The discovery of leptin and its effect on food intake and body weight fueled great excitement about a possible novel therapy to treat obesity. In humans, plasma leptin levels increase with increasing adipose tissue mass and most obese patients have high leptin levels (Maffei et al., 1995). Thus, it seems paradoxical that obese patients are unable to lose weight despite elevated leptin levels. This led to the idea that obese patients develop resistance to the hormone and are unable to effectively respond to plasma leptin levels to regulate adipose tissue mass. Prolonged exposure to high leptin levels, hyperleptinemia has been shown to be the cause of leptin resistance (Knight et al., 2010), though the precise cellular and molecular mechanisms involved in the development of leptin resistance still remain unclear.

Neural Components of Energy Homeostasis

Brain lesion and stimulation studies performed in the 1940s first implicated the hypothalamus as a major anatomical region controlling body weight and food intake. Lesion of specific hypothalamic areas such as the ventromedial, paraventricular and dorsomedial nuclei induced hyperphagia and obesity. In contrast, lesions of the lateral hypothalamus caused hypophagia (ANAND and Brobeck, 1951; Brobeck, 1946; Brobeck et al., 1943; Hetherington, 1944; Hetherington and Ranson, 1942). Similarly, electrical stimulation of the ventromedial hypothalamic nucleus suppressed food intake whereas stimulation of the lateral hypothalamus invoked feeding (Bray et al., 1990).

Since these findings, our knowledge of the discrete neuronal subpopulations that regulate energy homeostasis has expanded greatly. Among the most-studied and well-characterized neural populations are those that coexpress neuropeptide Y (NPY) and

agouti-related protein (AgRP)(Hahn et al., 1998). NPY is a potent orexigenic peptide that induced acute and robust feeding behavior when delivered intracerebroventricularly(Clark et al., 1984) while AgRP acts as an antagonist of the melanocortin-4 receptor (MC4R). AgRP/NPY neurons are situated almost exclusively in the arcuate nucleus of the hypothalamus, adjacent to the floor of the third ventricle and majority of these neurons also express the active form of the leptin receptor(Baskin et al., 1999). Optogenetic activation of AgRP/NPY neurons stimulate feeding, regardless of nutritional state(Aponte et al., 2011; Atasoy et al., 2012) and it is not surprising that leptin actually inhibits these cells(Spanswick et al., 1997; van den Top et al., 2004). In leptin deficient *ob/ob* mice, AgRP and NPY gene expressions are elevated and these neurons are strongly activated, functionally linking AgRP/NPY neurons to the hyperphagia observed in these mice(Schwartz et al., 1996).

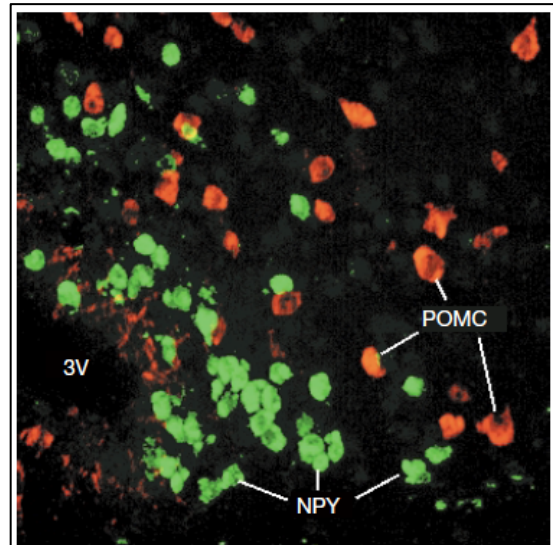
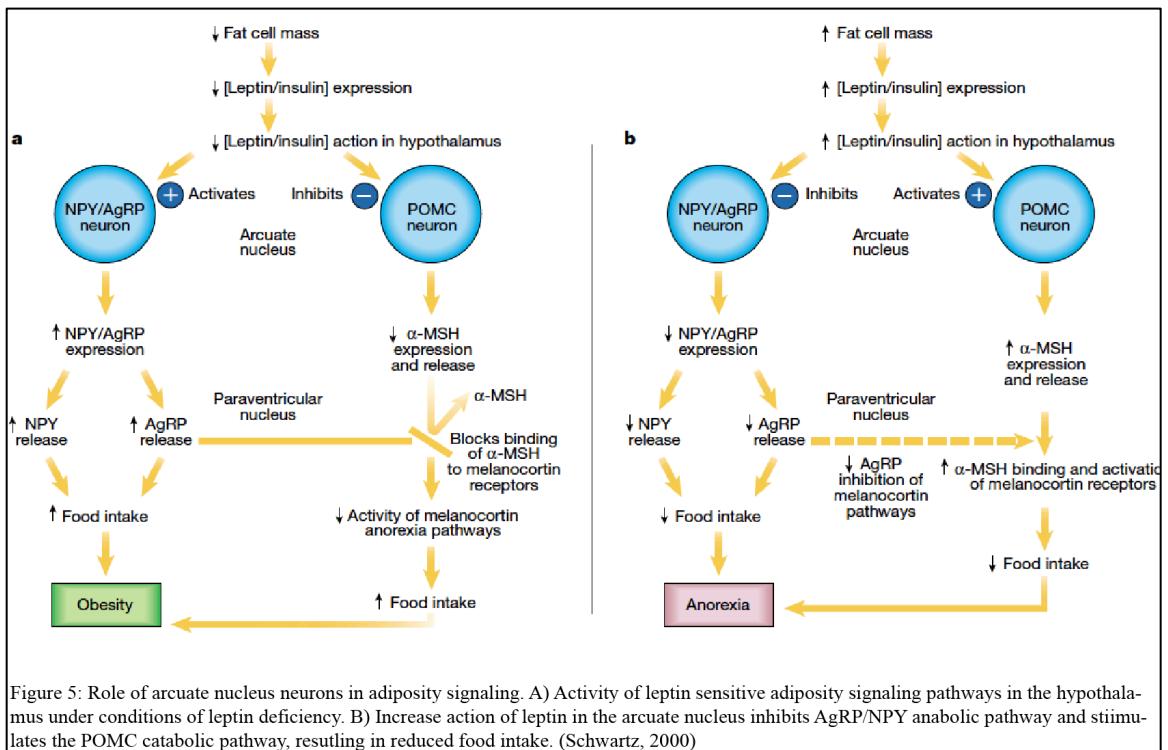


Figure 4: Fluorescence in situ hybridization of mRNA of NPY (green) and POMC (red) in the arcuate nucleus, adjacent to the third ventricle (3V). NPY and POMC are expressed in discrete, non-overlapping population of cells. (Schwartz, 2000)

Located adjacent to AgRP/NPY neurons are neurons that express pro-opiomelanocortin (POMC) and releases α -melanocyte stimulating hormone (α -MSH)(Figure 4), which inhibits food intake by binding to and activating melanocortin receptors. POMC neurons also express the leptin receptor(Cheung et al., 1997) but, unlike AgRP/NPY neurons, are activated by leptin(Cowley et al., 2001). It is highly unlikely that an animal can be both sated and hungry at the same time, thus when

AgRP/NPY neurons are activated to drive food consumption, POMC neurons, which inhibit food intake, should be silent and vice versa. Indeed, POMC neurons are inhibited by GABAergic inputs from AgRP/NPY neurons (Cowley et al., 2001), though inhibition of AgRP/NPY neurons by inputs from POMC neurons still remains to be definitively demonstrated. Figure 5 summarizes the contrasting effects of leptin on AgRP/NPY and POMC neurons.



Despite the importance of AgRP/NPY and POMC neurons in maintaining energy balance, only a mild obesity phenotype is observed when leptin receptors are deleted from AgRP/NPY, POMC or both AgRP/NPY and POMC neurons (Balthasar et al., 2004; van de Wall et al., 2008) while deletion of leptin receptor in the entire hypothalamus or in GABAergic neurons recapitulates the severe obesity and hyperphagia phenotype of *db/db* mice (Ring and Zeltser, 2010; Vong et al., 2011). Taken together these data suggest that there are other leptin receptor expressing neuronal populations, possibly those that use

the classical inhibitory neurotransmitter GABA, in the hypothalamus that are crucial for metabolic homeostasis.

Melanocortin System in Energy Homeostasis

The prominence of AgRP and POMC cells in modulating food intake via direct leptin action has also drawn significant focus to the melanocortin system. Melanocortins are neuropeptides (ie α -MSH, ACTH) cleaved from the POMC precursor molecule and exert their effects by binding to a family of melanocortin receptors(Cone et al., 1996). The MC3- and MC4-receptors are primarily expressed in the central nervous system(Mountjoy et al., 1994). Mice deficient in MC4R become hyperphagic and are obese(Huszar et al., 1997) demonstrating that tonic signaling on MC4R suppresses food intake and body fat mass. In humans, a dominant frame-shift mutation in the MC4R gene results in obesity(Vaisse et al., 1998). In fact, mutation at the MC4R gene locus is the most common monogenic form of human obesity described thus far, accounting for up to 6% of early onset or severe adult obesity(Farooqi et al., 2000; 2003). Similarly, loss of α -MSH in POMC knockout mice also causes hyperphagia and obesity(Yaswen et al., 1999). Further evidence for the importance of melanocortin signaling can be discerned from studies of agouti (A^y/a) mice. This is an autosomal dominant mutant of genetic obesity characterized by a yellow coat color. The agouti protein acts as an antagonist of cutaneous MC1R. By blocking MC1R signaling, agouti lightens the coat color. Agouti is also expressed ectopically throughout the body and the obese phenotype is caused by the antagonism of MC4R in the brain(Cone et al., 1996).

Neural Circuits for Feeding

The expression of ObRb in AgRP/NPY and POMC neurons and the role of their respective peptides in regulating central melanocortin signaling makes it compelling that these two neuronal subpopulations in the ARC are integral components of a neural circuitry that determine behavior in response to changes in nutritional state. Indeed, acute ablation of either AgRP/NPY or POMC neurons in adult mice, by expressing the human diphtheria toxin receptor and administering diphtheria toxin, results in profound metabolic phenotypes. Loss of POMC neurons leads to increase food intake and body weight whereas loss of AgRP/NPY neurons results in anorexia, eventually causing death by starvation (Gropp et al., 2005; Luquet et al., 2005). Interestingly, when diphtheria toxin was delivered to neonatal pups, animals remained viable, suggesting a compensatory mechanism during a period of elevated neuronal plasticity in development (Luquet et al., 2005). The advent of optogenetics and DREADDs (designer receptor exclusively activated by a designer drug) has enabled investigation into the feeding effects induced by activating or inhibiting molecularly defined neural populations in live, conscious animals (Kramer et al., 2013; Packer et al., 2013; Urban and Roth, 2014).

Recent reports have demonstrated the paraventricular nucleus (PVN) is downstream of AgRP/NPY neurons in the ARC. PVN neurons characterized by single-minded homolog 1 (SIM1) is inhibited by AgRP/NPY neurons and activation of SIM1 neurons reduces food intake and voracious feeding due to AgRP/NPY photoactivation (Atasoy et al., 2012). Furthermore, MC4R is abundantly expressed in the PVN (Mountjoy et al., 1994), this area is heavily innervated by AgRP/NPY and POMC neurons (Cowley et al., 1999) and expression of MC4R in SIM1 neurons in the PVN of

MC4R null animals rescues the hyperphagia phenotype of these animals, suggesting that the PVN is a crucial downstream first-order site of melanocortin signaling.

Biological Rhythms and Metabolism

Apart from the basic cellular and molecular components that maintain energy balance, biological clocks can also play a role in metabolic homeostasis. Many biological processes ranging from metabolic pathways to physiology and behavior show 24 hour rhythms driven by endogenous circadian clocks. The periodicity of 24 hours is commonly found

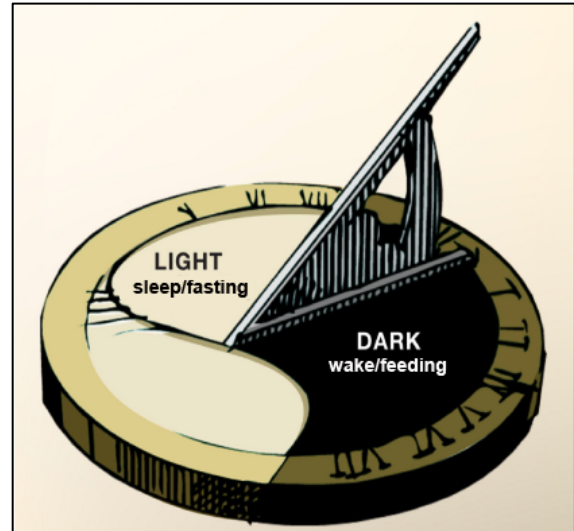


Figure 6: Genetic and molecular evidence suggest that within both the central nervous system and peripheral tissue, co-regulation of the daily alteration between sleep/wake and fasting/feeding cycles reflects coupling of both behavior and metabolic pathways. Because the availability of food and the risk of predators are tied to the environmental cycle of light and darkness, these interlinked cycles may have provided selective advantages. (Green et al, 2008)

in nature from unicellular organisms to complex species such as humans (Pittendrigh, 1993), strongly implicating evolutionary selection for this periodicity. Biological rhythms enable organisms to anticipate changes in the environment and adapt their behavior and physiology accordingly. There is increasing evidence that many aspects of metabolism show daily rhythmicity including many circulating and intracellular metabolites, feeding-related hormones and ingestive behaviors. For instance, leptin is expressed in mice according to a diurnal pattern, with relatively higher levels during the dark phase (Ahima et al., 1998). Metabolism and circadian clocks are deeply intertwined: clocks drive metabolic processes and many metabolic parameters affect clocks, forming complex feedback relationships (Figure 6). Microarray studies that have examined gene expression profiles throughout the circadian cycle in various mammalian tissues such as liver,

skeletal muscle, brown and white adipose tissue show that from 3-20% of genes assayed exhibit rhythmic expression(Akhtar et al., 2002; Kita et al., 2002; McCarthy et al., 2007; Panda et al., 2002; Reddy et al., 2006; Storch et al., 2002; Ueda et al., 2002; Zvonic et al., 2006), suggesting that a good proportion of the transcriptomes in these tissues are under circadian control. Clinical and epidemiologic studies have provided evidence that circadian disruption is associated with cardiovascular and metabolic complications across large segments of the human population(Laposky et al., 2008). Cross-sectional studies have also revealed increased incidences of metabolic syndrome, high BMI and cardiovascular issues in shift workers(Ellingsen et al., 2007; Karlsson et al., 2001). Taken together, these data suggests that misalignment of rest and activity cycles, as well as fasting and feeding, may contribute to pathogenesis of obesity and metabolic syndrome.

Biological Clocks

In mammals, a structure within the anterior hypothalamus called the suprachiasmatic nucleus (SCN) generates daily rhythms using light/dark cues from the environment relayed through the retina(Hastings et al., 2003; Lowrey and Takahashi, 2004)(Figure 7). When explants of the SCN were maintained in vitro, robust rhythmicity still persisted(Groos and Hendriks, 1982) and when SCN tissue from one animal was transplanted to another animal with lesioned SCN, the recipient of the transplanted SCN exhibited behavioral rhythms of the donor(Ralph et al., 1990), confirming that the SCN is indeed the master pacemaker of circadian rhythm. The molecular mechanism underlying circadian rhythms is composed of a set of interlocking transcriptional-translational feedback loops(Buhr and Takahashi, 2013). The primary loop consists of the gene products of the Clock and Bmal1 genes. Clock/Bmal1 heterodimers initiate transcription

of the negative limb of the feedback loop including Period (Per1 and Per2) and

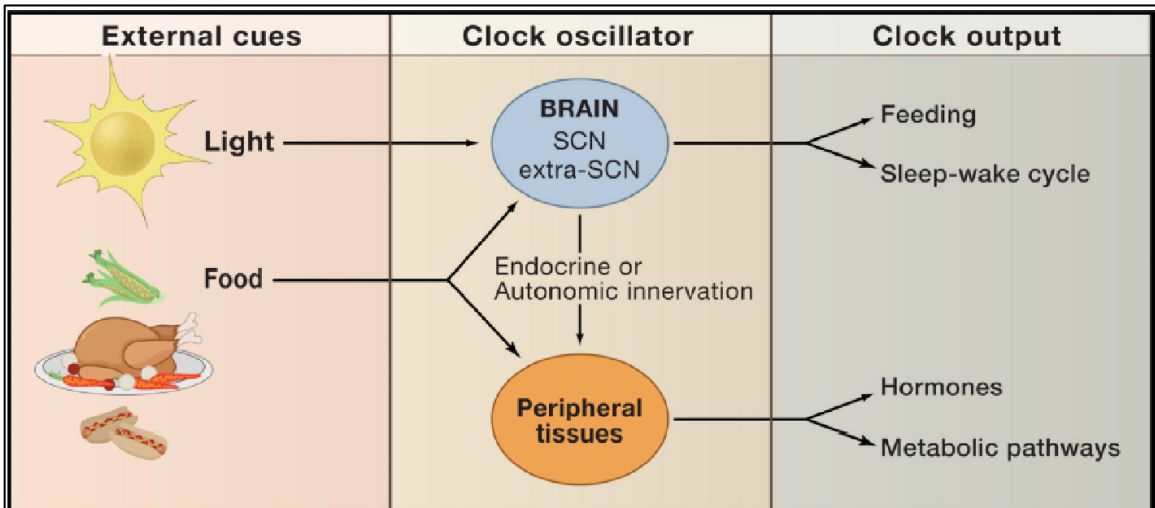


Figure 7: The predominant external cue (zeitgeber) of the SCN is light. Clocks in peripheral tissue such as the liver can be entrained by food. Nutrient and hormonal cues may also affect the period and phase characteristics of the master clock neurons, although little is known about how metabolic signals are communicated to the SCN. Outputs of both the SCN and peripheral clocks impact behavioral and metabolic responses such as feeding, sleep-wakefulness, hormone secretion and metabolic homeostasis. (Green et al., 2008)

cryptochrome (Cry1 and Cry2) genes. Per/Cry proteins dimerize and inhibit Clock/Bmal1 transcription, allowing the cycle to repeat from a low level of transcriptional activity. Interestingly, homozygous deletion of the Clock gene in mice on the C57BL/6J genetic background have severe alterations in energy balance including obesity, hyperlipidemia, elevated blood glucose and low plasma insulin (Turek et al., 2005). Feeding rhythms in Clock mutants are altered with increased food intake during the day, causing increased overall food intake.

The relationship between metabolism and circadian rhythms is complicated by the contribution of multiple tissues and cell types to metabolic homeostasis. Rhythmic expression of clock genes in non-SCN brain areas and many peripheral tissues including liver, lungs and skeletal muscle (Balsalobre et al., 1998; Guilding and Piggins, 2007; Yamazaki et al., 2000) indicate that individual organs possess their own circadian rhythms. The SCN coordinates the many peripheral clocks so that they maintain proper

phase-relationships with each other. A common analogy used to describe this organization refers to the SCN as a conductor of an orchestra and peripheral tissues representing individual musicians. Each musician is able to generate his own time but requires the conductor to ensure that they all maintain correct time relative to each other to produce a cohesive performance. Peripheral clocks can themselves be entrained by various stimuli, with food availability being a dominant zeitgeber (Figure 7). In rodents, a scheduled feeding paradigm where food is only available for a few hours during the light phase (a time when nocturnal animals do not normally eat) decouples the phase-lock rhythm of the SCN and peripheral tissues, even when the SCN remains entrained to light/dark cycle (Damiola et al., 2000; Hara et al., 2001; Stokkan et al., 2001; Wakamatsu et al., 2001).

The Food Entrainable Oscillator

The understanding of the effects of food on the circadian system is further complicated by the presence of a rather mysterious oscillator, the food entrainable oscillator (FEO). This oscillator controls daily rhythms of food anticipatory activity (FAA) entrained by food availability. When rodents are subjected to a scheduled feeding paradigm, where food is only available for a few hours in the middle of the day, they show increased activity before the time that food becomes available within a few days (Mistlberger, 2011; Stephan, 2002). FAA exhibits the hallmarks of bona fide circadian rhythms namely that it persists for several days even if food is withheld. The FEO is anatomically distinct from the SCN as lesions of the SCN, which cause animals to become arrhythmic, do not abolish FAA (Krieger et al., 1977; Stephan et al., 1979). Intriguingly, genetic deletions of canonical clock such as *Per1*, *Per2* and *Bmal1* do not

eradicate FAA(Storch and Weitz, 2009), suggesting that novel clock genes might underlie the mechanism of this rhythm. The dorsomedial hypothalamic nucleus (DMH) has been implicated as the site of the FEO. In situ hybridization for Per2 transcript demonstrated a robust rhythm in the DMH only when mice are entrained to scheduled feeding.(Mieda et al., 2006). However, disparate results were reported for DMH lesion experiments. One study observed significant loss of FAA after DMH lesions(Gooley et al., 2006) while another observed robust FAA after lesions(Landry et al., 2006). The difficulty to definitively identify the FEO has raised the possibility that the FEO may not reside in a single anatomical region (ie the SCN for light/dark cycle) but may be distributed among many sites.

Chapter 2:

Materials and Methods

Animal Treatment

All experiments were carried out in accordance to regulations of the Institutional Animal Care and Use Committee at the Rockefeller University. All transgenic mice used in this study were previously published. The following line was used to express Cre recombinase in AgRP cells: AgRP-IRES-Cre (Jackson Labs Stock 012899, $AgRP^{tm1(cre)Lowl/J}$). The following line was used to express Cre recombinase in MCH cells: MCH BAC transgenic (Jego et al., 2013). The following line was used to expression Cre recombinase in Gal cells: Gal BAC transgenic (MMRRC Stock 031060, $Tg(Gal-cre)KI87Gsat/Mmucd$). The following line was used to delete *Tsc1* in MCH cells: loxP sites flanking exon 17 and exon 18 of the *Tsc1* gene (Jackson Labs Stock 005680, $Tsc1^{tm1Djk/J}$). The following line was used to express the diphtheria toxin alpha chain in Gal cells: Rosa-loxSTOPlox-DTA (Jackson Labs Stock 009669, B6.129P2-Gt(ROSA)^{26Sortm1(DTA)Lky/J}). The following GFP reporter lines were used: Pomc-eGFP (Jackson Labs Stock 009593, C57BL/6J-Tg(Pomc-EGFP)1Low/J), NPY hrGFP (Jackson Labs Stock 006417, B6.FVB-Tg(NPY-hrGFP)1Low1/J), Pmch-eGFP (Jackson Labs Stock 008324, B6.Cg-Tg(Pmch-MAPT/CFP)1Rck/J), CRH-eGFP (Alon et al., 2009) and Gad67-eGFP (Tamamaki et al., 2003). The following reporter line was used, where a lox-STOP-lox sequence prevents expression of the reporter in the absence of Cre recombinase: Rosa-loxSTOPlox-tdTomato (Jackson Labs Stock 007909, B6.Cg-Gt(ROSA)^{26Sor^{tm9(CAG-tdTomato)Hze}}/J) and Rosa-loxSTOPlox-YFP (Jackson Labs Stock

006148, B6.129X1-Gt(ROSA)26Sor^{tm1(EYFP)^{Cos}/J}). The following line was used to delete Vgat in MCH and Gal cells: loxP sites flanking exon 2 of the gene Slc32a1 (Jackson Labs Stock 012897, Slc32a1^{tm1Lowl}/J). AgRP DTR animals were generated by crossing heterozygous AgRP-IRES-Cre animals with animals homozygous for ROSA-loxSTOPlox-iDTR (Jackson Labs Stock 007900, C57BL/6-Gt(ROSA)26Sor^{tm1(HBEGF)^{Awai}/J}). Animals heterozygous for AgRP-IRES-Cre and ROSA-loxSTOPlox-iDTR were termed AgRP DTR and animals heterozygous for only ROSA-loxSTOPlox-iDTR were termed DTR. MCH DTR animals were generated by crossing heterozygous MCH CRE animals with animals homozygous for ROSA-loxSTOPlox-iDTR (Jackson Labs Stock 007900, C57BL/6-Gt(ROSA)26Sor^{tm1(HBEGF)^{Awai}/J}). Animals heterozygous for MCH Cre and ROSA-loxSTOPlox-iDTR were termed MCH DTR and animals heterozygous for only ROSA-loxSTOPlox-iDTR were termed DTR. Unless otherwise stated, mice were group housed under a standard 12h light/dark cycle (lights on from 8:00 A.M. to 8:00 P.M.) and fed regular chow (LabDiet 5053). To ablate AgRP neurons, post natal day 3 (P3) litters were injected once with diphtheria toxin [50ng/g, subcutaneous (s.c), Sigma-Aldrich D0564]. For osmotic stimulation experiments, animals were given an intraperitoneal (i.p) injection of 2M NaCl (350ul), water was removed from the cage and mice were sacrificed 120 minutes later. For dehydration experiments, water was removed from the cage and mice perfused 24 hours later. For fasting experiments, animals were transferred to new cages and food deprived for at least 18 hours before they were either perfused for immunohistochemistry or re-fed. For ghrelin experiments, animals were given ghrelin (66ug, intraperitoneal, i.p, Tocris Bioscience #1465) and subsequent food intake measured. Animals were sacrificed 70 minutes after

ghrelin injection for immunohistochemistry. Food was removed from cages for animals used for immunohistochemistry. For scheduled feeding, mice were allowed access to food between ZT4 and ZT7 or between ZT15 and ZT18 each day for 14 days and body weight and food intake were measured each day. For drug treatments, mice were given intraperitoneal injection of the following dose and then sacrificed at the indicated time: cocaine (30mg/kg, 60 minutes), kainate (12.5mg/kg, 120 minutes), olanzapine (20mg/kg, 120 minutes), clozapine (10mg/kg, 45 minutes). For car odor experiments, a domestic cat was fitted with a fabric collar for 3 weeks; the collar was removed, mice were exposed to the collar for 60 minutes and then were perfused. For the resident intruder test, a male mouse was single caged for at least 2 weeks, a foreign male was introduced to the cage, animals were monitored for attacks and the resident was perfused after 60 minutes.

Leptin treatment

Miniosmotic pumps (Alzet, 2001) with mean pump rate of 0.98 ul/h were filled with leptin (Amylin Pharmaceutical) to achieve dose of 2.5ug/h for 8 days. Pumps were incubated in sterile PBS at 37°C for at least 6 hours before subcutaneous (s.c) implantation into animals. Animals were anesthetized with isoflurane when pumps were implanted or removed.

Treatment with kappa-opioid receptor antagonists

JDTic was delivered by intraperitoneal injections (10mg/kg). Norbinaltorphimine (5ul of a 1mg/mL solution) was delivered via Hamilton syringe into the lateral ventricle by using the coordinates L/M 1.0mm from Bregma, A/P -0.4mm from Bregma and 2.5mm beneath the cortex.

Locomotion analysis

10-12 weeks old male AgRP DTR and DTR mice were acclimatized to the experimental chambers for at least 24 hours prior to data collection using the Oxymax Lab Animal Monitoring System (Columbus Instruments). Only ambulatory beam breaks in the x and y axis were included in the analysis.

Ribosome Immunoprecipitation

150ul protein A Dynabeads (Invitrogen 10002D) were loaded with 4ug of pS6 antibody (Cell Signaling #2215) in Buffer A (10mM HEPES, pH 7.4, 150mM KCl, 5mM MgCl₂, 1% NP40, 0.05% IgG-free BSA). Beads were washed 3 times with Buffer A immediately before use. Mice were sacrificed by cervical dislocation. The hypothalamus was rapidly dissected in Buffer B (1xHBSS, 4mM NaHCO₃, 2.5mM HEPES, pH 7.4, 35mM glucose, 100ug/mL cycloheximide) on ice. Hypothalami were pooled (typically 10-20 per experiment), transferred to a glass homogenizer (Kimble Kontes 20) and resuspended in 1.35mL of Buffer C (10mM HEPES, pH 7.4, 150mM KCl, 5mM MgCl₂, 100nM calyculin A, 2mM DTT, 100U/mL RNasin, 100ug/mL cycloheximide, protease and phosphatase inhibitor cocktails). Samples were homogenized 3 times at 250rpm and 9 times at 750rpm on a variable –speed homogenizer (Glas-Col) at 4°C. Homogenates were transferred to a microcentrifuge tube and clarified at 2000x g for 10 minutes at 4°C. The low-speed supernatant was transferred to a new tube on ice and 90ul of 10% NP40 and 90ul of 1,2-diheptanoyl-sn-glycero-3-phosphocholine (DHPC, Avanti Polar Lipids: 100mg/0.69mL) was added to the supernatant. This solution was mixed and then clarified at 17000x g for 10 minutes at 4°C. The resulting high-speed supernatant was transferred

to a new tube and 20ul of a 0.05mM stock solution of 3P peptide (synthesized by United Peptide and has the sequence biotin-QIAKRRRLpSpSLRApSTSKSESSQK where pS is for phosphoserine) was added. A 20ul aliquot of this solution was removed, transferred to a new tube containing 350ul buffer RLT (QIAGEN, RNeasy Micro kit, 74004) and stored at -80°C for purification as input RNA. The remainder was used for immunoprecipitation. Immunoprecipitations were allowed to proceed for 10 minutes at 4°C. The beads were then washed 4 times with Buffer D (10mM HEPES, pH 7.4, 350mM KCl, 5mM MgCl₂, 2mM DTT, 1% NP40, 100U/mL RNasin and 100ug/mL cycloheximide). During the third wash the beads were transferred to a new tube and allowed to incubate at room temperature for 10 minutes. After the final wash, the RNA was eluted by addition of 350ul buffer RLT to the beads on ice, the beads removed by magnet and the RNA purified using RNeasy Micro kit (QIAGEN, RNeasy Micro kit, 74004). RNA was assessed using an Agilent 2100 bioanalyzer. For microarray analysis, cDNA was prepared using the Ovation RNA AmplificationSystem V2 (Nugen) and hybridized to MouseRef-8 v2 BeadChips (Illumina). For RNA-seq analysis cDNA was prepared using the SMARTer Ultralow Input RNA for Illumina Sequencing kit (Clontech, 634935) and then sequenced using an Illumina HiSeq 2000.

Immunohistochemistry

Mice were first anesthetized with isoflurane followed by transcardial perfusion with PBS and then 10% formalin. Brains were dissected, incubated in 10% formalin overnight at 4°C and 40um sections were prepared using a vibratome. Free floating sections were blocked for 1 hour at room temperature in blocking buffer (PBS, 0.1% Triton-X, 2% goat serum, 3% BSA) and then incubated overnight at 4°C with primary

antibodies. For pS6 244 staining, the pS6 240/244 polyclonal antibody (Cell Signaling, #2215) was combined to the 3P peptide (250nM final concentration). The next day, sections were washed in washing buffer (PBS, 0.1% Triton-X) 3 times for 20 minutes, incubated with dye-conjugated secondary antibodies at 1:1000 for 1 hour at room temperature, washed in washing buffer and then mounted. For vasopressin staining, it was noted that goat anti-rabbit secondary antibodies cross react with guinea pig primary antibodies; therefore primary antibody incubations were performed sequentially. For fosB staining, primary antibody incubations were allowed to proceed for 72 hours. For co-localization studies using 2 rabbit primary antibodies, the following 2 strategies were used. In the first approach, sections were stained with rabbit anti-cfos overnight, washed, stained with Alexa Fluor conjugated goat anti-rabbit Fab fragment (Jackson ImmunoResearch), washed, stained with rabbit anti-pS6, washed and then stained with Alexa Fluor conjugated goat anti-rabbit. In the second approach, sections were stained with rabbit anti-cfos overnight, washed, stained with Alexa Fluor conjugated goat anti-rabbit, washed and then stained with Alexa Fluor-488 conjugated pS6 235/236. The fidelity of double staining was confirmed by noting that cfos staining was exclusively nuclear while pS6 staining was cytoplasmic. Primary antibodies used were rabbit anti-NPY (1:2000, Bachem T4070) and rabbit anti-cfos (1:1000, Santa Cruz, sc52), rabbit anti-pS6 240/244 (Cell Signaling, #2215), rabbit anti-pS 235/236 (1:500, Cell Signaling, #4858), rabbit anti-pS6 235/236 (1:250, Cell Signaling, #4803), rabbit anti-rpL26 (Novus Biologicals, NB100-2131), rabbit anti-rpL7 (Novus Biologicals, NB100-2269), mouse anti-oxytocin (1:1000, Millipore, MAB5296), guinea pig anti-vasopressin (1:3000, Peninsula Laboratories, T5047), chicken anti-GFP (1:1000, Abcam, ab13970), rabbit

anti-fosB (1:25, Cell Signaling, #2251), rabbit anti-CXCL1 (1:200, Abcam, ab17882), mouse anti-rpS6 (250ng/mL, Cell Signaling, #2317), rabbit anti-MCH (1:1000, Phoenix Pharmaceuticals, H07047).

Fluorescent In Situ Hybridization

For vasoactive intestinal peptide a 527 base pair anti-sense digoxigenin-labeled riboprobe was generated based on sequences from the Allen Brain Atlas. For galanin, a 633 base pair anti-sense digoxigenin-labeled riboprobe was synthesized chemically based on sequences from the Allen Brain Atlas. For prodynorphin, a 592 base pair anti-sense digoxigenin-labeled riboprobe was synthesized chemically based on sequences from the Allen Brain Atlas. 40um cryostat free-floating sections were incubated in 3% H₂O₂ for 1 hour at room temperature to quench endogenous peroxidase activity. Sections were treated with 0.20% acetic anhydride followed by 1% Triton-X for 30 minutes each. Prehybridization was carried out at 62°C using hybridization buffer (50% formamide, 5x Denhardtts, 250ug/mL baker's yeast RNA, 500ug/mL ssDNA) for 1 hour before overnight hybridization with riboprobe at 62°C. Sections were washed in 5x SSC followed by 2 washes with 0.2x SSC at 62°C. When immunohistochemistry was combined with FISH, the primary antibody was added together with the riboprobe at the appropriate dilution. Brief washes with 0.2x SSC and Buffer B1 (0.1M Tris, pH 7.5, 0.15M NaCl) were performed and sections were blocked in TNB (1% blocking reagent in B1, Roche, #1096176) for 1 hour at room temperature. Anti-digoxigenin-POD antibody (1:100, Roche, #11207733910) was applied overnight at 4°C. When immunohistochemistry was combined with FISH, a secondary antibody conjugated to Alexa Fluor was applied to the sections for 1 hour at room temperature before riboprobe was detected. Riboprobe was

developed using the TSA Plus Fluorescence System (Perkin Elmer, #NEL744) according to the manufacturer's instructions.

Cell Culture

Wildtype and S6^{SSA} MEFs (a gift from David Sabatini) were cultured in DMEM supplemented with 10% FBS and penicillin-streptomycin. Cells were grown to confluence, starved for 6 hours in 0.25% DMEM/FBS and restimulated with 20% DMEM/FBS supplemented with 100nM insulin for 30 minutes. Cells were washed with PBS, trypsinized, collected by centrifugation and then lysed in a 1% NP40 buffer containing protease and phosphatase inhibitors. Lysates were clarified, immunoprecipitated using pS6 antibodies and the recovered RNA quantified using Agilent Bioanalyzer 2100.

Microscopy and Quantification

Free-floating sections were stained, mounted and then imaged using either Zeiss LSM 510 or Zeiss LSM 810 laser scanning confocal microscope. pS6 was quantified in specific neuronal populations as follows. Sections were double immunostained for pS6 244 and the relevant neuropeptide or GFP expressed from a transgenic mouse line. For each of 3 animals from both experimental and control groups, 3 sets of z-stacks were acquired from sections 160um apart. The surfaces corresponding to each labeled cell in the field were reconstructed using Imaris software (Bitplane), each surface was examined manually to confirm that the calculated surface corresponded to a cell and the mean intensity in the pS6 channel within the volume bounded by the surface of each labeled cell was recorded. This data was then plotted using a scatter dot plot, with the mean and

standard error indicated. Images for comparison in the manner were collected using identical microscope and camera settings on tissue samples processed in parallel. In cases where the absolute number of pS6 positive cells within an anatomical region was desired, the number was obtained through manual counts. Fluorescence intensity and cfos counts were carried out using ImageJ.

TaqMan Quantitative PCR Array Analysis and Measurements

Primers and internally quenched probes were synthesized (IDT DNA) to detect 225 genes that mark discrete populations of hypothalamic neurons. Probes were distributed to 96-well plates in duplicated, cDNA was prepared using the Quantitect Reverse Transcriptase kit (QIAGEN) and reactions were run using the TaqMan Gene Expression Master Mix (Applied Biosystems) on an Applied Biosystems 7900HT system. For each experiment (stimulus or control), the abundance of each gene in the input RNA and in the pS6 immunoprecipitated RNA was measured in duplicate. The RNA abundance was determined, normalized to an rpL27 probe that was present in every plate and the ratio (IP/input) was calculated. The entire experiment from animal sacrifice to RNA measurement was repeated the following number of times for each stimulus or control: no stimulation at ZT 5 (6 experiments), osmotic stimulation (5 experiments), scheduled feeding (4 experiments), ghrelin (3 experiments), no stimulation at ZT 23 (4 experiments), overnight fast (4 experiments). Each of these experiments utilized 10-20 animals. These values were then averaged and the differential enrichment calculated (ratio of IP/input stimulus over IP/input control). The log-transformed fold enrichment values for each gene were analyzed by calculating a p value (unpaired 2-tailed student t test) and a q value to estimate the false discovery rate at different thresholds of

significance. Follow-up analysis focused on the most highly enriched genes in each experimental condition, which were validated by histology.

List of Hypothalamic Marker Genes used in TaqMan Array

Gene Symbol	Gene Name	Class
PENK	Pro-enkephalin	Neuropeptide
POMC	Pro-opiomelanocortin	Neuropeptide
PDYN	Pro-dynorphin	Neuropeptide
PNOC	Prepro-nociceptin	Neuropeptide
AVP	Vasopressin	Neuropeptide
OXT	Oxytocin	Neuropeptide
GAST	Gastrin	Neuropeptide
CCK	Cholecystokinin	Neuropeptide
SST	Somatostatin	Neuropeptide
CORT	Cortistatin	Neuropeptide
NPVF	RF-amide related peptide, Neuropeptide VF	Neuropeptide
NPFF	Neuropeptide FF	Neuropeptide
NPY	Neuropeptide Y	Neuropeptide
CALCA	Calcitonin 1, CGRP (calcitonin related polypeptide)	Neuropeptide
CALCB	Calcitonin 2	Neuropeptide
IAPP	Amylin, Islet amyloid polypeptide	Neuropeptide
ADM	Adrenomedullin	Neuropeptide
NPPA	Atrial natriuretic factor	Neuropeptide
NPPC	Natriuretic peptide precursor C	Neuropeptide
GRP	Gastrin releasing peptide	Neuropeptide

NMB	Neuromedin B	Neuropeptide
EDN3	Endothelin 3	Neuropeptide
SCT	Secretin	Neuropeptide
VIP	Vasoactive intestinal peptide	Neuropeptide
ADCYAP1	Pituitary adneylcyclase-activated peptide	Neuropeptide
GHRH	Growth hormone releasing hormone	Neuropeptide
CRH	Corticotropin releasing hormone	Neuropeptide
UCN	Urocortin	Neuropeptide
UCN2	Urocortin 2	Neuropeptide
UCN3	Urocortin 3	Neuropeptide
TAC1	Prepro-tachykinin A, substance P, Neurokinin A	Neuropeptide
TAC2	Prepro-tachykinin B, Neuromedin K, Neurokinin B	Neuropeptide
NMS	Neuromedin S	Neuropeptide
NMU	Neuromedin U	Neuropeptide
AGT	Angiotensin	Neuropeptide
NTS	Neurotensin	Neuropeptide
CHGA	Chromogranin A	Neuropeptide
CHGB	Chromogranin B	Neuropeptide
SCG2	Secretogranin II	Neuropeptide
SCG3	Secretogranin III	Neuropeptide
SCG5	SGNE1, Secretory granule neuroendocrine protein	Neuropeptide
VGF	VGF nerve growth factor	Neuropeptide
GAL	Galanin	Neuropeptide
GALP	Galanin-like peptide	Neuropeptide
GnRH1	Gonadotropin-releasing hormone 1	Neuropeptide
NPB	Neuropeptide B	Neuropeptide

NPW	Neuropeptide W	Neuropeptide
NPS	Neuropeptide S	Neuropeptide
NXPH1	Neurexophilin-1	Neuropeptide
NXPH2	Neurexophilin-2	Neuropeptide
NXPH3	Neurexophilin-3	Neuropeptide
NXPH4	Neurexophilin-4	Neuropeptide
UTS2D	Urotensin-2-related peptide	Neuropeptide
RLN1	Relaxin 1	Neuropeptide
RLN3	Relaxin 3	Neuropeptide
TRH	Thyrotropin releasing hormone	Neuropeptide
PTH1H	Parathyroid hormone-like hormone	Neuropeptide
PMCH	Melanin concentrating hormone	Neuropeptide
HCRT	Hypocretin	Neuropeptide
CARTPT	Cocaine and amphetamine regulated transcript	Neuropeptide
AGRP	Agouti related protein	Neuropeptide
APLN	Apelin	Neuropeptide
KISS1	Kisspeptin, Metastasis-suppressor KiSS	Neuropeptide
DBI	Diazepam-binding inhibitor	Neuropeptide
CBLN1	Cerebellin-1	Neuropeptide
CBLN2	Cerebellin-2	Neuropeptide
CBLN4	Cerebellin-4	Neuropeptide
ADIPOQ	Adiponectin	Neuropeptide
RETN	Resistin	Neuropeptide
NUCB2	Nucleobindin 2, Nesfatin	Neuropeptide
UBL5	Ubiquitin-like 5	Neuropeptide
SERPINA3K	serine (or cysteine) peptidase inhibitor, clade A, member 3K	Other

NPY1R	Neuropeptide Y receptor 1	Receptor
CITED1	Cbp/p300-interacting transactivator with Glu/Asp-rich carboxy-terminal domain 1	Transcription factor
ESYT3	extended synaptotagmin-like protein 3	Other
PRLR	Prolactin receptor	Receptor
ASB4	ankyrin repeat and SOCS box-containing 4	Other
RGS9	regulator of G-protein signaling 9	Other
PLAGL1	pleiomorphic adenoma gene-like 1	Other
GABRE	gamma-aminobutyric acid (GABA) A receptor, subunit epsilon	Receptor
TMEM176A	transmembrane protein 176A	Other
Ecel1	Endothelin converting enzyme-like 1	Other
PEG10	paternally expressed 10	Other
GRIK3	glutamate receptor, ionotropic, kainate 3	Receptor
Tbx3	T-box 3	Transcription factor
IRS4	Insulin receptor substrate 4	Other
TMED3	transmembrane emp24 domain containing 3	Other
GPX3	glutathione peroxidase 3	Other
DLK1	delta-like 1 homolog	Transcription factor
ARL10	ADP-ribosylation factor-like 10	Other
SPINT2	serine protease inhibitor, Kunitz type 2	Other
GPR165	G protein-coupled receptor 165	Receptor
Clcn5	chloride channel 5	Channel/Transporter
Celf6	CUGBP, Elav-like family member 6	Other
Rxfp3	Relaxin family peptide receptor 3	Receptor
Nnat	Neuronatin	Other
Mesdc2	mesoderm development candidate 2	Other

Slc2a1	Glut-1; Solute carrier family 2, facilitated glucose transporter member 1	Channel/Transporter
VAT1	vesicle amine transport protein 1 homolog (T californica)	Channel/Transporter
Adcyap1r1	adenylate cyclase activating polypeptide 1 receptor 1	Receptor
Fezf1	Fez family zinc finger 1	Transcription factor
Slit3	slit homolog 3 (Drosophila)	Other
Gda	guanine deaminase	Other
Rreb1	ras responsive element binding protein 1	Transcription factor
AMIGO2	adhesion molecule with Ig like domain 2	Other
Doc2b	double C2, beta	Other
Pvr13	poliovirus receptor-related 3	Other
Icam5	intercellular adhesion molecule 5, telencephalin	Other
Gla1	glycine receptor, alpha 1 subunit	Receptor
Chrm5	cholinergic receptor, muscarinic 5	Receptor
Camk1g	calcium/calmodulin-dependent protein kinase I gamma	Other
Itpr1	inositol 1,4,5-triphosphate receptor 1	Other
Lmo3	LIM domain only 3	Transcription factor
Cacna2d1	calcium channel, voltage-dependent, alpha2/delta subunit 1	Channel/Transporter
Kcnab1	potassium voltage-gated channel, shaker-related subfamily, beta member 1	Channel/Transporter
Syt10	synaptotagmin 10	Other
Lhx1	LIM homeobox protein 1	Transcription factor
Vipr2	VIP receptor 2	Receptor
Rasl11b	Ras like 11b	Other
Rgs16	Regulator of G-protein signaling 16	Other

Rorb	RAR-related orphan receptor beta	Transcription factor
Prokr2	prokineticin receptor 2	Receptor
Rora	RAR-related orphan receptor alpha	Transcription factor
NR1D1	nuclear receptor subfamily 1, group D, member 1	Transcription factor
Zim1	zinc finger, imprinted 1	Transcription factor
Flrt3	fibronectin leucine rich transmembrane protein 3	Other
Zic1	zinc finger protein of the cerebellum 1	Transcription factor
Slc2a13	solute carrier family 2 (facilitated glucose transporter), member 13	Channel/Transporter
Npsr1	Neuropeptide S receptor 1	Receptor
Fezf2	Fez family zinc finger 2	Transcription factor
Tacr3	Tachykinin receptor 3	Receptor
Ly6H	Lymphocyte antigen 6 complex, locus H	Other
Ntsr1	Neurotensin receptor 1	Receptor
Pitx2	Paired-like homeodomain transcription factor 2	Transcription factor
Gabrq	Gamma-aminobutyric acid (GABA) A receptor, subunit theta	Receptor
Calcr	Calcitonin receptor	Receptor
GPR101	GPCR 101	Receptor
Pou6f2	POU domain, class 6, transcription factor 2	Transcription factor
Crhr2	Corticotropin releasing hormone receptor 2	Receptor
Htr1a	5-hydroxytryptamine (serotonin) receptor 1A	Receptor
Htr1b	5-hydroxytryptamine (serotonin) receptor 1B	Receptor
Htr2a	5-hydroxytryptamine (serotonin) receptor 2A	Receptor
Htr2c	5-hydroxytryptamine (serotonin) receptor 2C	Receptor
Htr3b	5-hydroxytryptamine (serotonin) receptor 3B	Receptor
Htr4	5-hydroxytryptamine (serotonin) receptor 4	Receptor

Htr5A	5-hydroxytryptamine (serotonin) receptor 5A	Receptor
Htr6	5-hydroxytryptamine (serotonin) receptor 6	Receptor
Zfx4	zinc finger homeodomain 4	Transcription factor
Ar	Androgen receptor	Transcription factor
Trhr	Thyrotropin releasing hormone receptor	Receptor
Cnr1	Cannabinoid receptor 1	Receptor
MC4R	Melanocortin 4-receptor	Receptor
NPY5R	Neuropeptide Y receptor 5	Receptor
NPY2R	Neuropeptide Y receptor 2	Receptor
PGR	progesterone receptor	Transcription factor
OXTR	oxytocin receptor	Receptor
Gpr83	G protein-coupled receptor 83	Receptor
Pcsk1	Proprotein convertase subtilisin/kexin type 1	Other
LHX9	Lim homeobox protein 9	Transcription factor
Sim1	single minded 1	Transcription factor
Gsbs	G substrate	Other
Calb1	calbindin 1	Other
Calb2	calbindin 2	Other
Chrna3	cholinergic receptor, nicotinic, alpha polypeptide 3	Receptor
Chrna4	cholinergic receptor, nicotinic, alpha polypeptide 4	Receptor
Chrna7	cholinergic receptor, nicotinic, alpha polypeptide 7 (Chrna7)	Receptor
Avpr1a	arginine vasopressin receptor 1A	Receptor
GBX2	gastrulation brain homeobox 2	Transcription factor
DDC	dopa decarboxylase	Other
SYTL4	synaptotagmin-like 4	Other
NGB	neuroglobin	Other

NHLH2	nescient helix loop helix 2	Transcription factor
nkx2-1	NK2 homeobox 1	Transcription factor
isl1	ISL1 transcription factor	Transcription factor
BRS3	bombesin-like receptor 3	Receptor
Slc18a2	solute carrier family 18 (vesicular monoamine), member 2	Channel/Transporter
NR5A1	nuclear receptor subfamily 5, group A, member 1; SF1	Transcription factor
P2RY1	purinergic receptor P2Y, P2Y	Channel/Transporter
Esr1	estrogen receptor alpha	Transcription factor
rpl27	ribosomal protein L27	Other
rpl23	ribosomal protein L23	Other
Actb	Actin	Other
Syt1	synaptotagmin 1	Other
slc1a2	solute carrier family 1 (glial high affinity glutamate transporter), member 2	Channel/Transporter
nefl	neurofilament, light	Other
slc12a5	solute carrier family 12, member 5; KCC2	Channel/Transporter
snap25	synaptosomal associated protein 25	Other
gfap	glial fibrillary acidic protein	Other
HDC	Histidine decarboxylase	Other
Ache	Acetylcholinesterase	Other
Mal	myelin and lymphocyte protein, oligodendrocyte marker	Other
FA2H	fatty acid 2-hydroxylase, oligodendrocyte marker	Other
Slc6a3	Dopamine Transporter; dopamine marker	Channel/Transporter
TH	Tyrosine hydroxylase; dopamine marker	Other
GAD2	glutamic acid decarboxylase 2	Other

GAD1	GAD67, glutamic acid decarboxylase 1	Other
NOS1	nitric oxide synthase 1, neuronal	Other
Fxyd6	FXYD domain-containing ion transport regulator 6	Other
hap1	huntingtin-associated protein 1	Other
Slc17a7	Vglut1; solute carrier family 17 member 7	Channel/Transporter
Slc17a6	Vglut2; solute carrier family 17 member 6	Channel/Transporter
Slc1a1	EAAT3, neuronal/epithelial high affinity glutamate transporter	Channel/Transporter
Sgsm1	small G protein signaling modulator 1	Other
Susd2	sushi domain containing 2	Other
Pcsk1n	proprotein convertase subtilisin/kexin type 1 inhibitor	Neuropeptide
Ghsr	Growth hormone secretagogue receptor	Receptor
Npr3	natriuretic peptide receptor 3 (NPR-C)	Receptor
Crabp1	cellular retinoic acid binding protein	Transcription factor
Scn9a	sodium channel, voltage-gated, type IX, alpha	Channel/Transporter
Scn7a	sodium channel, voltage-gated, type VII, alpha	Channel/Transporter
kcnk2	potassium channel subfamily K member 2	Channel/Transporter
Adra2a	alpha 2A adrenergic receptor	Receptor
Per1	Period homolog 1	Transcription factor
Per2	Period homolog 1	Transcription factor
Drd2	Dopamine receptor 2	Receptor
GPR50	G protein coupled receptor 50	Receptor
Drd1a	Dopamine receptor 1a	Receptor
Aplnr	Apelin Receptor	Receptor
Fzd5	frizzled homolog 5	Transcription factor
Pou2f2	POU domain, class 2, transcription factor 2	Transcription factor
Sox3	SRY (sex determining region Y)-box 3	Transcription factor

Six3	sine oculis-related homeobox 3 homolog	Transcription factor
Qrfpr	pyroglutamylated RFamide peptide receptor	Receptor
Oprl1	opiod receptor like 1	Receptor
Gck	glucokinase	Other
MC3R	melanocortin 3-receptor	Receptor
Fos	FBJ osteosarcoma oncogene	Transcription factor
FosB	FBJ murine osteosarcoma viral oncogene homolog B	Transcription factor
Egr1	early growth response 1; NGFI-A	Transcription factor
Egr4	early growth response 4	Transcription factor
Nr4a1	Nur77; NGFI-B, immediate early gene	Transcription factor
Arc	activity-regulated cytoskeleton-associated protein; Arg3.1	Transcription factor
Cxcl1	Chemokine (C-X-C motif) ligand 1	Chemokine
Nupr1	Nuclear protein 1	Activity dependent gene

Statistical Analysis

Data was presented as mean \pm standard error of the mean (SEM). Student's t test was used to determine significance of the difference of the mean between experiment and control animals. $p < 0.05$ represented statistical significance.

General Considerations for pS6 Profiling Experiments

The efficiency and reproducibility of the pS6 induction by the stimulus is a critical determinant to the success of these experiments. Stimuli that produce small changes in pS6 will produce small fold enrichment values. Likewise, stimuli that induce pS6 inconsistently between animals will result in lower fold enrichment values because

tissue are pooled for immunoprecipitation. When testing a new paradigm, a time course of staining for both pS6 and cfos in brain sections (ie 30, 60 and 120 minutes) was performed. Different stimulus conditions (ie dose, time of day) was also tested, starting from parameters that have been previously reported in the cfos literature. The key parameters that determine the degree of induction of pS6 (or cfos) may not be obvious. For instance, overnight fast has been reported to induce pS6 in the arcuate nucleus (Villanueva et al., 2009) but we found that this pS6 induction was sensitive to both the duration of the fast and the time of day the mice were sacrificed. Fasted mice sacrificed during the light phase showed less pS6 in the arcuate nucleus than mice sacrificed at the end of the dark phase. Similarly, the optimal fasting duration was approximately 15 hours and lower levels of pS6 were observed when mice were fasted 24 hours or longer. It is important to note that for activity-dependent and other induced genes, the level of mRNA (rather than protein) in the activated neurons at the time of sacrifice will determine the fold enrichment. For example, in the salt loading experiment, cfos was enriched 2-fold by TaqMan and 3.6-fold by RNA-seq following salt challenge despite the observation that more significant induction of cfos protein was seen using immunohistochemistry. The discrepancy arises from the fact that cfos protein and mRNA have different kinetics and that for salt loading, the animals were sacrificed 2 hours after the stimulus. Although this time point is at the approximate peak for cfos protein induction (Miyata et al., 2001; Penny et al., 2005) as well as pS6, it is long after the peak of cfos mRNA expression, which peaks within 30 minutes and has returned to baseline by 3 hours following salt challenge (Kawasaki et al., 2005). In contrast, greater enrichment for fosB was observed because fosB gene expression has been shown to

remain elevated for several hours after salt loading(Miyata et al., 2001; Penny et al., 2005).

A polyclonal pS6 240/244 antibody (Cell Signaling, #2215) combined with a pS6 240 containing peptide gave the highest and most reproducible fold-enrichment values among several commercially available pS6 antibodies that were tested. Acceptable results using a polyclonal pS6 244/247 antibody (Life Technologies, 44-923G) were also obtained. Monoclonal antibodies targeting pS6 (Cell Signaling, #4858 and #5364) immunoprecipitated many non-specific proteins and therefore are not recommended.

A typical experiment using the pooled hypothalami from 20 mice yielded approximately 10ng of total RNA from the pS6 immunoprecipitate after purification (20ul of a 0.5ng/ul solution). This corresponds to an immunoprecipitate yield of 0.02%-0.1% of the total input RNA. Increasing the percent yield above this level (by relaxing the stringency of the immunoprecipitation) tended to decrease the fold-enrichment values, presumably because the most highly phosphorylated polysomes are preferentially immunoprecipitated. For RNA-seq experiments, we used approximately 0.5ng of total RNA from pS6 immunoprecipitation to prepare amplified cDNA. This amount has been shown to be sufficient for reproducible coverage of the transcriptome by sequencing(Ramsköld et al., 2012).

The RNA quantification data is analyzed in 2 steps. First the RNA in the immunoprecipitate for each gene is divided by the input to determine the fold-enrichment (IP/input). This measures the degree to which the transcript is enriched in the pS6 immunoprecipitate relative to the tissue as a whole. Since the immunoprecipitate is

divided by the input, changes in the absolute expression level of a transcript within the tissue have no effect on the fold-enrichment. This analysis is performed separately for stimulus and control experiments. The fold-enrichment values for the stimulus are then divided by the fold-enrichment values for the control to calculate the differential enrichment. The differential enrichment is calculated to identify neuronal markers that become enriched or depleted specifically in response to the stimulus. Normalization to the control group accounts for the fact that each neural marker has a different enrichment at baseline, reflecting different baseline pS6 for each cell population. For transcripts that may not be present at detectable levels in the pS6 immunoprecipitate from the control group (ie immediate early genes and other inducible transcripts), the data are analyzed as fold-enrichment in the stimulus group only.

Chapter 3:

Molecular Profiling of Activated Neurons by Phosphorylated Ribosome Capture

Introduction

A basic goal of neuroscience is to link the activity of specific neuronal cell types to the various functions of the brain. This task is complicated by the extraordinary cellular diversity of the mammalian central nervous system (CNS)(Lichtman and Denk, 2011; Masland, 2004; Nelson et al., 2006; Stevens, 1998) and the fact that most neurons cannot be identified solely based on their morphology or location(Isogai et al., 2011; Siegert et al., 2009). Comprehensive analyses of gene expression in the CNS such as the GENSAT project and the Allen Brain Atlas have revealed extensive heterogeneity in gene expression across brain regions(Gong et al., 2003; Lein et al., 2007), but there are significant gaps in our understanding of how this molecular diversity is linked to function.

The ability to profile genes uniquely expressed in neurons that respond to a stimulus would facilitate the systematic molecular identification of the cell types that control behavior. The molecular identification of these cells would also enable their in vivo manipulation using technologies that make it possible to activate or inhibit neurons with light(Yizhar et al., 2011), generate transcriptional profiles from neurons using tagged ribosomes(Heiman et al., 2008; Sanz et al., 2009) or label using fluorescent reporters to facilitate electrophysiological recordings(Gong et al., 2003). These tools achieve their selectivity by targeting protein expression using a promoter from a cell-type

specific marker gene. However, in many cases marker genes that identify a functional population of neurons are lacking(Zhang et al., 2007).

Immediate early genes such as *cfos* have been widely used to visualize neurons that respond to numerous stimuli(Morgan and Curran, 1991). Despite its utility in marking neurons that have been biochemically activated, *cfos* immunostaining does not reveal genetic identity of the labeled cells. Characterizing the co-expression of an activation marker such as *cfos* with even a limited set of candidate genes requires processing large numbers of histological sections(Isogai et al., 2011). For this reason, systematic methods are needed to profile gene expression from discrete subpopulations of activated neurons in the brain.

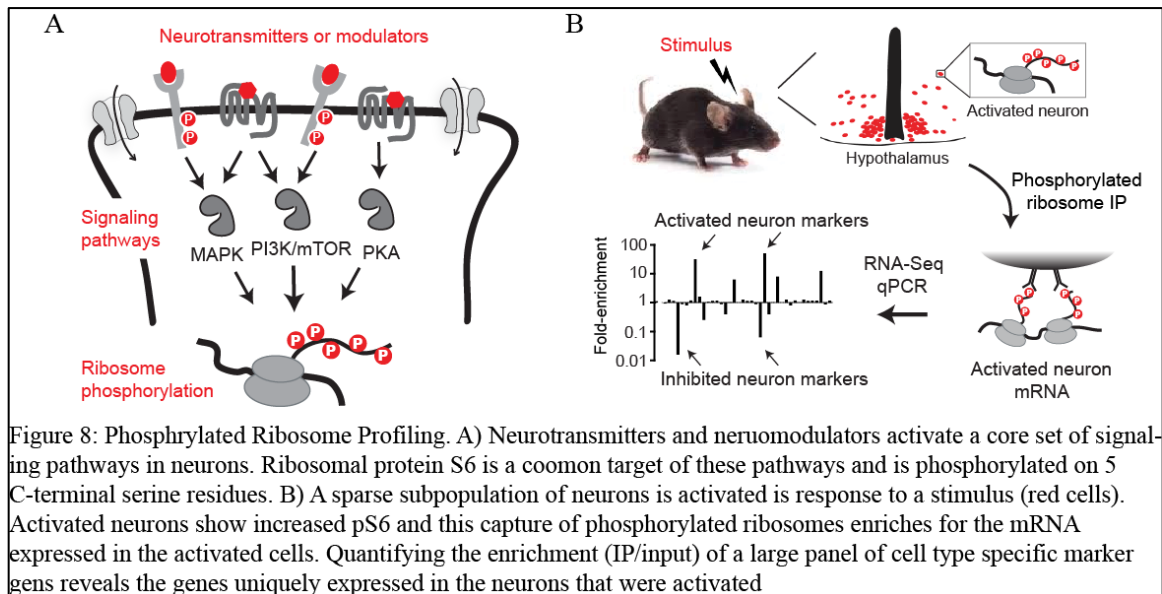
Here, I show that phosphorylation of the ribosome can be used as a molecular tag to selectively retrieve RNA from activated neurons. This enables the unbiased discovery of the genes that are uniquely expressed in functionally activated neurons. By quantifying in parallel the enrichment of many such markers, it is possible to assess the activation or inhibition of numerous cell types in a complex tissue, revealing the coordinated regulation of ensembles of neurons in response to an external stimulus.

Results

Ribosome Phosphorylation Often Correlates with Neural Activity

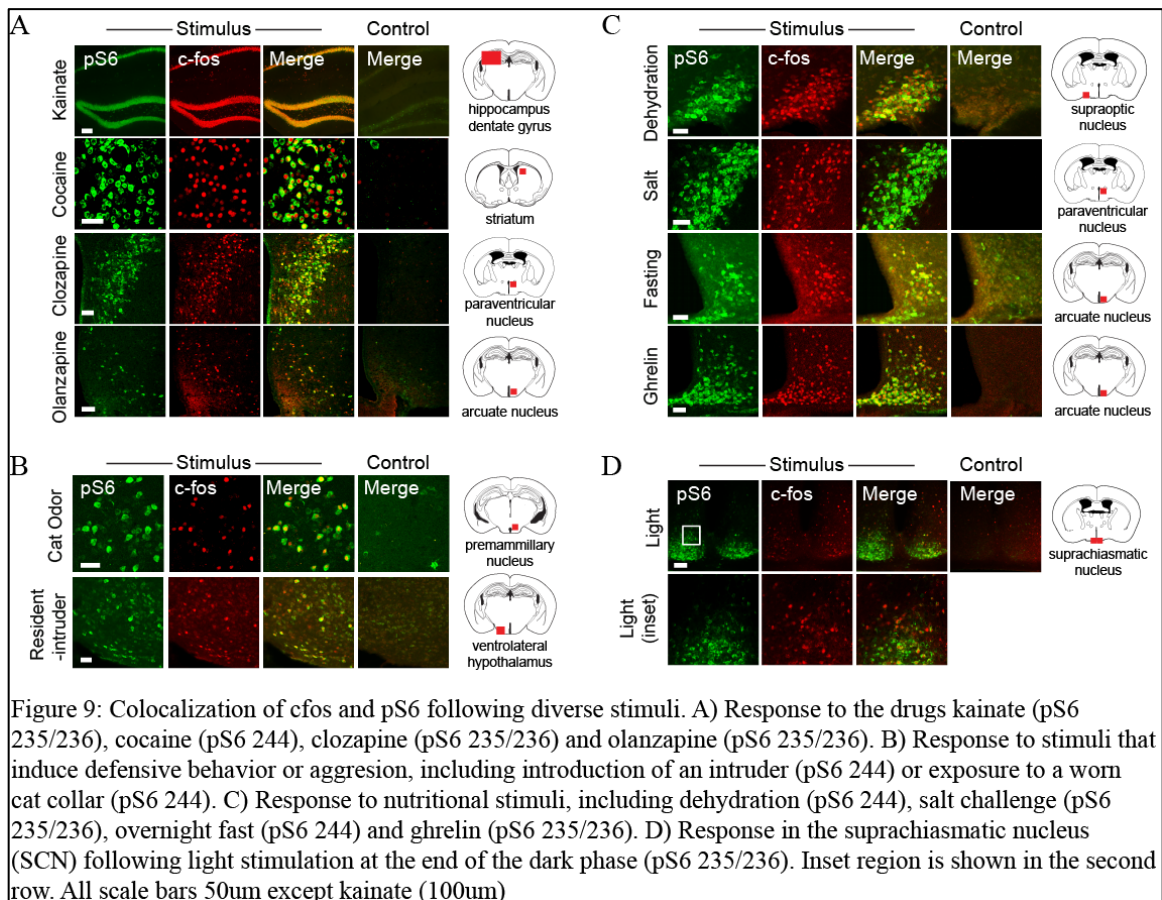
Immediate early genes such as *cfos* are widely used to mark activated neurons in the mouse brain(Morgan and Curran, 1991) but *cfos* immunostaining does not reveal the molecular identity of the labeled cells. I thus set out to develop a method for generating expression profiles from activated neurons. I noted that many stimuli that trigger *cfos*

expression in activated neurons also induce phosphorylation of ribosomal subunit S6 (Cao et al., 2008; Valjent et al., 2011; Villanueva et al., 2009; Zeng et al., 2009). S6 is a structural component of the ribosome that is phosphorylated downstream of PI3-K/mTOR, MAPK and PKA signaling (Figure 8A) (Meyuhas, 2008; Valjent et al., 2011). These same pathways regulate the transcription of activity-dependent genes such as *cfos* (Flavell and Greenberg, 2008). I reasoned that because S6 phosphorylation introduces a tag on ribosomes that resides in biochemically activated neurons, it might be possible to immunoprecipitate these phosphorylated ribosomes from mouse brain homogenates and thereby enrich for messenger RNA (mRNA) expressed in the activated cells (Figure 8B). By comparing the abundance of each transcript in the pS6 immunoprecipitate to its abundance in the tissue as a whole, it would therefore be possible to rank in an unbiased way the genes that are uniquely expressed in a population of neurons that respond to a stimulus.



To confirm that S6 was phosphorylated in cells expressing *cfos*, I exposed mice to a diverse panel of stimuli and then performed double immunohistochemistry for *cfos* and

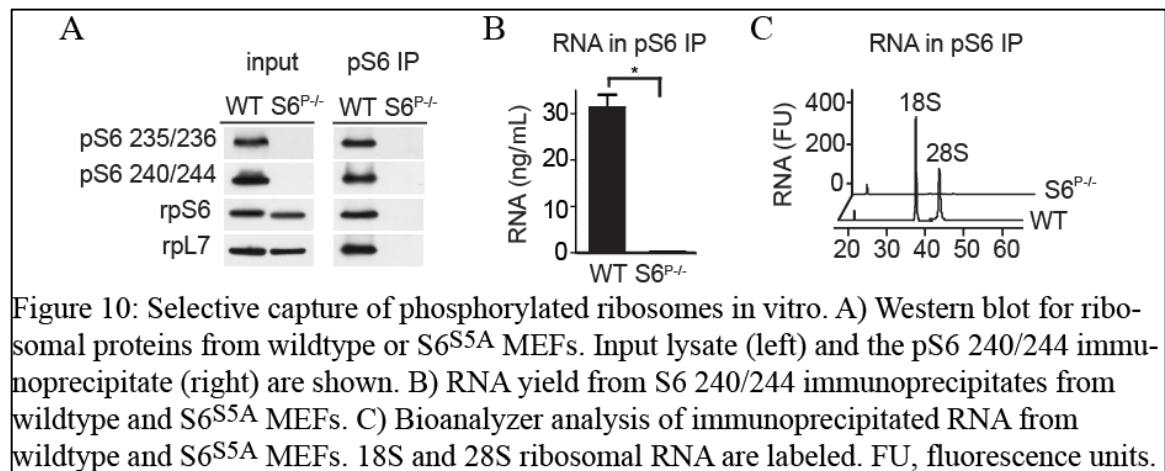
pS6 in brain slices (Figure 9). Treatment of mice with drugs such cocaine (a stimulant), kainate (a convulsant), clozapine and olanzapine (antipsychotics) all induced colocalization of pS6 and cfos in a variety of brain regions (Figure 9A). Exposure of male mice to an intruder induced an overlapping pattern of cfos and pS6 expression in brain regions that are known to mediate aggression such as the ventrolateral hypothalamus (Figure 9B) (Lin et al., 2011). A cat odorant, which signals to rodents the presence of a predator, induced cfos and pS6 in the dorsal preammillary nucleus, a region known to mediate fear and defensive responses (Figure 9B) (Dielenberg et al., 2001). A wide variety of nutritional stimuli including fasting, dehydration, salt challenge and ghrelin treatment also resulted in extensive colocalization of cfos and pS6 in regions of the hypothalamus that are known to regulate water and food intake (Figure 9C). In some



cases, one of these markers labeled a broader population of activated neurons than the other. For example, light induced strong pS6 but only scattered cfos within the suprachiasmatic nucleus (Figure 9D), a region that regulates circadian rhythms and receives input from the retina(Cao et al., 2008). However, in general, a wide range of stimuli induced expression of cfos and pS6 in largely overlapping neural populations throughout the brain.

Selective capture of Phosphorylated Ribosomes

I next set out to confirm that I could selectively isolate phosphorylated ribosomes and their associate mRNA. I prepared lystates from wild-type mouse embryonic fibroblasts (MEFs) as well as knockin MEFs in which each of the 5 serine phosphorylation sites on S6 was mutated to alanine (Ser 235, 236, 240, 244 and 247; S6^{S5A})(Ruvinsky et al., 2005). Antibodies that recognize pS6 240/244 efficiently immunoprecipitated ribosome from lysates of wild-type MEFs but not from S6S5A cells (Figure 10A). Approximately 100-fold more RNA was isolated in pS6 immunoprecipitates from wild-type MEFs compared to S6^{S5A} controls (Figure 10B and 10C), confirming that phosphorylated ribosomes can be captured with high selectivity.



To confirm that mRNA from a single neuronal cell type can be enriched *in vivo*, I generated mice in which the gene encoding Tsc1 was selectively deleted in melanin-concentrating hormone (MCH) neurons of the lateral hypothalamus (MCH^{Cre} Tsc1^{fl/fl}). Deletion of Tsc1 activated the mTORC1 pathway, resulting in constitutive S6 phosphorylation (Figure 11A and 11B). Consistent with prior reports, deletion of Tsc1 also results in increased cell size (Figure 11B) (Meikle et al., 2007). I prepared tissue homogenates from hypothalami of these mice, immunoprecipitated phosphorylated ribosomes and analyzed the purified RNA. Commercially available antibodies that recognize either pS6 235/236 or 240/244 could enrich for Pmch mRNA by ~4 fold. (Figure 11C and 11D) Because Tsc1 deletion results in uniform and complete S6 phosphorylation in targeted cells (Meikle et al., 2007), this 4-fold enrichment represents an upper limit on the RNA enrichment that can be achieved. At this level of enrichment, it was challenging to identify markers for cell types that underwent graded or heterogeneous activation in response to a physiologic stimulus. A way to capture RNA from activated neurons more selectively was needed.

Phosphorylation of S6 is believed to occur sequentially (in the order Ser 235, 236, 240, 244 and 247) such that the most C-terminal sites (Ser 244 and 247) are phosphorylated at much lower stoichiometry than the N-terminal sites at baseline (Figure 11C) (Meyuhas, 2008). Thus it is possible that phosphorylation of these C-terminal sites exhibit a wider dynamic range in response to changes in neural activity and that an antibody recognizing only one of the C-terminal sites might enable greater enrichment of cell type specific transcripts. After extensive optimization, I discovered that a polyclonal antibody targeting pS6 240/244 can be made more selective by pre-incubation with a

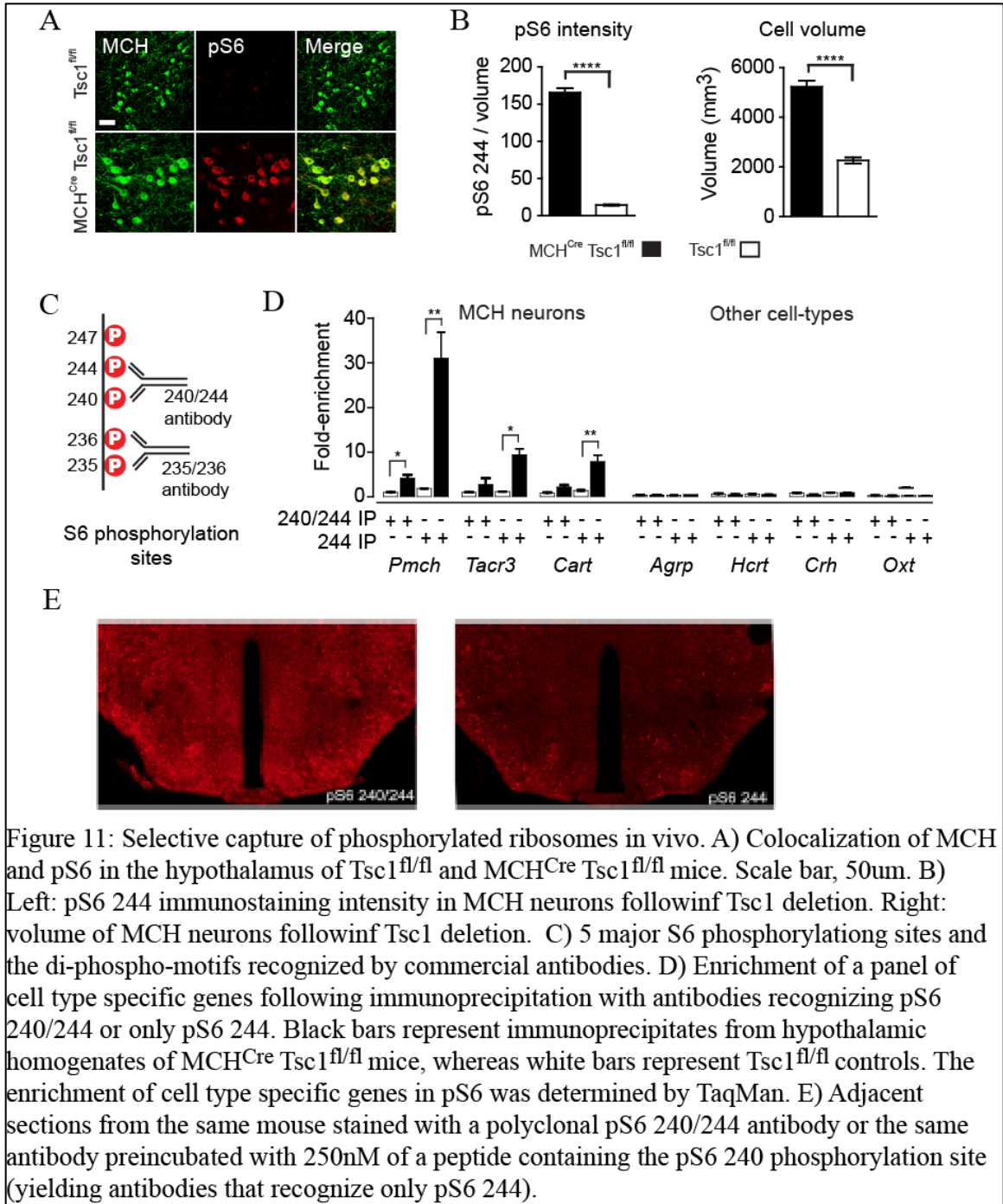


Figure 11: Selective capture of phosphorylated ribosomes in vivo. A) Colocalization of MCH and pS6 in the hypothalamus of *Tsc1^{fl/fl}* and *MCH^{Cre} Tsc1^{fl/fl}* mice. Scale bar, 50um. B) Left: pS6 244 immunostaining intensity in MCH neurons following *Tsc1* deletion. Right: volume of MCH neurons following *Tsc1* deletion. C) 5 major S6 phosphorylation sites and the di-phospho-motifs recognized by commercial antibodies. D) Enrichment of a panel of cell type specific genes following immunoprecipitation with antibodies recognizing pS6 240/244 or only pS6 244. Black bars represent immunoprecipitates from hypothalamic homogenates of *MCH^{Cre} Tsc1^{fl/fl}* mice, whereas white bars represent *Tsc1^{fl/fl}* controls. The enrichment of cell type specific genes in pS6 was determined by TaqMan. E) Adjacent sections from the same mouse stained with a polyclonal pS6 240/244 antibody or the same antibody preincubated with 250nM of a peptide containing the pS6 240 phosphorylation site (yielding antibodies that recognize only pS6 244).

phosphopeptide containing the S6 Ser240 phosphorylation site, thereby yielding antibodies that recognize only phosphorylation at Ser244 (hereafter referred to as pS6 244 antibodies) (Figure 11C). Immunoprecipitation of phosphorylated ribosomes by using S6 244 antibodies resulted in more than 30-fold enrichment of *Pmch* transcripts from

MCH^{Cre} Tsc1^{fl/fl} mice, but not Tsc1^{fl/fl} controls (Figure 11D). Importantly, robust enrichment (8- to 10-fold) for genes co-expressed in only a subset of MCH neurons such as *Cart* and *Tacr3* was observed (Croizier et al., 2010). There was no enrichment for genes expressed in a set different hypothalamic cell types such as the neuropeptides *Hcr*, *Oxt*, *Agrp* and *Crh* (Figure 11D). Consistent with this quantitative PCR (qPCR) data, brain slices stained by using pS6 244 antibodies showed enhanced contrast between pS6-positive and pS6-negative neurons compared to slices stained with commercial antibodies that recognize a broader set of phosphorylation sites (Figure 11E). Using this optimized approach, we were able to achieve highly selective enrichment of transcripts expressed in neurons after induction of pS6 in vivo.

Molecular Identification of Hypothalamus Neurons at Baseline

I observed that wildtype mice exhibit strong pS6 immunostaining in the suprachiasmatic nucleus (SCN) during the day with variable but low levels of pS6 detectable in other anatomical regions (Figure 12A). The SCN controls circadian rhythms in response to input from the retina and light has been shown to induce pS6 in a subpopulation of neurons in the SCN (Cao et al., 2011; 2010). These pS6-positive cells are predominantly negative for vasopressin but their neurochemical identity is otherwise unknown.

I sacrificed wild-type mice near the midpoint of the circadian day (ZT 5), prepared tissue homogenates from the hypothalamus and immunoprecipitated ribosomes using pS6 244 antibodies. The fold-enrichment (IP/input) for a panel of 20 neuropeptides that represent markers for a series of well-characterized hypothalamic cell types was

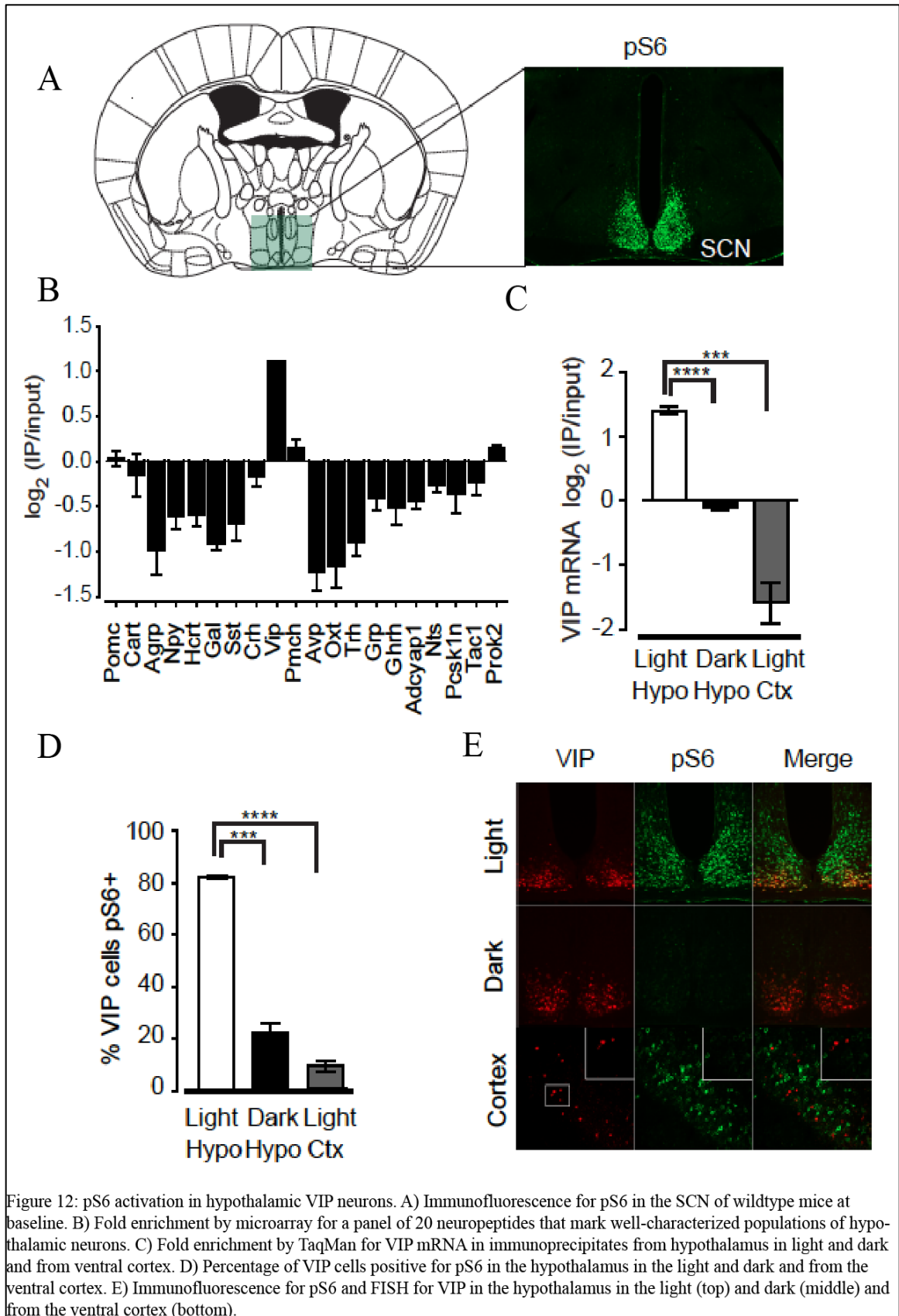


Figure 12: pS6 activation in hypothalamic VIP neurons. A) Immunofluorescence for pS6 in the SCN of wildtype mice at baseline. B) Fold enrichment by microarray for a panel of 20 neuropeptides that mark well-characterized populations of hypothalamic neurons. C) Fold enrichment by TaqMan for VIP mRNA in immunoprecipitates from hypothalamus in light and dark and from ventral cortex. D) Percentage of VIP cells positive for pS6 in the hypothalamus in the light and dark and from the ventral cortex. E) Immunofluorescence for pS6 and FISH for VIP in the hypothalamus in the light (top) and dark (middle) and from the ventral cortex (bottom).

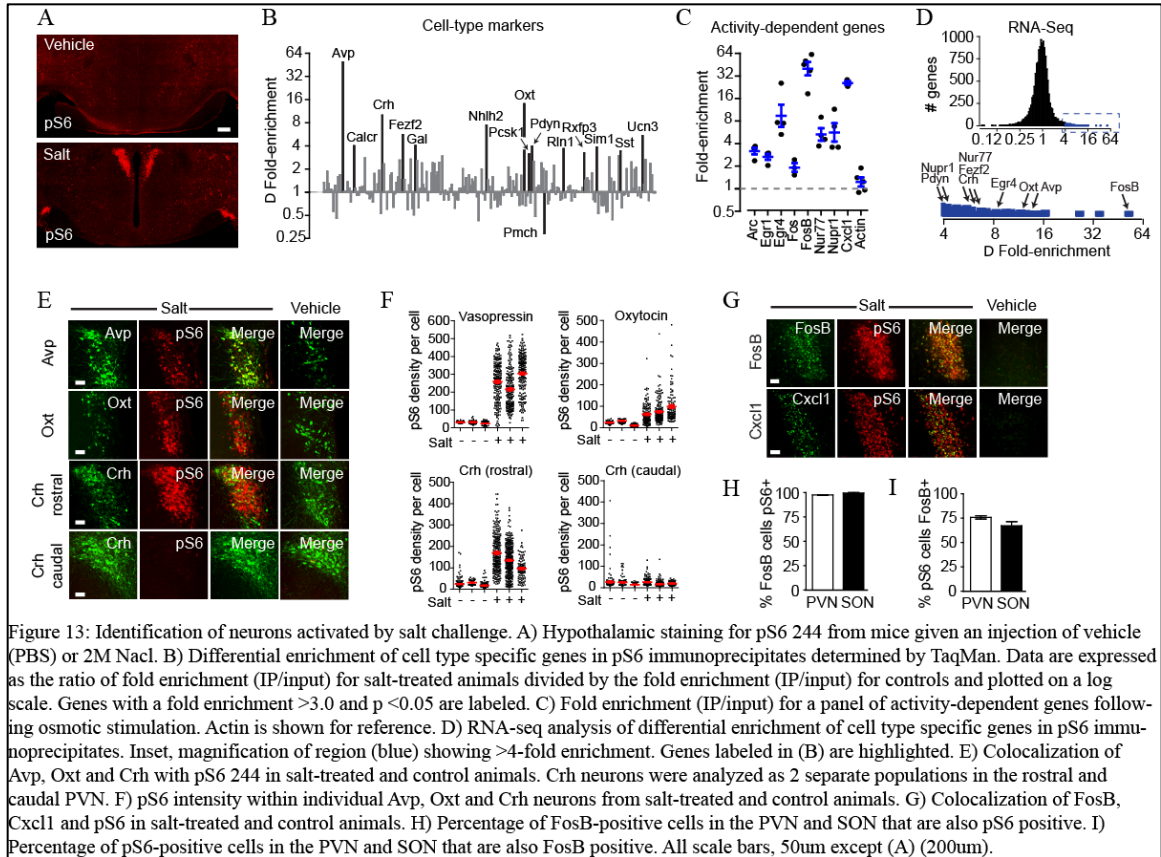
determined (Figure 12B). Vasoactive intestinal peptide (VIP) was the only neuropeptide significantly enriched in pS6 immunoprecipitates at baseline. I then confirmed by immunohistochemistry that 82% of VIP cells in the SCN were pS6 positive (Figure 12C and 12 D). pS6 in the SCN is regulated by circadian time and stimulated by light, suggesting that the enrichment observed for VIP should be sensitive to the time of day in which the experiment was performed. Mice were sacrificed in the dark phase, at the midpoint of the circadian night (ZT 18) and the RNA recovered in pS6 immunoprecipitates analyzed. Night-time dissection abolished the enrichment for VIP mRNA in S6 immunoprecipitates (Figure 12C) and we confirmed by immunohistochemistry that mice sacrificed in the dark had significantly fewer pS6 positive VIP neurons in the SCN (Figure 12D and 12E). VIP is also expressed in the cortex, where it defines a major class of interneuron that is functionally unrelated to VIP neurons in the SCN. There was little co-localization between pS6 and VIP neurons in the cortex by immunostaining (Figure 12D and 12E). Consistent with this result, VIP mRNA was markedly depleted in pS6 immunoprecipitates from the cortex (Figure 12C). Thus, these data clearly demonstrates that pS6 capture can reveal cell type specific changes in activity across circadian time and anatomical space.

Molecular Identification of Hypothalamic Neurons Activated by Salt

I next asked if I could identify neurons activated by a well-characterized stimulus. Plasma osmolarity is controlled by a hypothalamic system that includes vasopressin and oxytocin neurons. The levels of these neuropeptides are known to increase in response to salt loading. Mice were challenged with a concentrated salt solution and brain sections were stained for pS6 244.

Salt challenge induced a dramatic increase in regions of the hypothalamus that mediate osmoregulation, including the paraventricular nucleus (PVN), supraoptic nucleus (SON) and median eminence (Figure 13A). Phosphorylated ribosomes were immunoprecipitated from hypothalamic homogenates of salt-challenged and control animals and mRNA analyzed for enrichment. To enable the rapid and sensitive quantification of low abundance transcripts, I used a custom array of 225 TaqMan probes comprising of marker genes that show anatomically restricted expression within the hypothalamus, including neuropeptides, receptors and transcription factors. The expression data for these genes were plotted as the log of the differential enrichment for each gene in response to the stimulus (Figure 13B). Similar results were obtained using RNA sequencing (Figure 13D).

Markers for the major neural populations that respond to salt challenge were among the most highly enriched genes in pS6 immunoprecipitates. These included vasopressin (Avp; 49-fold enriched), oxytocin (Oxt; 14-fold enriched) and corticotrophin-releasing hormone (Crh; 10-fold) (Figure 13B). The degree of enrichment for these marker genes correlated with the quantitative induction of pS6 in the corresponding cells as assayed by immunohistochemistry (Figure 13E and 13F). Specific enrichment for genes that partially overlap in expression with Avp and Oxt such as the neuropeptides galanin (Gal; 4-fold enriched) and prodynorphin (Pdyn; 3.9-fold enriched) and the PVN-specific transcription factors Nhlh2 (7.4-fold enriched), Fezf2 (5.6-fold enriched) and Sim1 (3.8-fold enriched) (Figure 13B) (Gai et al., 1990; Sherman et al., 1986) were also detected at lower levels of enrichment. These data indicate that pS6 immunoprecipitation



can enrich for transcripts that identify activated cell types and that the fold enrichment of these genes reflects their selective expression in the activated cells.

Some of the genes enriched in pS6 immunoprecipitates identify neural populations not previously known to be activated by salt challenge. For example, relaxin-1 (Rln1; 3.7-fold enriched) a neuropeptide that stimulates water intake and activates vasopressin and oxytocin neurons but has not been characterized in the hypothalamus due to low expression level (Thornton and Fitzsimons, 1995). Other enriched neuropeptides include urocortin 3 (Ucn3; 5.4-fold enriched), which is related to Crh and is expressed in a small population of neurons in the perifornical region and somatostatin (Sst; 3.4-fold enriched) which is known to promote vasopressin release (Brown et al., 1988).

In addition to these cell type specific markers, biochemical markers that are known to be induced by neural activity were also enriched (Figure 13C). The most highly enriched activity-dependent gene was FosB (43-fold enriched) and immunostaining revealed essentially complete colocalization of FosB and pS6 in the PVN and SON (Figure 13G and 13H). Cxcl1 (26-fold enriched), a chemokine that is not expressed in the hypothalamus at baseline but is selectively induced in the PVN by salt (Koike et al., 1997), was also enriched (Figure 13G). These data confirm that by capturing phosphorylated ribosomes and analyzing the associated mRNA, genetic markers for neurons that are activated by a stimulus can be systematically identified, revealing the coordinated response of numerous intermingled cell types to a physiologic signal.

Hypothalamic Respond to Fasting

A different set of neurons in the hypothalamus regulate food intake and the response to food restriction. To identify components of this system, mice were exposed to a series of nutritional perturbations beginning with fasting. Mice were fasted overnight and sacrificed at the end of the dark phase and extent of ribosome phosphorylation was assayed by immunostaining. Fasting induced strong pS6 in the arcuate nucleus (ARC) of the hypothalamus as well as in the dorsomedial hypothalamus (DMH) and scattered cells of the medial preoptic area (MPA) (Figure 14A). To identify fasting-regulated neurons in each of these regions, I immunoprecipitated phosphorylated ribosomes from hypothalamic homogenates of fasted and fed animals and analyzed the enrichment of cell type specific RNAs.

Markers for many cell types that are known to regulate feeding were differentially enriched in pS6 immunoprecipitates. Two of the most enriched transcripts in response to fasting were *Agrp* and *Npy* (Figure 14B). These two neuropeptides are coexpressed in critical neurons of the ARC that promote food intake (Elmqvist et al., 2005). Selective increase of pS6 in these cells were confirmed with histology (Figure 14C) (Villanueva et al., 2009). Ghrelin receptor (*Ghr*), which is expressed in most *AgRP/NPY* neurons (Willeesen et al., 1999), and neuropeptide *Vgf*, which is induced in *AgRP* neurons following fasting (Hahm et al., 2002) were also enriched.

The neuropeptide galanin was one of the most strongly enriched genes in pS6 immunoprecipitates from fasted animals (Figure 14B). Galanin has been shown to stimulate feeding when injected directly into the hypothalamus (Parker and Bloom, 2012) but the regulation of galanin neurons by changes in nutritional state has not been described (Schwartz et al., 1993). I found that fasting induced a marked increase in pS6 in a specific subset of galanin neurons located in the DMA and MPA (Figure 14E). Galanin neurons in these 2 regions also expressed *cfos* after an overnight fast, confirming that they are activated by food restriction (Figure 14F).

As it is possible that all neurons have a basal level of ribosome phosphorylation, neural inhibition might result in a decrease in pS6, which would be detected as the depletion of transcripts from pS6 immunoprecipitates in the analysis. Consistent with this reasoning, the neuropeptide *Pomc* was the most depleted transcript in response to fasting (Figure 14D). *Pomc* is expressed in a key population of neurons in the ARC that inhibit food intake and *Pomc* expression is downregulated during food deprivation (Elmqvist et al., 2005), whereas leptin increases *cfos* in *Pomc* neurons as well as the firing rate of

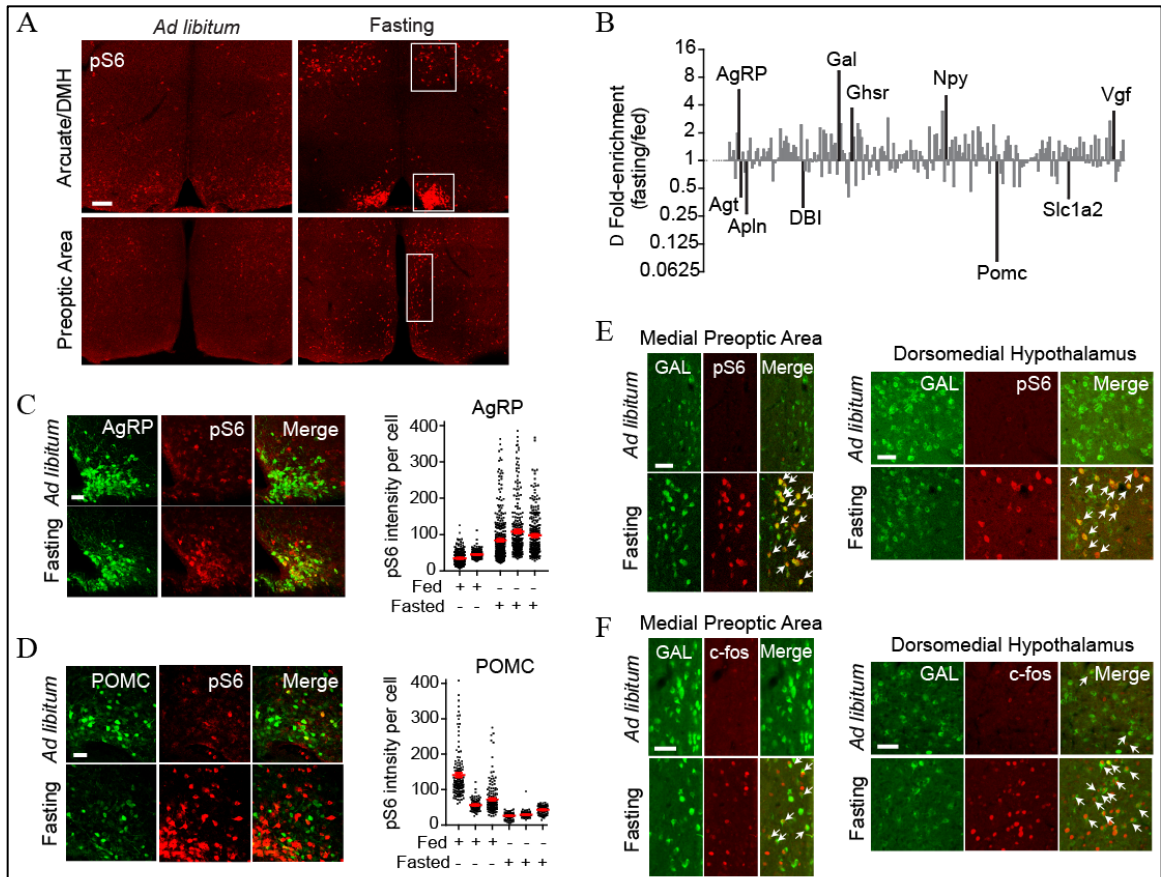


Figure 14: Identification of neurons activated by fasting. A) Hypothalamic staining for pS6 244 from fasting and fed mice. Top panels show the arcuate nucleus and DMH. Bottom panels show the preoptic area. B) Relative enrichment of cell type specific genes in pS6 immunoprecipitates from fasted and fed animals. Data are expressed as the ratio of fold enrichment (IP/input) for fasted animals divided by the fold enrichment (IP/input) for fed controls and are plotted on a log scale. Genes with fold enrichment >2.5 and $p < 0.05$ are labeled. C) Left: colocalization of AgRP and pS6 244 in fed and fasted mice. Right: pS6 intensity in AgRP neurons. D) Left: Colocalization of POMC and pS6 244 in fed and fasted mice. Right: pS6 intensity in POMC neurons. E) Colocalization of Gal and pS6 244 in fed and fasted mice in the MPA and DMH. F) Colocalization of Gal and c-fos in fed and fasted mice in the MPA and DMH. All scale bars, 50um except (A) (100um).

these cells (Cowley et al., 2001). Although fasting increases the level of pS6 in the ARC overall (largely as a result of AgRP neuron activation, Figure 14A), quantitative imaging reveals that fasting decreases the density of pS6 specifically within Pomc cells (Figure 14D). Thus, the depletion of specific transcripts from pS6 immunoprecipitates can be used to identify inhibited neurons. It is important to emphasize that the depletion observed for Pomc is not the result of change in gene expression level as only the ratio of RNA in the immunoprecipitate versus tissue as a whole (IP/input) was analyzed. Rather, enrichment or depletion of RNA from neurons is based on whether the state of activation of that neuron has changed. This ability to detect inhibition by ribosome profiling

contrasts with cfos immunostaining, which is limited in its ability to detect downregulation due to low level of cfos expression in most cells at baseline.

In addition to Pomc, several other neuropeptides that inhibit feeding such as apelin (Apln, which is co-expressed in a subset of Pomc neurons), angiotensin (Agt) and diazepam-binding inhibitor (Dbi) were also depleted (Figure 14B), suggesting that these peptides may reside in a population of fasting-inhibited cells (de Mateos-Verchere et al., 2001; Porter and Potratz, 2004; Reaux-Le Goazigo et al., 2011).

Scheduled Feeding Synchronizes Ribosome Phosphorylation with Food Availability

Although fasting can reveal the response to chronic energy deficit, most human feeding takes place intermittently at regular times in the day and the timing of meals is associated with many biochemical and behavioral responses. Similarly, rodents allowed daily access to food only during a scheduled window are known to synchronize their metabolism and activity to the time of food availability (Mistlberger, 2011). This behavioral adaptation is known as food-anticipatory activity (FAA) and is associated with the activation of neurons in multiple hypothalamic regions, including the DMH and ARC. Despite extensive investigation into the mechanism of FAA, the identity of the activated cell types and their specific roles are largely unknown. Thus, I sought to identify neurons with a specialized function associated with scheduled feeding. Unlike fasting, scheduled feeding also allows for more precise synchronization of behavior, enabling a more refined analysis of temporal changes in cell activation.

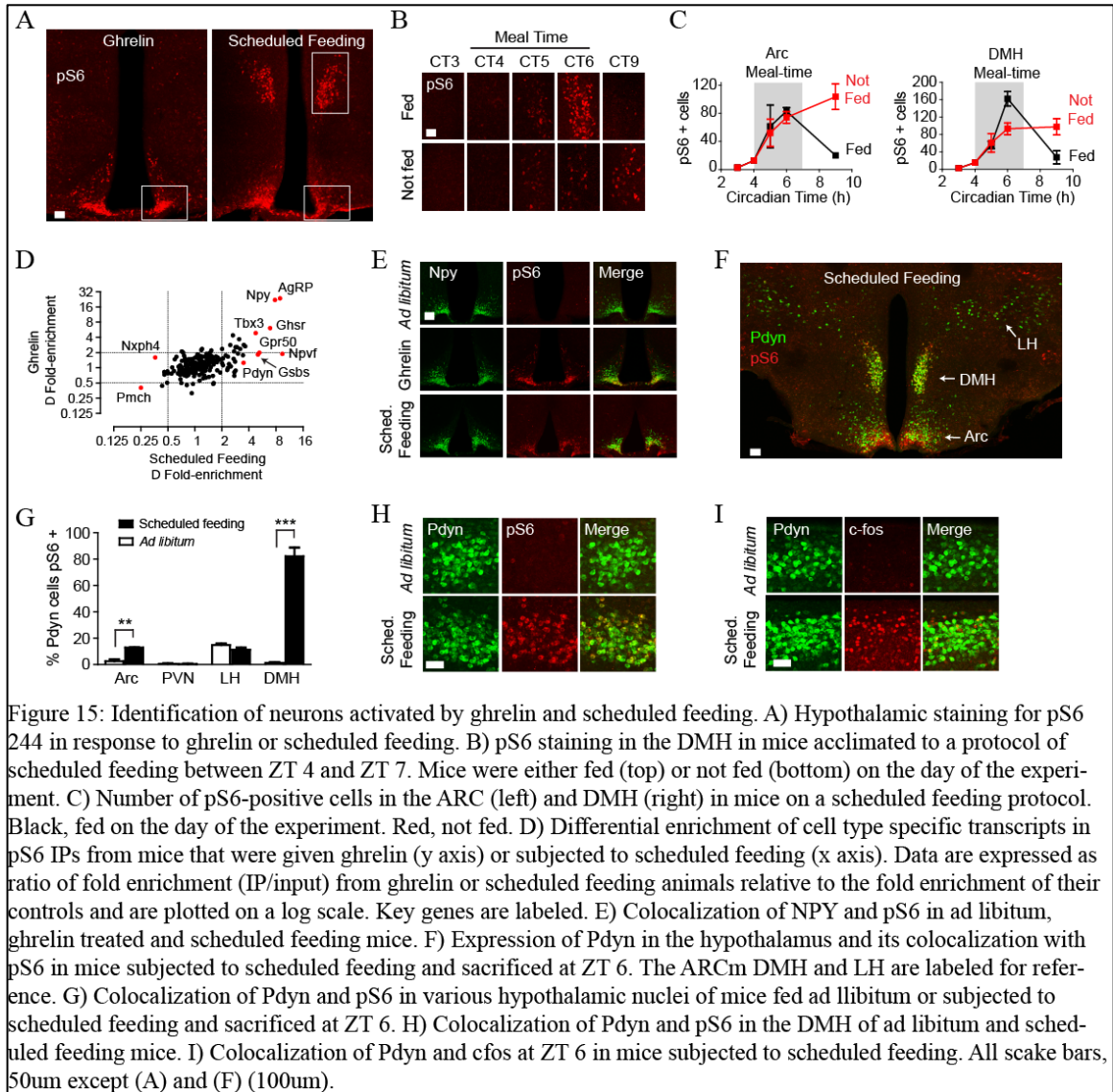
Food access of mice was restricted to a 3 hour window in the middle of the light phase, which resulted in robust FAA within 10 days. Next, I performed pS6 staining of

brain sections from these mice at several time points to establish the dynamics of ribosome phosphorylation in the hypothalamus. Scheduled feeding induced intense pS6 staining in the DMH and ARC (Figure 15A) that peaked within the meal window and declined to baseline thereafter (Figure 15B and 15C). DMH staining was concentrated in the compact part of the DMH, a region that does not show changes in ribosome phosphorylation after a single overnight fast (Figure 14A). Once the mice were entrained, this pattern of S6 phosphorylation no longer depended on the presence of food because brain sections from mice that acclimated to scheduled feeding but were not fed on the day of experiment showed a similar pattern of pS6 (although with lower intensity in the DMH; Figure 15B and 15C). This suggests the existence of unidentified neural populations that are regulated in part by a circadian signal entrained by food availability.

To identify neurons activation during scheduled feeding, I immunoprecipitated phosphorylated ribosomes from the hypothalamus of animals sacrificed 2 hours after food presentation and analyzed the enriched mRNAs. To provide a comparison data set, I also performed ribosome profiling from mice that received an injection of the gut hormone ghrelin. Levels of plasma ghrelin increase prior to meal time and this increase has been hypothesized to promote scheduled feeding (LeSauter et al., 2009; Mistlberger, 2011; Verhagen et al., 2011). Ghrelin induced strong pS6 in the ARC but had little effect on pS6 in the DMH (Figure 15A). Comparison of these 2 profiles was performed to segregate enriched cell type markers according to their potential anatomical location and function.

Both ghrelin injection and scheduled feeding induced strong enrichment of *Agrp* (24-fold and 8.9 fold respectively), *Npy* (22-fold and 7.8-fold) and *Ghsr* (6.1-fold and

6.9-fold). This result was confirmed by extensive colocalization of pS6 and AgRP/NPY neurons in the ARC under both conditions (Figure 15E). The activation of AgRP/NPY is consistent with voracious eating displayed by animals acclimated to scheduled feeding following food presentation and demonstrates that ghrelin and scheduled feeding activate a common set of neural targets in the ARC.



In contrast to the enrichment of *AgRP* and *Npy* transcripts, *Pmch* was consistently depleted from pS6 immunoprecipitates during scheduled feeding (Figure 15D). Double

immunostaining for pS6 and MCH in brain slices of these animals showed selective decrease in pS6 localized to MCH neurons from mice subjected to scheduled feeding relative to ad libitum fed controls. This decrease in ribosome phosphorylation was specific to MCH neurons as neighboring pS6-positive cells were observed in the lateral hypothalamus in the same sections. Therefore, MCH neurons appear to be selectively inhibited during scheduled feeding. Interestingly, a second neuropeptide Nphx4, which is expressed in the lateral hypothalamus, was also depleted (Figure 15D). As deletion of both *Pmch* and its receptor *Mch1r* has been reported to induce hyperactivity in mice (Zhou et al., 2005), inhibition of these neurons may be related to the locomotor phenotype observed during scheduled feeding.

Molecular Identification of Activated Neurons in the DMH during Scheduled Feeding

Since the understanding of function and identity of cell types in the DMH that regulate feeding is limited, I turned my attention to identifying neurons in this region. Four transcripts: *Npvf*, *Pdyn*, *Gpr50* and *Gsbs* were enriched in pS6 immunoprecipitates from mice subjected to scheduled feeding relative to ghrelin treatment (Figure 15D). Analysis of in situ hybridization data from the Allen Brain Atlas confirmed that these transcripts show localized expression in the DMH. Among these transcripts, the neuropeptide *Npvf* has previously been shown to colocalize with *cfos* in a sparse population of DMH cell activated during FAA (Acosta-Galvan et al., 2011) and the G-protein coupled receptor *Gpr50* is known to be regulated by leptin and nutritional state (Ivanova et al., 2008) but has not been previously linked to scheduled feeding.

I further characterized the neurons in the DMH that express *Pdyn*, a neuropeptide

that has complex effects on mood, nociception and reward but has not been previously linked to scheduled feeding. Immunostaining revealed extensive colocalization of pS6 and Pdyn across the rostrocaudal axis of the DMH. 82% of Pdyn neurons in the DMH were positive for pS6 in mice subjected to scheduled feeding compared to just 1% in ad libitum fed controls (Figure 15F-H). A smaller increase in colocalization of pS6 and Pdyn in the ARC was observed but there was no change in the level of pS6 in Pdyn neurons in the PVN or lateral hypothalamus (Figure 15F and 15G). These data suggest that Pdyn neurons in the DMH represent a functionally distinct population with a specialized role in feeding. Immunostaining for cfos also revealed extensive colocalization with Pdyn neurons in the DMH during scheduled feeding but not ad libitum feeding (Figure 15I), confirming that Pdyn neurons are biochemically active when mice are subjected to the feeding protocol. cfos expression was also observed in other cells in the DMH, indicating existence of additional populations of activated neurons in this region.

Prodynorphin Restrains Bouts of Intense Feeding

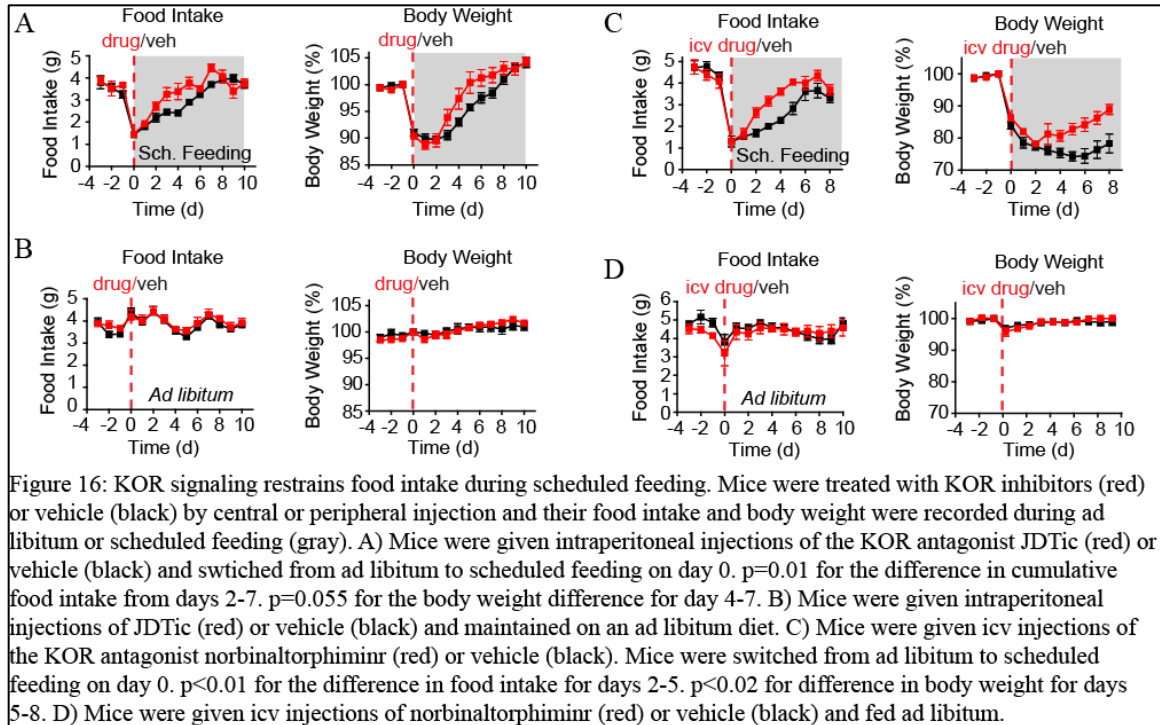
I hypothesized that Pdyn might play a role in meal termination following bouts of intense feeding. This is because, pS6 induction in Pdyn neurons is only evident late in the meal window (Figure 15B and 15C), requires food presentation for full expression (Figure 15B and 15C) and is not observed in response to orexigenic signals such as fasting or ghrelin injection (Figure 14A and 15A). Pdyn signals through the κ -opioid receptor (KOR) and potent, highly selective KOR antagonists have been developed (Bruchas et al., 2007; Carroll et al., 2004). Using pharmacological inhibitors of KOR, the function of Pdyn during scheduled feeding was assessed. An intraperitoneal injection of either a selective KOR antagonist (JDTic) or vehicle was given to mice. Mice

were divided into 2 groups: one exposed to scheduled feeding paradigm and the other fed ad libitum. Because KOR antagonists have a characteristic long duration of action in vivo (up to 3 weeks), only a single dose was required (Bruchas et al., 2007; Carroll et al., 2004).

Vehicle-treated animals initially consumed less food each day and lost weight after shifting to scheduled feeding. Their weight gradually recovered over the course of 7 days. (Figure 16A) Mice treated with JD1c show a similar decrease in food intake and body weight at first but their food intake increased more rapidly, relative to controls, and they showed a more rapid regain of body weight (Figure 16A). In contrast, JD1c had no impact on food intake or body weight in ad libitum fed animals (Figure 16B), indicating that the increased feeding induced by the drug is only evident under conditions in which Pdyn neurons are activated.

To test whether this effect was mediated by central KOR signaling, I delivered a second, structurally unrelated KOR antagonist (norbinaltorphimine) to mice by intracerebroventricular (icv) injection and then exposed these animals to scheduled feeding protocol. Norbinaltorphimine-treated animals consumed approximately 50% more food during scheduled feeding than vehicle-treated controls (Figure 16C). Drug-treated animals likewise gained weight much faster than controls (Figure 16C). Remarkably, this effect was specific to scheduled feeding paradigm as icv norbinaltorphimine had no effect on food intake or body weight of ad libitum fed animals (Figure 16D). Taken together, these data show that Pdyn neurons in the DMH are selectively activated during scheduled feeding and that central KOR signaling downstream of Pdyn acts to limit food intake following the intense feeding that

accompanies this paradigm. As Pdyn neurons are also found in other brain regions, it is possible that Pdyn produced outside the DMH also contributes to the effects observed here. Understanding how Pdyn signaling is able to selectively regulate episodic feeding will require further characterization of the Pdyn cells in the DMH and their relation to other elements of the circuitry that control food intake.



Discussion

A vast array of experiments has sought to establish functional importance of discrete neuronal populations in controlling behavior (Lichtman and Denk, 2011). However, these efforts are often limited by a lack of molecular information about the relevant cell types. In 2001, Francis Crick and Christof Koch predicted that the development of techniques “based on the molecular identification and manipulation of discrete and identifiable subpopulations” of neurons would enable elucidation of the functional anatomy of the CNS (Koch and Crick, 2001). With the development of

optogenetics and related methods, the means for manipulating cells are now available. In contrast, there has been less progress toward the development of approaches for the molecular identification of functional populations of neurons and for many neural functions, the molecular identity of the relevant cell types remains unknown. This problem of linking cell type function has persisted despite increasingly sophisticated analyses of the molecular heterogeneity of the brain as a whole (Gong et al., 2003; Lein et al., 2007).

Here, I report a conceptually distinct way to map the functional organization of gene expression in the brain. This approach takes advantage of the fact that marker genes can be used to identify specific cell types within an anatomic region such as the hypothalamus (Siegert et al., 2009). It is possible to capture RNA from cells proportionate to their activity, quantify the enrichment of these cell type specific marker genes and then use this information to assay in parallel the functional state of a large number of intermingled cell types. A key advantage of this approach is that it enables the use of powerful molecular biology tools such as qPCR or RNA sequencing to make measurements of cellular activity that would otherwise require analysis of large numbers of samples by histology. Thus, it is possible to identify in an unbiased way the specific genes that are most uniquely expressed in a co-regulated population of neurons in the brain. Once identified, such genes can serve as markers that enable the functional interrogation of those cells by using optogenetics or other approaches.

In this chapter, I demonstrate that phosphorylation of ribosomal protein S6 can be used as a tag to enable capture of mRNA from activated cells. This is possible because the same signaling pathways that trigger S6 phosphorylation are also correlated with

neural activity(Flavell and Greenberg, 2008; Meyuhas, 2008; Valjent et al., 2011). As the phosphorylation sites on S6 are evolutionarily conserved(Meyuhas, 2008), this approach can in principle be used to study a range of species, including those that are not amenable to genetic modification. Moreover, as S6 phosphorylation is controlled by extracellular stimuli in all cells(Meyuhas, 2008), this strategy could also reveal the regulation of non-neural cell types that reside in other complex tissues such as the immune system, lung, intestine and kidney just to name a few. The fidelity of this approach has been validated by identifying many neurons known to be activated or inhibited in response to well-characterized stimuli such as salt challenge and fasting. In addition to recapitulating known components of these system, I have identified markers for activated neurons that have been overlooked such as Gal neurons during fasting and Pdyn neurons during scheduled feeding. As many functional populations of neurons have been visualized by cfos staining but not molecularly characterized(Dielenberg et al., 2001; Lin et al., 2011; Wu et al., 2012), phosphorylated ribosome profiling provides a general way to identify these cells. Once marker genes for these cell types have been identified, techniques such as BacTRAP or Ribotag can be used to genetically deliver tagged ribosomes to these cell, enabling deep profiling of their transcriptomes(Heiman et al., 2008; Sanz et al., 2009).

Although the data suggest that this approach will find broad application in neuroscience, it is important to emphasize that pS6, like other surrogates for neural activity such as cfos, measures only 1 dimension of ‘neural activity’ and therefore will not retrieve markers for all neurons that become activated in all contexts. It is possible that neurons that show induction of cfos and pS6 are most responsive to stimuli that modulate neuropeptides and biogenic amines since both cfos and pS6 are triggered by

biochemical activation of neurons. Although I have shown here that many stimuli that activate neurons induce pS6, it is not fully understood to what extent the induction of pS6 is correlated with action potentials and changes in firing rate.

Different stimuli induce pS6 with varying efficiency and for this reason it is important to optimize the stimulus protocol to maximize the fold enrichment of relevant neural markers. For the stimuli explored here, pS6 is induced with kinetics that range from tens of minutes to 2 hours. This is comparable to the expression of many immediate early genes but is somewhat slower than *cfos* transcription, which is often complete within 20 minutes of stimulation. In addition, experiments described here have focused on the hypothalamus but brain regions that have a high level of pS6 at baseline may be less amenable to this approach.

Several large-scale efforts are currently underway to map the functional organization of the mammalian brain (Alivisatos et al., 2012; Gong et al., 2003; Koch and Reid, 2012). These projects are being supported by efforts to develop new imaging technologies that can probe the complex anatomy of this tissue (Lichtman and Denk, 2011). The approach described here represents a complementary way to link structure to function of the nervous system. Unlike existing efforts, this approach suggests a way to simultaneously measure the activity of every cell type within a region of brain, a goal not addressed by existing technology. Although the use of ribosome phosphorylation to identify activated neurons was focused on the hypothalamus, it should be possible to capture ribosomes and its associated mRNA in response to other signals that reflect the functional state of a cell. For instance, many proteins dynamically associate with polysomes in response to extracellular stimuli and these proteins could also function as

ribosome tags that enable enrichment of RNA from cells that received specific signals. Alternatively, it might be possible to engineer ribosomes that are modified in response to the expression of immediate early genes such as cfos or use mass spectrometry to identify posttranslational modifications of the ribosomes that correlate with specific stimuli. The combination of such approaches may eventually enable the use of RNA sequencing to measure the functional state of complex tissues along multiple dimensions and at the resolution of molecularly defined cell types.

Chapter 4:

Ablation of AgRP Neurons Impairs Adaptation to Scheduled Feeding

Introduction

Molecular clocks play a key role in coordinating physiology and behavior with environmental cues (Rosenwasser et al., 1981). The circadian oscillator in the suprachiasmatic nucleus (SCN) is regulated by environmental light/dark cues conveyed from the retina and controls the sleep/wake cycle and other behaviors in mammals (Hastings et al., 2003; Lowrey and Takahashi, 2004). At the molecular level, this circadian clock relies on daily oscillations in the transcription and translation of a set of evolutionarily conserved clock genes (Reppert and Weaver, 2002). In the SCN, circadian oscillations in clock gene expression change cellular activity within this structure to control circadian rhythms (Fuller et al., 2008; Gavrilá et al., 2008). Circadian rhythms in clock gene expression are also observed in many brains outside the SCN (Guilding and Piggins, 2007) as well as in peripheral, non-neuronal tissues (Balsalobre et al., 1998; Yamazaki et al., 2000).

While a light-entrained oscillator regulates the sleep/wake cycle and other processes, this is not the only biological clock. When food availability is restricted to a single period during a fixed time of the day, over the course of a few days animals adapt to this schedule and increase their feeding during the window of food availability, even if it is during the light phase, a time when animals do not normally eat. In addition, in this scheduled feeding paradigm, animals show a marked increase in locomotor activity shortly before onset of the time when food is made available. This increased activity is

referred to as food anticipatory activity, FAA(Mistlberger, 1994; Stephan, 2002). FAA is associated with increase in body temperature, adrenal corticosterone secretion and gastrointestinal motility. This biological rhythm, timed to a window of food availability is unaffected by SCN ablation, confirming the existence of a food-entrainable oscillator (FEO) that is separate from the SCN(Krieger et al., 1977; Stephan et al., 1979). Moreover, previous reports have demonstrated that scheduled feeding can entrain and shift the circadian rhythms in peripheral tissues as well as brain areas outside the SCN even when oscillation in the SCN remains phase-locked to the light/dark cycle(Damiola et al., 2000; Hara et al., 2001; Stokkan et al., 2001; Wakamatsu et al., 2001). These findings show that the timing of food availability can cause a phase uncoupling among multiple circadian oscillators outside the SCN and can even dominate the circadian oscillator. However, while the demonstration that FAA and other physiologic responses develop after scheduled feeding, the anatomic sites and neuronal populations that comprise the food entrained oscillator have not been elucidated.

In the previous chapter, I employed a new profiling technology to identify cell types in the hypothalamus that are activated in response to an acute or chronic stimulus(Knight et al., 2012). I used this method to identify neural populations in the hypothalamus that are activated when food availability of animals are restricted to a 3 hour window during the light phase. In the previous chapter, I reported that dynorphin neurons in the dorsomedial hypothalamus play a role in the response to scheduled feeding. I also found that AgRP/NPY neurons in the arcuate nucleus are activated when animals are subjected to a scheduled feeding paradigm. AgRP neurons in the arcuate nucleus of the hypothalamus co-express NPY(Hahn et al., 1998) and regulate food intake

and metabolism. Optogenetic activation of these neurons promote food intake (Aponte et al., 2011; Atasoy et al., 2012). These neurons also express the ghrelin receptor (Willeßen et al., 1999) and are responsive to plasma ghrelin which has been shown to rise prior to meal times and has been hypothesized to promote feeding during scheduled feeding (LeSauter et al., 2009; Mistlberger, 2011; Verhagen et al., 2011).

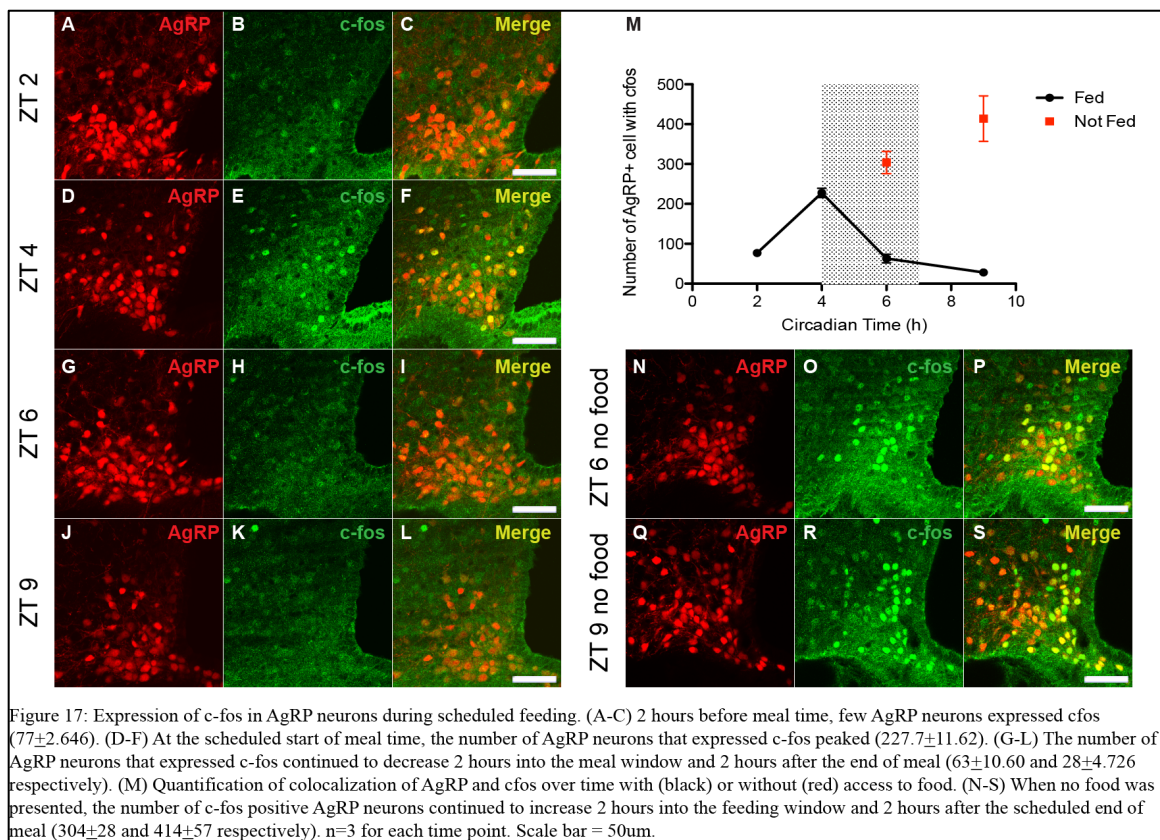
I thus set out to evaluate the possibility that AgRP neurons also play a role in the response to scheduled feeding and the development of FAA. In this chapter, I confirm a key role for AgRP/NPY neurons in the response to scheduled feeding suggesting that it is a key neural component of the food entrainable oscillator.

Results

AgRP Neurons are Activated during Scheduled Feeding (SF)

Although the role of AgRP neurons in metabolic homeostasis is well studied, their role in circadian-regulated feeding behavior is less clear. I first used *cfos* expression to test whether scheduled feeding activates these neurons. I mated AgRP-Cre mice to a lox-STOP-lox tdTomato reporter line to generate AgRP tdTomato animals that express the fluorescent reporter tdTomato only in AgRP cells. These animals were then subjected to a SF paradigm in which animals were only allowed access to food during a 3 hour window between ZT 4 and ZT 7. As mentioned, mice normally eat between ZT 12 and ZT 24. After 10 days of SF, animals were perfused at different times during the day and the expression of the immediate early gene, *cfos*, was probed using immunohistochemistry. *cfos* expression in AgRP neurons was low 2 hours before the start of the scheduled feeding window but increased thereafter peaking at ZT 4 just prior to food being made

available (Figure 17A-F, 17M). *c-fos* expression in these neurons then fell during the feeding window and remained low 2 hours after the feeding window ended (Figure 17G-M). However, if food was withheld during ZT 4 and ZT 7 in fully trained animals, the number of AgRP neurons that expressed *c-fos* continues to rise during the feeding window and was still increasing 2 hours after the feeding window ie ZT 9 (Figure 17M-S). These observations suggest that the activity of AgRP neurons is synchronized with food availability and that they might play a role in the behavioral response to scheduled feeding.



Ablation of AgRP Neurons

To study the functional role of AgRP neurons in scheduled feeding, I ablated these neurons by generating mice that expressed the human diphtheria toxin receptor only

in AgRP neurons by mating AgRP-Cre animals with a lox-STOP-lox iDTR line. I then injected diphtheria toxin (DTX; 50ng/g) subcutaneously in neonatal animals. I used neonatal animals because prior reports showed that injection into adult animals resulted in profound hypophagia and death (Gropp et al., 2005; Luquet et al., 2005). In contrast, these same reports showed that neonatal animals develop normally and fail to show any phenotypic effects after neonatal AgRP ablation suggesting that compensatory mechanisms enable neonatal animals to maintain normal food intake when fed ad libitum. Consistent with previous reports, there was a substantial decrease in the number of AgRP neurons after administration of DTX to neonatal animals (Figure 18A-L) (Gropp et al., 2005; Luquet et al., 2005). Subcutaneous injection of DTX at post natal day 3 led to loss of more than 50% of AgRP neurons on post natal day 7 with a similarly marked decrease in NPY immunoreactivity in AgRP DTR animals compared to controls.

I found that animals receiving DTX at 3 days of age still showed decreased NPY immunoreactivity in 8 weeks old animals (Figure 18D-F). The number of NPY fibers was similar in neonatal and adult animals after neonatal AgRP ablation suggesting very little regeneration of AgRP neurons took place after DTX treatment. I also found a marked decrease in NPY projections in the paraventricular hypothalamic nucleus (PVN) and the dorsal medial hypothalamic nucleus (DMH) (Figure 18G-L), sites where AgRP neurons are known to project.

Phenotypic Assessment of AgRP DTR animals

Previous studies of neonatal animals after AgRP ablation have shown that food intake is normal, in contrast to AgRP ablation of adult animals which leads to extreme

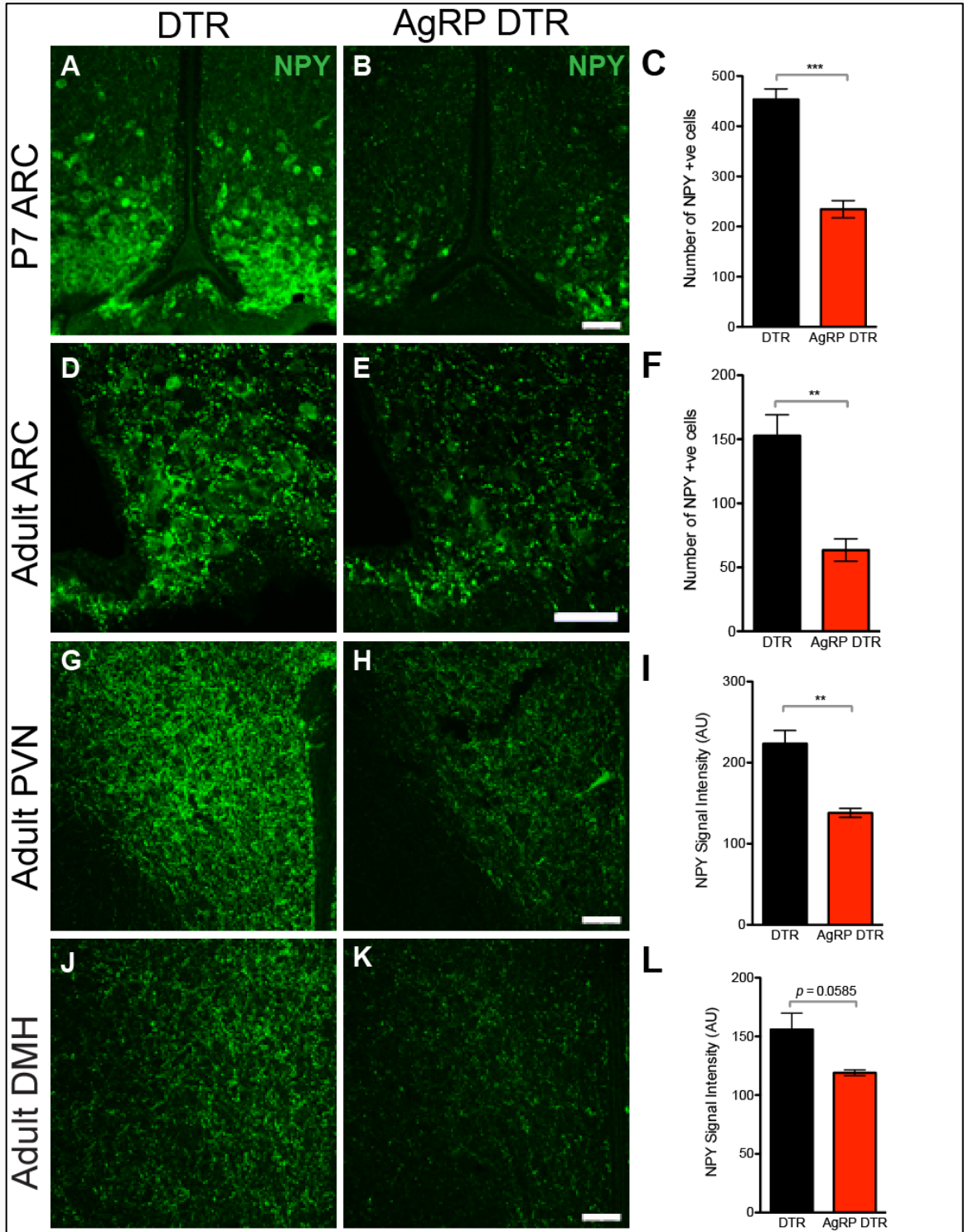
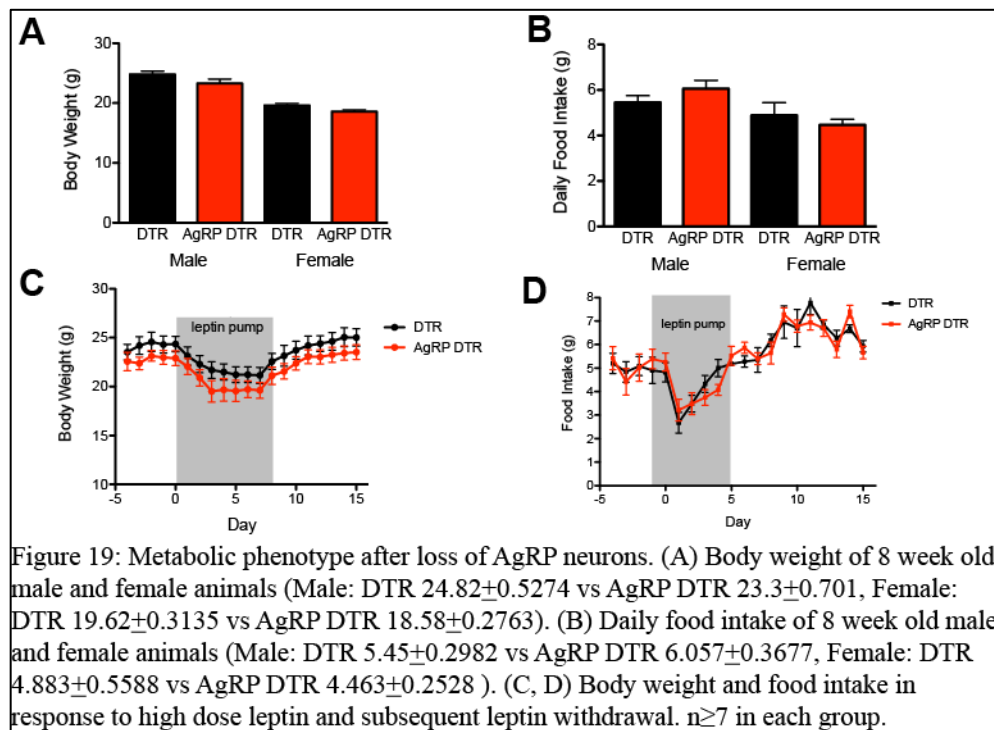


Figure 18: Ablation of AgRP neurons. (A-C) NPY immunostaining in the arcuate nucleus (ARC) at postnatal day 7 in control versus AgRP DTR animals (DTR 453 ± 21.13 vs AgRP DTR 234.5 ± 17.33 , $p < 0.001$). (D-E) Loss of NPY immunostaining in the ARC of 8 week old AgRP DTR animals (DTR 152.8 ± 16.49 vs AgRP DTR 63.33 ± 8.743 , $p < 0.01$). Decreased NPY signal intensity in the paraventricular nucleus (PVN) in adult AgRP DTR animals (DTR 223.3 ± 16.27 vs AgRP DTR 138 ± 5.508 , $p < 0.01$). (J-L) Decreased NPY signal intensity in the dorsal medial hypothalamic nucleus (DMH) in adult AgRP DTR animals (DTR 156 ± 13.87 vs AgRP DTR 119 ± 2.517 , $p = 0.0585$). $n \geq 3$ in each group. Scale bar = 50 μ m.

anorexia and death(Luquet et al., 2005). Consistent with these reports, I found that neonatal ablation of AgRP neurons did not alter viability. Body weight (Figure 19A) and food intake (Figure 19B) of both male and female neonatal ablated animals were comparable to littermate controls. Since AgRP neurons express the leptin receptor and are known leptin targets(Flier, 2004), I next assayed the leptin responsiveness of AgRP DTR animals after treatment with high dose leptin (2.5ug/h) via osmotic pumps for 8 days. The extent of weight loss and decrease of food intake following high dose leptin was similar in AgRP DTR animals versus littermate controls (Figure 19C and 19D). I also tested whether the response to hypoleptinemia was altered by measuring food intake after removing the leptin pumps from AgRP ablated and control animals. I found that after withdrawal of high dose leptin treatment, the food intake and weight gain was similar in animals with neonatal AgRP ablation versus controls (Figure 19C and 19D).



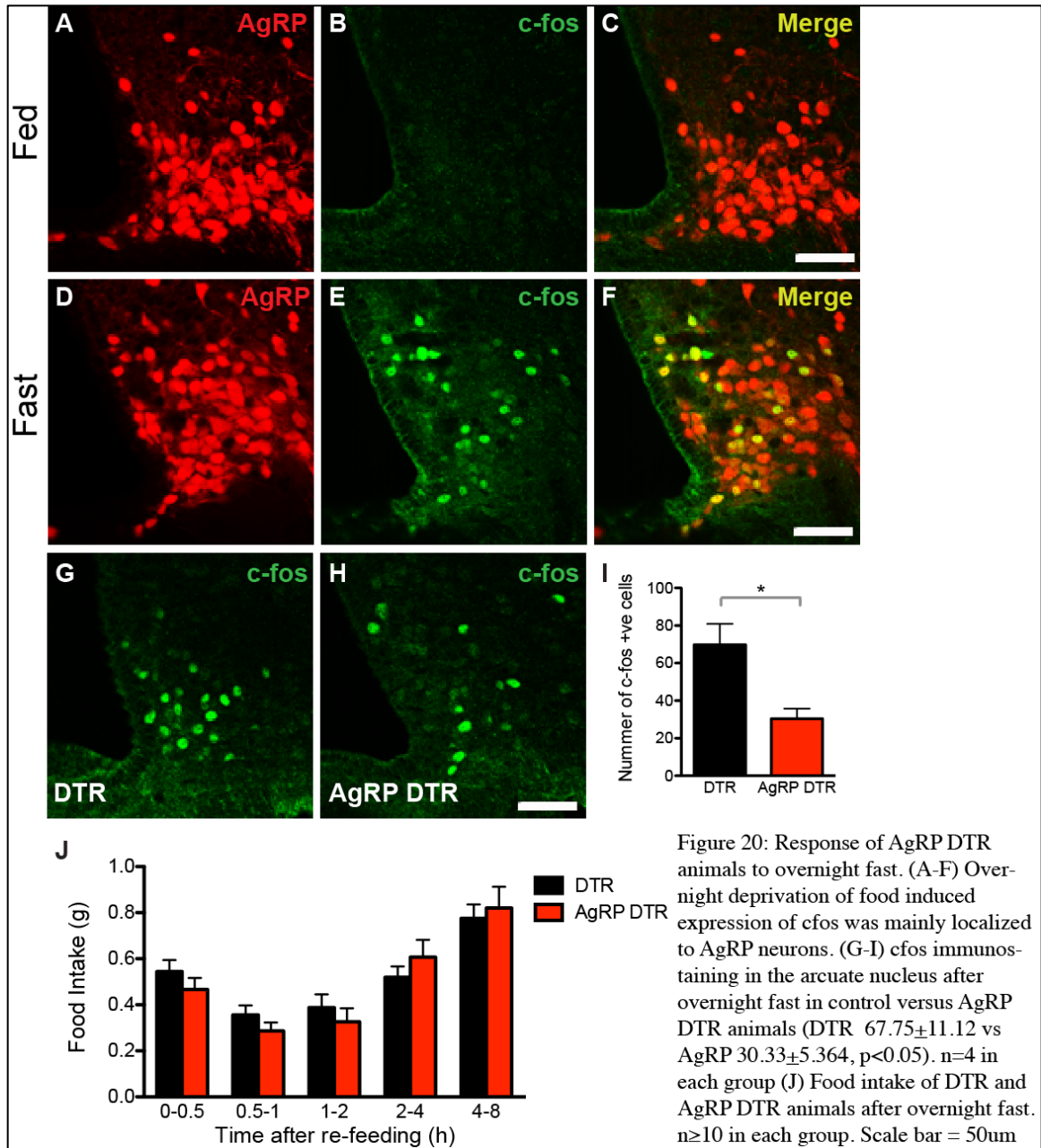


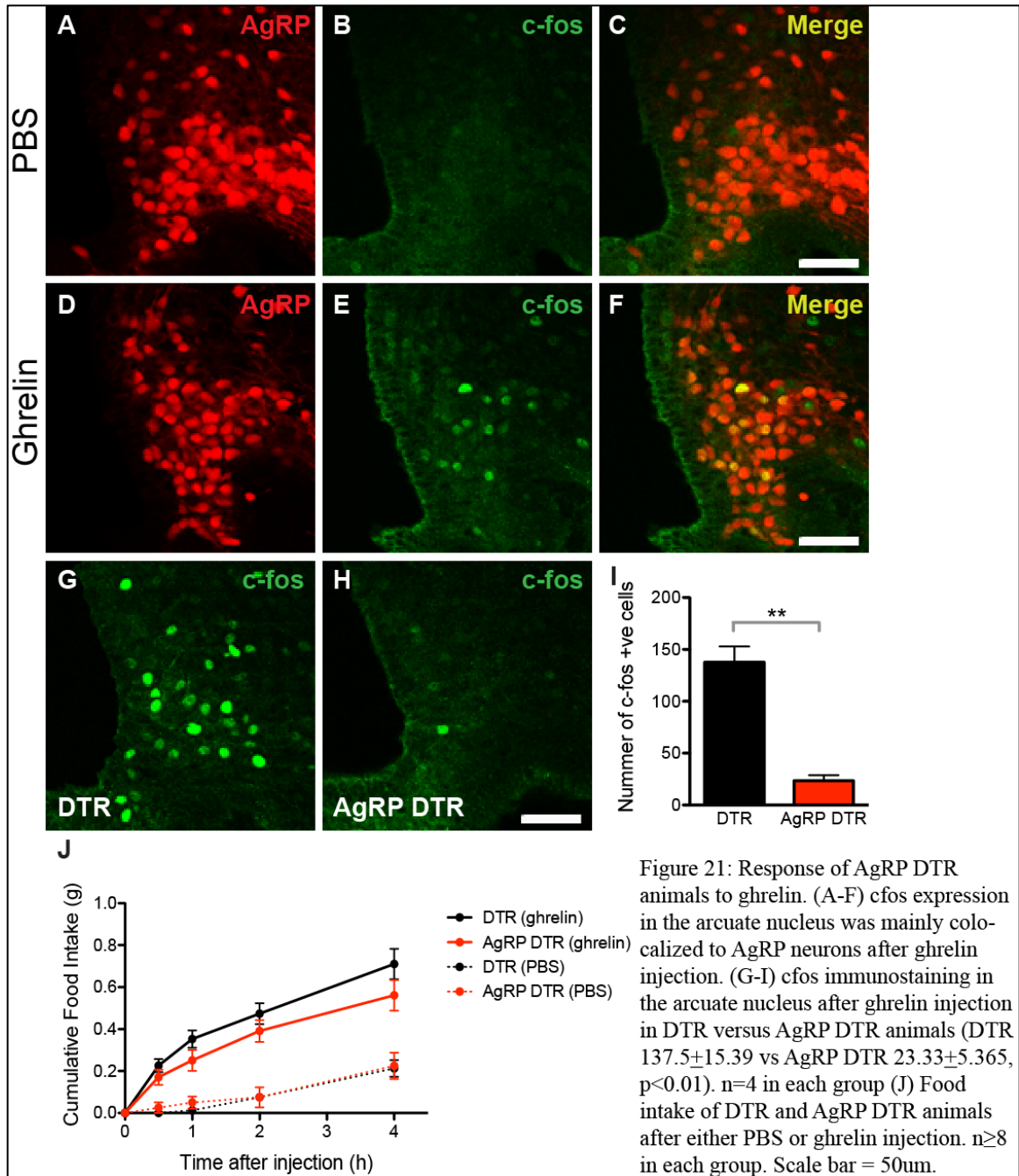
Figure 20: Response of AgRP DTR animals to overnight fast. (A-F) Overnight deprivation of food induced expression of *c-fos* was mainly localized to AgRP neurons. (G-I) *c-fos* immunostaining in the arcuate nucleus after overnight fast in control versus AgRP DTR animals (DTR 67.75 ± 11.12 vs AgRP 30.33 ± 5.364 , $p < 0.05$). $n=4$ in each group (J) Food intake of DTR and AgRP DTR animals after overnight fast. $n \geq 10$ in each group. Scale bar = 50um

AgRP neurons become activated when animals are deprived of food (Figure 20A-F) so I next assayed the response of AgRP DTR animals to a 24 hour fast. I first assayed *c-fos* expression in these neurons after food deprivation and found that there were significantly fewer *c-fos* positive cells in the arcuate nucleus of AgRP DTR animals compared to controls (Figure 20G-I). Note the reduction in the number of cells expressing *c-fos* was consistent with the loss of AgRP neurons suggesting that the *c-fos*

response in surviving cells was unchanged. Despite the loss of AgRP neurons and the similarly low number of cfos positive cells in AgRP DTR animals, the food intake of these animals after a 18 hour fast was unaltered compared to controls (Figure 20J). Because AgRP neurons also express the ghrelin receptor (Ghsr), I also assayed the response of AgRP DTR animals to ghrelin. I found that most of the cfos immunoreactivity in the arcuate nucleus colocalized with AgRP cells (Figure 21A-F). Similar to the case for food deprivation, ghrelin injection during the light phase resulted in much smaller number of cfos positive cells in the arcuate of AgRP DTR animals (Figure 21G-I). However, despite the decreased number of cfos positive cells, the food intake of AgRP DTR animals after ghrelin treatment was indistinguishable from that of control animals (Figure 21J). Taken together, these results show that animals with AgRP ablation do not show alterations in baseline food intake and body weight and that their responses to leptin treatment, leptin withdrawal, fasting and ghrelin treatment are all normal.

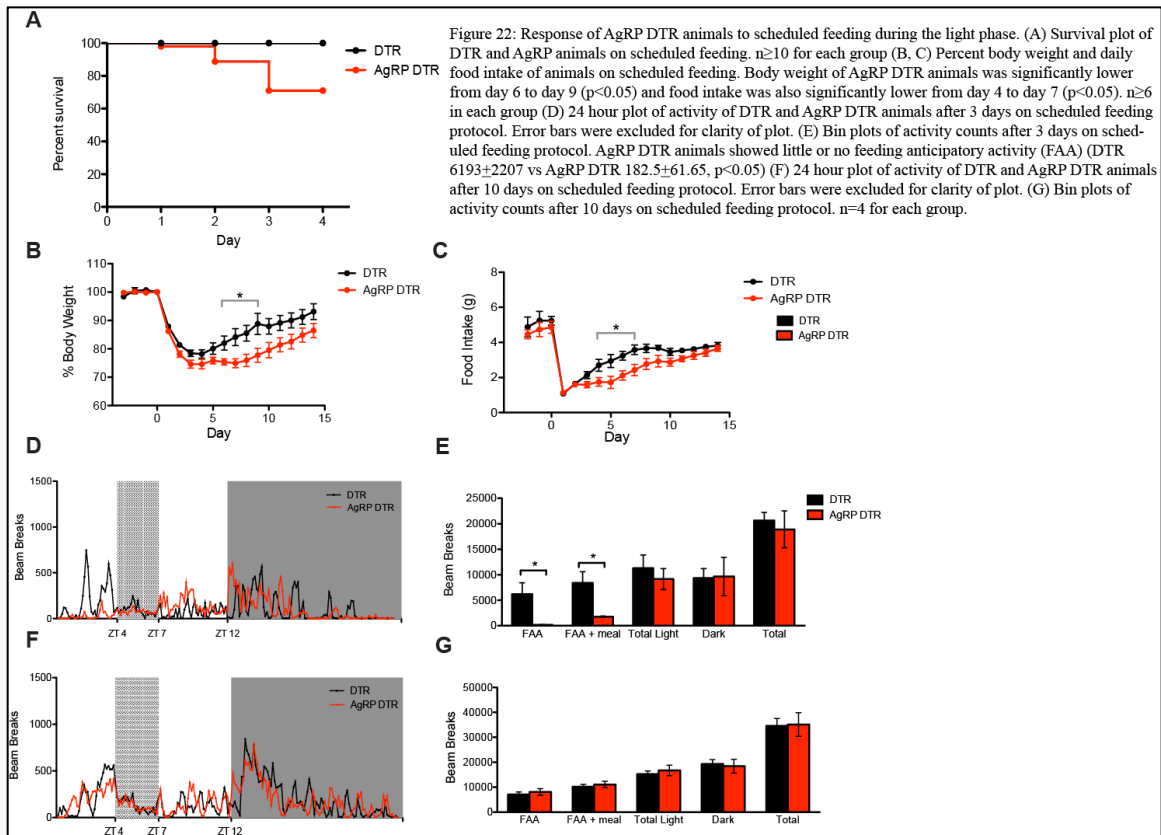
Response of AgRP DTR Animals to Scheduled Feeding in the Light Phase

I next compared the response to scheduled feeding of AgRP DTR animals that received DTX at 3 days of age to their littermate controls (also injected with DTX). 12 week old animals were maintained on a 12 hour light dark cycle since weaning at which time food availability was changed to a period between ZT 4 and ZT 7. This was continued for 14 days. Consistent with previous reports, control animals showed a transient reduction in food intake but quickly acclimated to this change, steadily increasing their food intake over the course of the experiment with no mortality. In contrast, I noted increased mortality among AgRP DTR mice with 10% mortality at day 2



and 30% mortality at day 4 (Figure 22A). Moreover, the AgRP DTR animals that survived the first 4 days of SF and remained viable through the end of the experiment failed to acclimate normally to the SF protocol. Wildtype mice that are given food only between ZT 4 and ZT 7 consume less food over the first 6 days as they acclimate to the change in food availability. However, by day 7 normal mice consume an equivalent

amount of food in the feeding window as they consume previously during the entire dark phase. In contrast, AgRP DTR animals consumed less food and weighed less than control mice from day 4 to day 9 with food intake only reaching that of control mice after day 10 (Figure 22B and 22C).



Animals that have become acclimated to the SF protocol exhibit markedly increased locomotor activity known as food anticipatory activity (FAA) beginning at ZT 2, 2 hours prior to the presentation of food. I next monitored the 24-hour activity of AgRP DTR animals after 3 days of SF, by which time wild type animals show robust FAA (Mistlberger, 1994). Consistent with the reduced food consumption at this time, AgRP DTR animals did not show an increase in locomotion in the 2 hour window prior to the scheduled meal 3 days after food availability was shifted to the light phase (Figure 22D and 22E). This defect in locomotion before meal time was not due to a general

deficit in locomotion since total activity counts for AgRP DTR animals was similar to controls. However, after 10 days of SF, the FAA of AgRP DTR animals were indistinguishable from controls. Taken together, these data demonstrate that AgRP neurons play an important role in the ability of animals to sense and adapt to a temporal change in food availability. The delayed acclimation to this change leads some animals to die of starvation while those animals that survive still show a significant delay in recovery of food intake and the onset of FAA.

Reponse of AgRP DTR Animals to SF in the Dark Phase

As a further control, I monitored survival, food intake weight and FAA in AgRP DTR mice when food availability was limited to 3 hours during the dark phase which, as mentioned, is when wild type mice, which are nocturnal, consume nearly all of their food. AgRP DTR animals given food only during a 3 hour window in the dark phase between ZT 15 and ZT 18 showed an equivalent increase of food intake and body weight compared to controls throughout the experiment (Figure 23A and 23B). After 3 days of SF in the dark phase, 24 hour activity analyses further revealed that AgRP DTR animals showed increased locomotion prior to the start of meal time, although the magnitude of FAA was significantly lower than controls (Figure 23C and 23D). Thus the deficit in adapting to SF was more profound when food was only available during the light phase, a time when mice generally move less and eat less.

Discussion

AgRP neurons which are localized in the arcuate nucleus are both necessary and sufficient for feeding in adult animals (Gropp et al., 2005; Luquet et al., 2005). However,

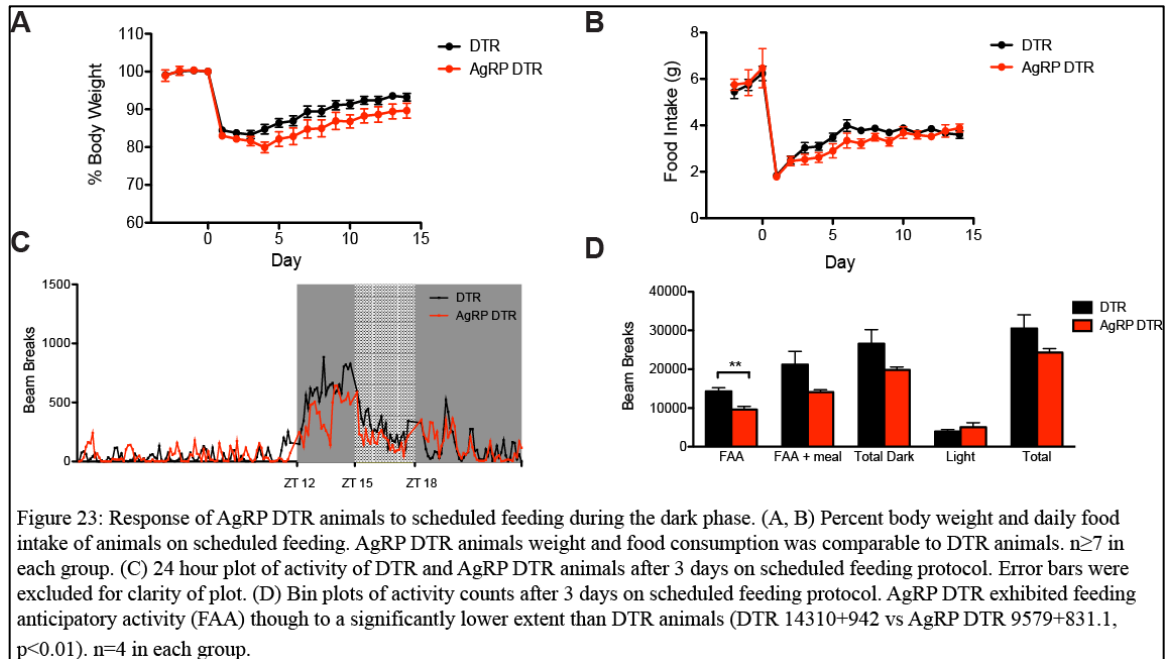


Figure 23: Response of AgRP DTR animals to scheduled feeding during the dark phase. (A, B) Percent body weight and daily food intake of animals on scheduled feeding. AgRP DTR animals weight and food consumption was comparable to DTR animals. $n \geq 7$ in each group. (C) 24 hour plot of activity of DTR and AgRP DTR animals after 3 days on scheduled feeding protocol. Error bars were excluded for clarity of plot. (D) Bin plots of activity counts after 3 days on scheduled feeding protocol. AgRP DTR exhibited feeding anticipatory activity (FAA) though to a significantly lower extent than DTR animals (DTR 14310+942 vs AgRP DTR 9579+831.1, $p < 0.01$). $n = 4$ in each group.

animals in which AgRP neurons are ablated as neonates survive suggesting that the increased plasticity of the central nervous system in younger animals allows such animals to survive after the loss of these neurons. Here I show that the ablation of AgRP neurons in neonatal animals results in significant abnormalities in the response to a temporal alteration of food availability. These abnormalities include increased mortality in animals subjected to a protocol that elicits FAA with a significant delay in the recovery of food intake and body weight and an absence of FAA even in those animals that survive. These abnormalities are not observed when food is limited to an equivalent window in the dark phase suggesting that AgRP neurons are essential for the ability of animals to adapt to a change in food availability at circadian times when food is uncoupled from the circadian oscillator (ie moved to the light phase). In contrast, the loss of AgRP neurons has no effect on baseline food intake, body weight or the response to food restriction, leptin and ghrelin treatment or leptin withdrawal. In aggregate, these findings suggest that AgRP neurons are a key component of a food entrained oscillator that allows animals to predict

in time when nutrient will be available and adjust their behavior accordingly. Moreover, the observation that AgRP neural ablation in neonatal animals affects only the response to SF suggests that a key function of these neurons is to control this set of responses.

In this study, I used a Cre-lox system to express the human diphtheria toxin receptor only in AgRP neurons and was able to ablate 50% of these neurons. This extent of ablation is consistent with a previous report using the same Cre-lox strategy (Gropp et al., 2005). We do note that in a separate report using a knockin strategy as reported by Luquet et al. (Luquet et al., 2005) there was more than 90% ablation of AgRP neurons. It is unclear why these strategies result in differing degrees of ablation. Interestingly, neonatal ablation of AgRP neurons using the knockin method (with near complete ablation) resulted in animals becoming obese after 12 weeks of age with a metabolic shift towards lipid oxidation which is somewhat paradoxical in light of the known effect of AgRP neurons to increase feeding (Joly-Amado et al., 2012). The animals with ~90% ablation exhibited decreased food intake after 24 hour fast and ghrelin challenge in contrast to a failure of a more limited ablation to have an effect as shown in this study. The aggregate data show that a loss of only 50% of AgRP cells is not sufficient to impair responses to food deprivation and ghrelin injection while the hyperphagia that develops after glucoprivation is not impaired even after the loss of the vast majority of AgRP neurons (Luquet et al., 2007). Though the extent of AgRP ablation observed here is incomplete, the key finding is that the response to SF in animals with AgRP ablation was still impaired even when 50% of AgRP neurons were intact, suggesting that the response to SF is quite sensitive to perturbations of AgRP neurons. The nutrient signal responsible for linking AgRP neuronal activity to circadian time is not known though recent studies

have shown that hypothalamic autophagy(Kaushik et al., 2011) and mitochondria dynamics(Dietrich et al., 2013) regulate AgRP neuronal function in response to changes in energy availability.

The SCN, which responds to light, is believed to be the primary circadian oscillator, but the biological rhythms that develop in response to changes in food availability are known to persist even in the absence of the SCN. These data have thus suggested that there is a food entrainable oscillator that separate and independent of the light entrained oscillator(Krieger et al., 1977; Stephan et al., 1979). Previous work to identify the anatomical sites of the food entrainable oscillator have focused on structures in the hypothalamus posterior to the SCN that regulate feeding behavior such as the dorsal medial hypothalamus (DMH) as well as the arcuate nucleus (ARC).

The possible role of the DMH was previously assayed by analyzing the periodicity of the expression of the canonical clock genes, Period 1 (Per1) and Period (Per2), both of which were expressed rhythmically in the DMH during SF(Mieda et al., 2006). However, lesioning studies of the DMH report disparate results. Thus while Landry et al(Landry et al., 2006) showed that radio-frequency induced lesions on the DMH did not impair FAA. Gooley et al(Gooley et al., 2006) reported that ibotenic acid induced lesions of the DMH attenuated FAA. The different findings of these studies may be attributed to a variety of factors including lesion type and behavioral assays that were used.

In addition to the DMH, rhythmic expression of clock genes was also reported in other brain regions, including the ARC, after a change in feeding schedule, though the

identity of which arcuate population was not determined(Moriya et al., 2009; Verwey et al., 2008). The clock genes Per1 and Per2 are also expressed in the ARC with RF(Mieda et al., 2006) while endogenous Per2 is expressed rhythmically in the ARC in slice preparations of a Per2 luciferase knockin mouse(Guilding et al., 2009). These data show that arcuate neurons show rhythmic behaviors and are consistent with our conclusion that AgRP neurons are a neural component of the food entrainable oscillator. While Mistlberger and Antle(Mistlberger and Antle, 1999) showed that monosodium glutamate (MSG) induced lesions of the ARC enhanced FAA in rats during SF, the possible role of AgRP neurons was not assessed and furthermore this finding is the opposite of what was observed after AgRP ablation which reduces FAA. However, it must be noted that lesions of the ARC using MSG not only results in the loss of AgRP neurons but also adjacent cell population such as POMC neurons. Thus the increase in FAA after non-specific ARC lesions is likely to be a result of the net effect of damage to several different cell types and the identity of the putative cell type(s) that normally suppress FAA is not known.

Arcuate neurons that co-express the neuropeptide AgRP and NPY(Hahn et al., 1998) also express the leptin receptor and are inhibited by leptin(Flier, 2004). NPY is a potent orexigenic neuropeptide and promotes feeding in sated or food-deprived animals was administered centrally(Billington and Levine, 1992) while AgRP is an antagonist of the melanocortin-4 receptor (MC4R), which when activated suppresses feeding(Ollmann et al., 1997). While the effect of AgRP/NPY neurons in metabolic homeostasis is well-characterized, their involvement in the temporal control of food intake has been less clear at least prior to the current study. Consistent with data presented here, studies of leptin deficient *ob/ob* mice and Zucker rats, which exhibit hyperphagia as well as increased

AgRP/NPY neural activity, revealed enhanced FAA after a change in food schedule and this effect can be suppressed by recombinant leptin treatment (Mistlberger and Marchant, 1999; Ribeiro et al., 2011). In addition, AgRP DTR animals exhibited a defect in adapting to SF during the light phase despite only a partial loss of AgRP neurons, suggesting that a full 'complement' of AgRP neurons is essential for the normal response of animals to this SF paradigm. It has been recently shown that AgRP neurons are heterogeneous with respect to their projections in the central nervous system (Betley et al., 2013) and it is possible that different AgRP populations suffer different degrees of cell loss after DTX treatment. It is also possible that the impairment to SF observed here could be due to developmental effects of neonatal AgRP neuronal ablation since development of downstream dopamine neurons in the ventral tegmental area (VTA) is altered after AgRP neurons ablation (Dietrich et al., 2012). Further studies will be necessary to understand whether distinct AgRP subpopulations are responsible for FAA as well as to elucidate the cellular mechanisms that couple food availability to the activity of these neurons. Since *Per1* and *Per2* are also expressed rhythmically in the arcuate nucleus during SF (Mieda et al., 2006), it is possible that arcuate AgRP neurons express the canonical clock genes in response to food availability. Intriguingly, mice lacking known canonical clock components in all tissue exhibited normal FAA and response to SF (Storch and Weitz, 2009), suggesting that oscillators that link nutrient availability to behavior may be different from the known clock genes that regulate circadian rhythm.

It has been hypothesized that the gut hormone ghrelin is a peripheral signal that targets hypothalamic nuclei to increase locomotor activity in anticipation to a scheduled meal. Ghrelin acts through the growth hormone secretagogue receptor (GHSR), which is

widely expressed throughout the hypothalamus, including in AgRP neurons in the ARC(Guan et al., 1997; Willesen et al., 1999; Zigman et al., 2006). Interestingly, animals under SF exhibited rhythmic patterns of ghrelin secretion with plasma levels peaking 2 hours prior to which when food was available(Drazen et al., 2006). Consistent with this study, GHSR knockout mice also exhibited attenuated FAA(Blum et al., 2009). The fact that FAA was not abolished but only impaired in GHSR knockout mice suggests that there must be other undiscovered peripheral cues that regulate meal pattern behavior. Intriguingly, ghrelin knockout mice displayed normal FAA(Szentirmai et al., 2010) suggesting that another unknown ligand of GHSR could induce FAA and/or compensate for the absence of ghrelin. Since GHSR is widely expressed in the hypothalamus, of which AgRP neurons are a small population, it is thus not surprising that FAA can still be observed in AgRP ablated animals that survive albeit with a significantly delayed onset. Furthermore, shRNA knockdown of GHSR in the DMH and the VMH of rats did not abolish FAA with some anticipatory activity still persisting(Merkestein et al., 2014). Taken together, these data suggest a distributed network of brain regions that regulate meal pattern behavior that includes AgRP neurons in the ARC. Thus, disrupting one node of this network only attenuates but does not completely abolish FAA.

It is well documented that circadian rhythm of the SCN is primarily determined by light/dark cues while food availability can entrain peripheral tissues(Damiola et al., 2000; Hara et al., 2001; Stokkan et al., 2001; Wakamatsu et al., 2001). It is intriguing to note that light availability (or lack of) can also be used as a cue for animals to begin food seeking behavior since animals have to be awake to consume food. SF during the light phase, when mice are usually at rest and do not feed, uncouples oscillations in peripheral

tissues from the central pacemaker to coordinate body physiology in response to food intake. At the same time, cues from the peripheral much influence non-SCN brain regions to change behavior from rest to food seeking. Data present here suggest that AgRP neurons in the ARC are a key site where peripheral and possibly other cues are detected independent of visual cues (ie light) that allow an animal to adapt to a new meal time during a period when mice are normally at rest and do not consume food.

Chapter 5:

Loss of MCH Neurons Enhances Adaptation to Scheduled Feeding

Introduction

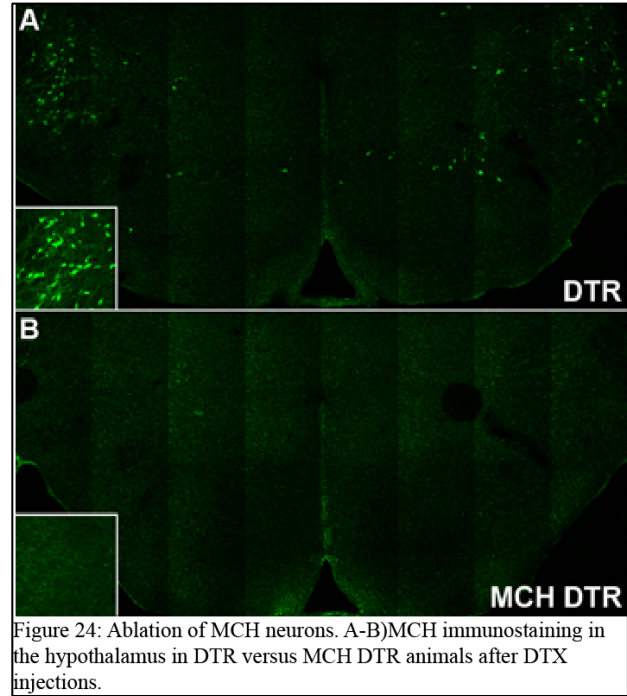
The neuropeptide melanin-concentrating hormone (MCH) was first discovered in teleost fish(Kawauchi et al., 1983) but is also expressed in mammals. MCH binds to a G-protein coupled receptor, MCHR1(Kokkotou et al., 2001) and is an orexigenic peptide because intracerebroventricular (icv) administration of MCH stimulates food intake(Rossi et al., 1997). To date, studies of the physiological role of MCH neurons have manipulated MCH or its receptor. MCH knockout mice are lean and hyperactive and exhibit increased wakefulness(Kokkotou et al., 2005; Shimada et al., 1998; Willie et al., 2008) while MCHR1 knockout mice are also hyperactive(Zhou et al., 2005). The function of MCH neurons was explored by expressing a toxic form of ataxin-3 in MCH neurons, which caused progressive cell death(Alon and Friedman, 2006). These mice developed a lean phenotype with enhanced metabolism consistent with MCH knockout mice. Acute ablation of MCH neurons also caused a mild lean phenotype and hyperactivity(Whiddon and Palmiter, 2013). However, the role of MCH neurons in scheduled feeding has never been explored.

In Chapter 3, I described that mRNA transcript for MCH was depleted during scheduled feeding, suggesting a role for MCH neurons in this paradigm. Here I investigate the role of MCH neurons using diphtheria toxin mediated cell ablation.

Results

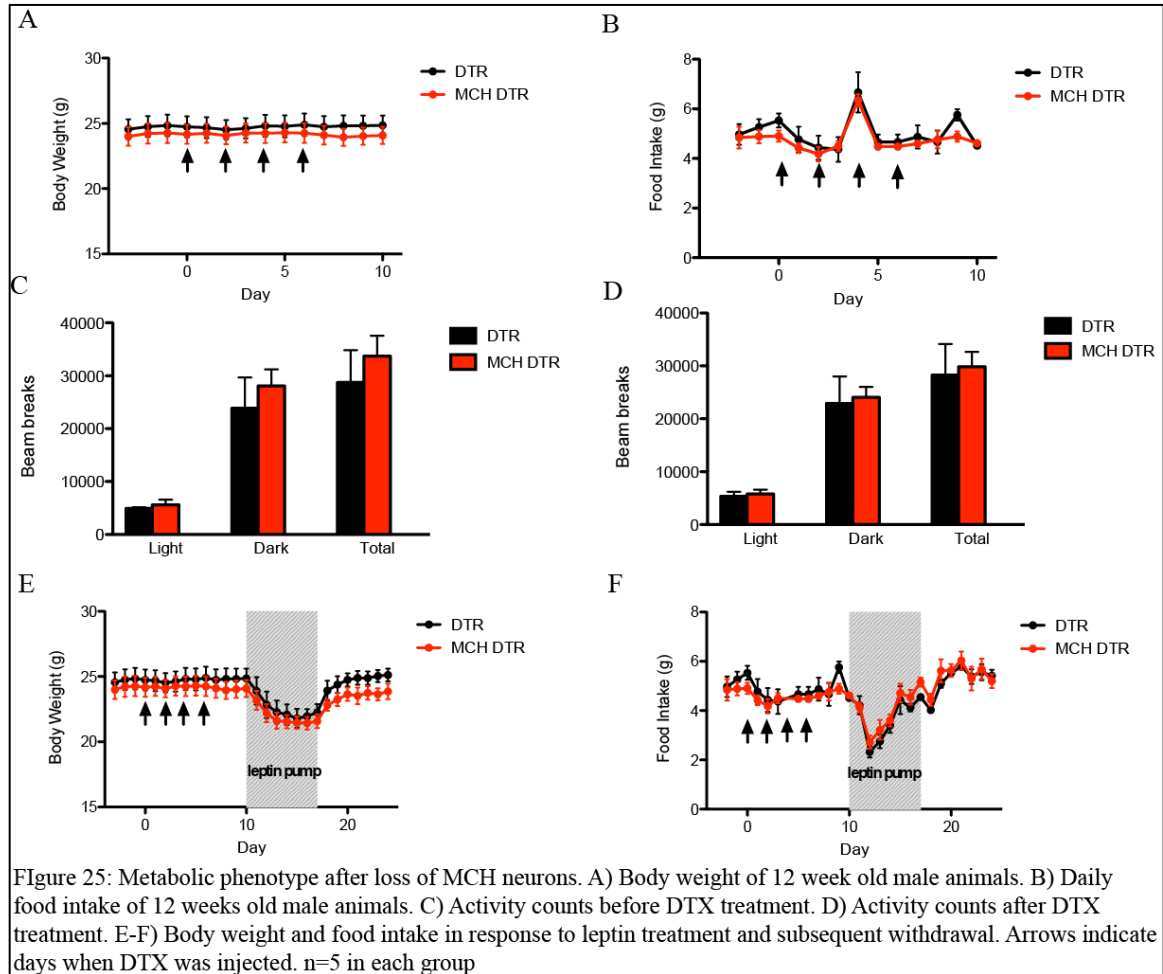
Ablation of MCH neurons

I generated mice expressing the human diphtheria toxin receptor only in cells expressing MCH by crossing a MCH Cre line to a lox-STOP-lox iDTR line. I then injected diphtheria toxin (DTX, 100ng) every other day for a total of 4 doses in adult mice. On the 10th day after the first DTX injection, I perfused control DTR and MCH DTR animals and performed immunostaining for MCH in brain slices of these animals. After DTX



injection, I observed a complete loss of MCH immuno-reactivity in MCH DTR brain slices while MCH was readily detected in the lateral hypothalamus of control animals (Figure 24A-B), confirming that DTX-mediated ablation of MCH was successful. Loss of MCH neurons only caused a small but insignificant loss in body weight and no changes in food intake were observed (Figure 25A-B). As animals null for MCH and the MCH receptor MCH1R become hyperactive (Zhou et al., 2005), the home cage locomotor activity of MCH DTR animals was recorded before and after DTX administration and no changes in activity counts were observed (Figure 25C-D). I also tested the response of MCH DTR animals to hyperleptinemia by administering leptin via osmotic pumps for 7 days. Decrease in body weight and daily food intake in MCH ablated animals was comparable to control animals (Figure 25E-F). Furthermore, the response in body weight

and food intake to hypoleptinemia was also unaltered in MCH DTR animals after removal of osmotic pumps (Figure 25E-F).



Response of MCH DTR animals to scheduled feeding.

The transcript for *Pmch* was depleted following immunoprecipitation of phosphorylated ribosomes during scheduled feeding (Figure 15D), suggesting that inhibition of MCH neurons may play a role in regulating the response to this paradigm. I next maintained animals with ablated MCH neurons on a scheduled feeding protocol where food was made available only during the light phase between ZT 4 and ZT 7. MCH DTR animals acclimated faster to the shift in food available as evidenced by the 25-50%

increase in food intake relative to controls on day 3 to day 5 and the normalization of daily food intake by day 8 versus day 12 for control animals (Figure 26B). Consistent with the earlier normalization of food intake, MCH DTR also regained body weight faster than controls (Figure 26A). 24 hour locomotor analysis after animals were entrained on the scheduled feeding protocol for 2 weeks revealed that MCH DTR animals exhibited greater amplitude of food anticipatory activity (FAA) in the hours before food presentation (Figure 26C-D). This observation is consistent with the inactivation of MCH neurons during scheduled feeding as uncovered by phosphorylated ribosome capture and functionally demonstrates that loss of activity in MCH neurons contributes to FAA.

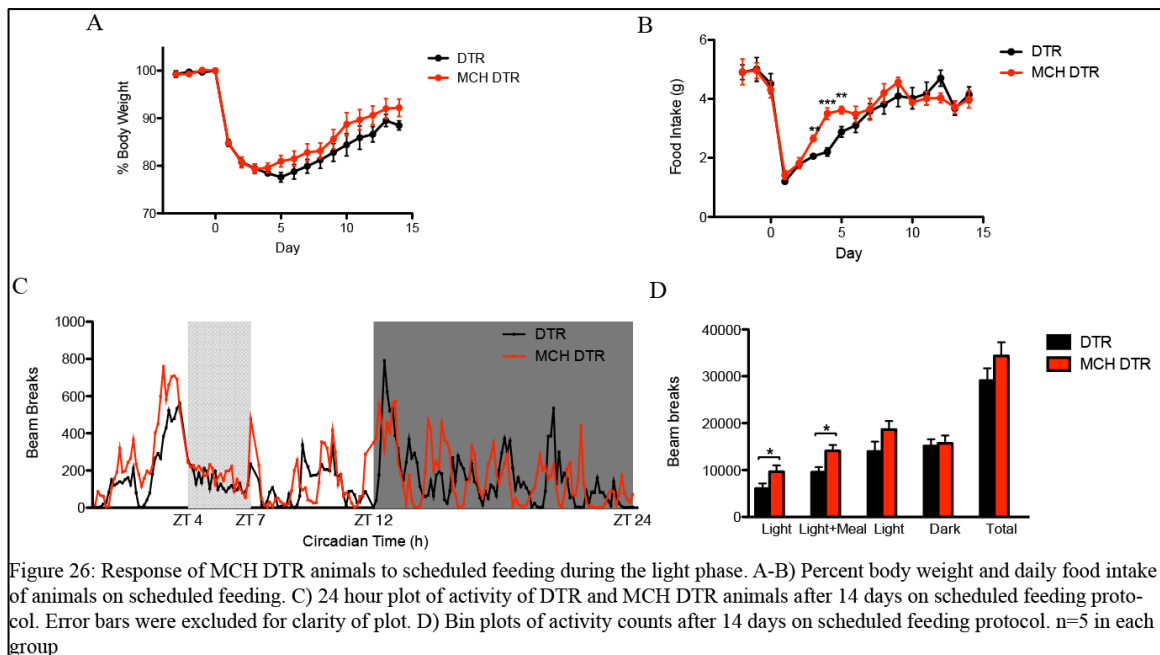


Figure 26: Response of MCH DTR animals to scheduled feeding during the light phase. A-B) Percent body weight and daily food intake of animals on scheduled feeding. C) 24 hour plot of activity of DTR and MCH DTR animals after 14 days on scheduled feeding protocol. Error bars were excluded for clarity of plot. D) Bin plots of activity counts after 14 days on scheduled feeding protocol. n=5 in each group

Response of MCH Vgat knockout animals to scheduled feeding

Besides neuropeptides, neurons also use classical neurotransmitters such as glutamate and gamma-aminobutyric acid (GABA) to convey information. I first determined whether MCH neurons are GABAergic by performing immunostaining for the MCH peptide in a glutamate decarboxylase, Gad67 (also known as Gad1) GFP

reporter mouse line. *Gad67* is a glutamate decarboxylase that catalyzes the decarboxylation of glutamate to GABA. I found that 60.23% ($\pm 0.6\%$) of MCH neurons overlapped with GFP (Figure 27A-C), suggesting that these neurons are GABAergic. Next, I generated mice with MCH neurons that are deficient in GABA signaling by mating a MCH Cre line with a *Vgat* flox/flox line. *Vgat* is an integral membrane protein for the packaging of GABA into synaptic vesicles. I then maintained MCH *Vgat* flox/flox animals on a scheduled feeding protocol. MCH *Vgat* knockout animals acclimated to the protocol as well as control animals as evidenced by comparable recovery of body weight and normalization of daily food intake (Figure 27D-E). However, after 2 weeks of entrainment to the protocol, conditional knockout animals exhibited FAA with significantly more locomotion than control animals (Figure 27F-G). This result suggests that GABA signaling from MCH contributes to locomotion during FAA.

Discussion

In this chapter, I investigate the role of MCH neurons during scheduled feeding. Diphtheria toxin mediated ablation of MCH neurons in adult animals resulted in complete loss of MCH immunoreactivity and led to a small but insignificant decrease in body weight although food intake, response to hyperleptinemia, hypoleptinemia and home cage locomotion were unaffected. However, animals with ablated MCH neurons acclimated faster to a scheduled feeding protocol as evidenced by earlier recovery of food intake and body weight in the first week of the protocol. Loss of MCH neurons also resulted in increased FAA locomotion after 2 weeks of entrainment to scheduled feeding.

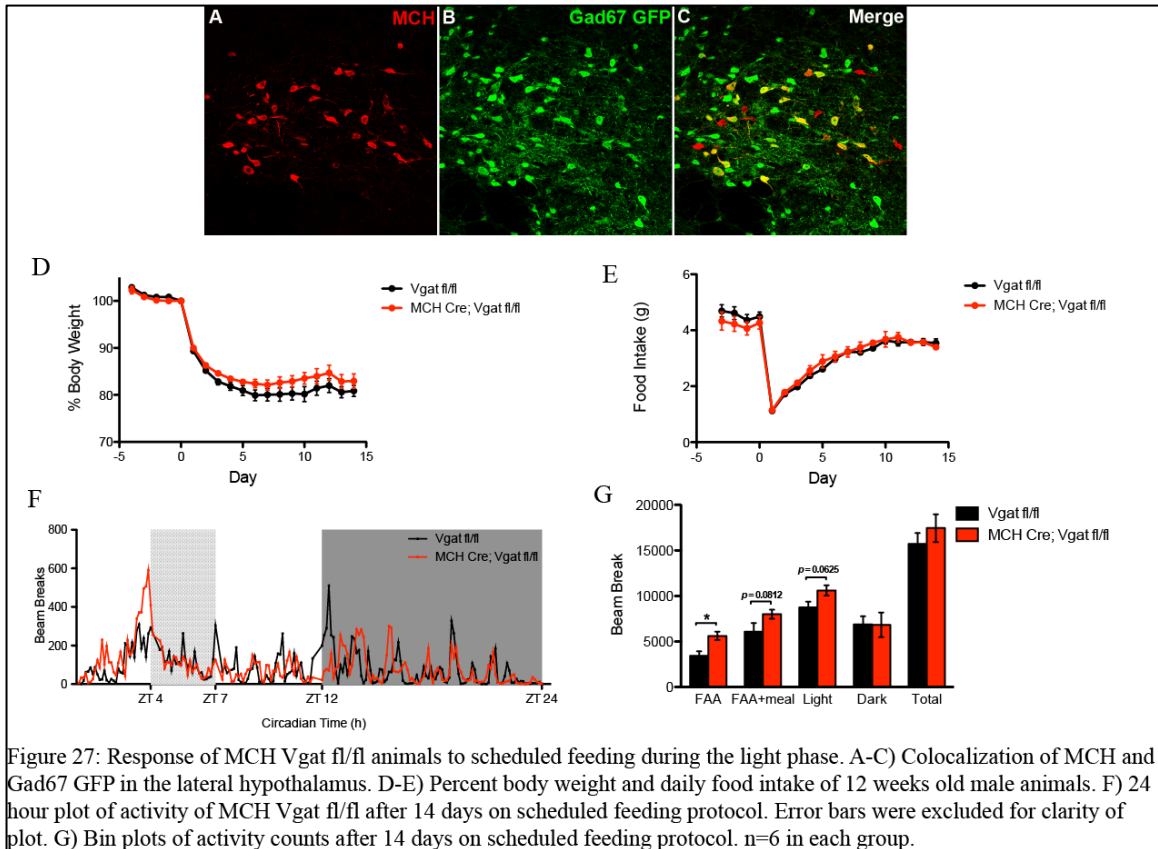


Figure 27: Response of MCH Vgat fl/fl animals to scheduled feeding during the light phase. A-C) Colocalization of MCH and Gad67 GFP in the lateral hypothalamus. D-E) Percent body weight and daily food intake of 12 weeks old male animals. F) 24 hour plot of activity of MCH Vgat fl/fl after 14 days on scheduled feeding protocol. Error bars were excluded for clarity of plot. G) Bin plots of activity counts after 14 days on scheduled feeding protocol. n=6 in each group.

This result combined with the finding that MCH neurons are inhibited during scheduled feeding, suggest that activity of MCH neurons acts to counter the adaptation of animals to a scheduled feeding paradigm and that silencing MCH neurons promotes this adaptation and may also account for the increased FAA locomotion after entrainment. MCH has been consistently shown to be an orexigenic peptide but the loss of MCH neurons in this study caused increased food intake during acclimatization to scheduled feeding is rather surprising.

I further determined that approximately 60% of MCH neurons are GABAergic and generated animals with impaired GABA signaling in MCH neurons. These animals did not show enhanced adaptation to scheduled feeding but did exhibit increased FAA compared to control animals after entrainment to scheduled feeding. Taken together,

these data demonstrate that different aspects of MCH neurons contribute to distinct behavioral phenotypes associated with scheduled feeding with the silencing of GABA signaling from MCH neurons contributing to locomotion during FAA. However, more studies need to be carried out to further tease apart and definitively show which aspects of MCH neurons contribute to which behavioral phenotype. For instance the scheduled feeding experiments can be performed in mice with genetic deletion of MCH, in mice with disrupted glutamate signaling in MCH neurons and in mice with disruption in both glutamate and GABA signaling in MCH neurons.

Chapter 6:

Loss of Galanin Neurons Results in Leanness

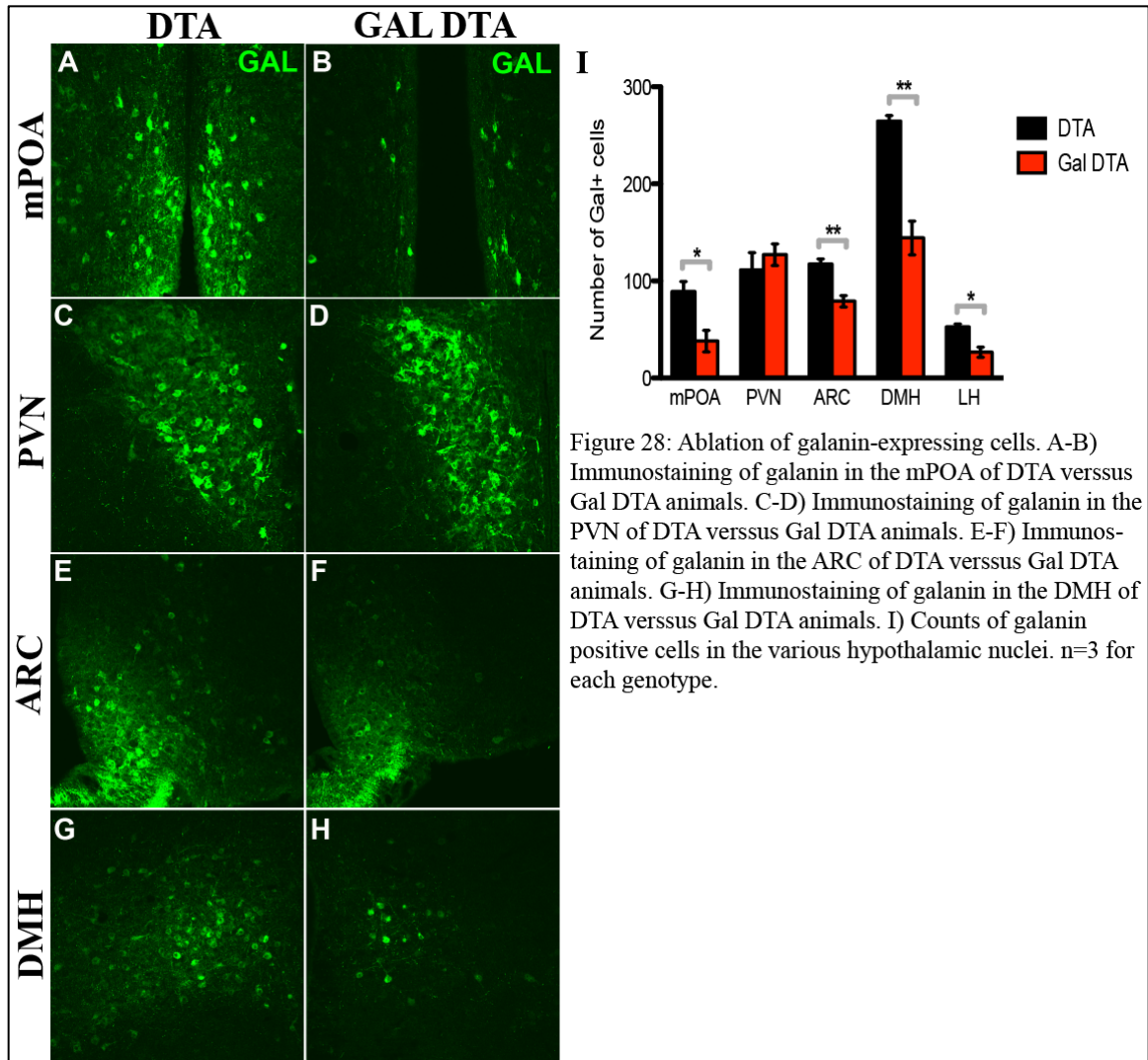
Introduction

Galanin is a neuromodulator in both the central and peripheral nervous system and is implicated in several neural functions including cognition(Wrenn et al., 2006), pain perception(Liu and Hökfelt, 2002; Xu et al., 2000) and neuronal protection and regeneration(Elliott-Hunt et al., 2004; Mahoney et al., 2003). Galanin is an orexigenic neuropeptide since central administration of galanin stimulates food intake(Crawley et al., 1990; Kyrkouli et al., 1986; 1990). However, genetic manipulations of the galanin gene do not cause changes in body weight and food intake(Hohmann et al., 2003; Wynick et al., 1998). Furthermore, food deprivation does not alter galanin gene expression levels(Schwartz et al., 1993). Thus, the role of galanin and galanin expressing cells in regulating metabolic homeostasis remains unclear. In chapter 3, I reported that galanin neurons were activated following an overnight fast, suggesting a role for galanin in response to food deprivation. Here, I investigate the role of galanin neurons in energy balance using diphtheria toxin alpha chain (DTA) mediated cell ablation.

Results

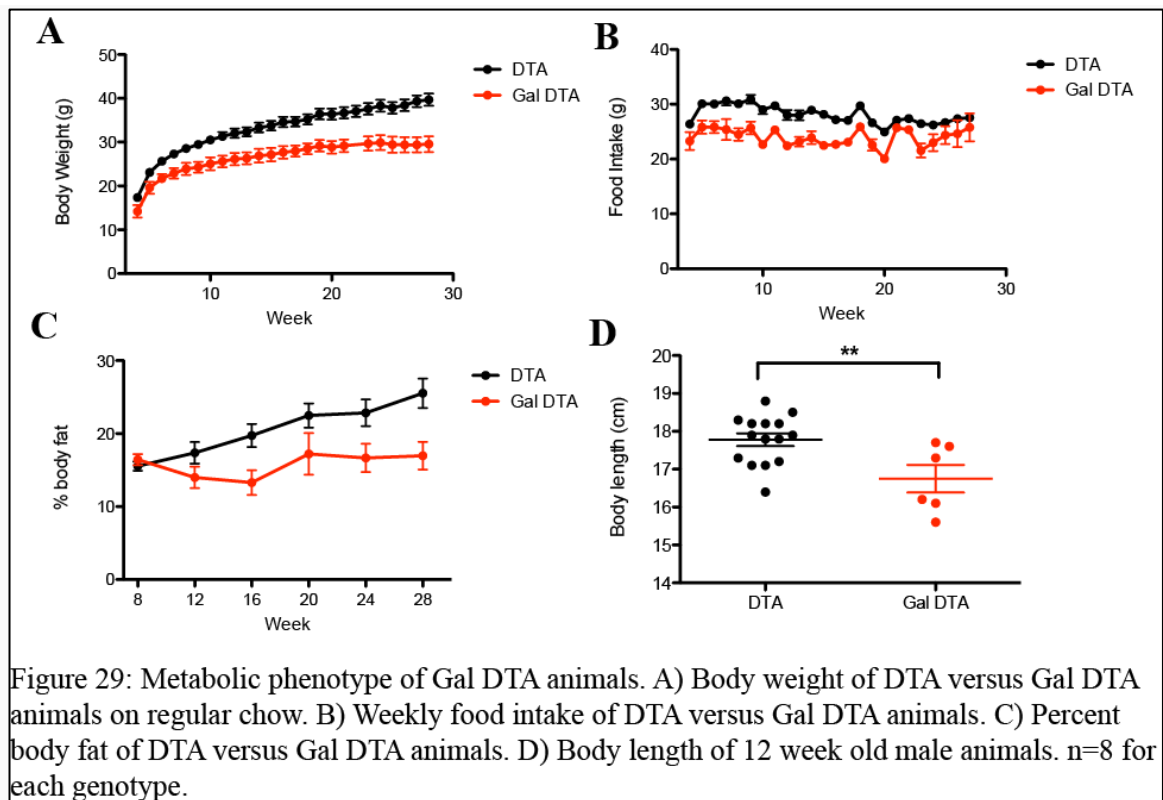
Ablation of Galanin neurons in the hypothalamus results in lean animals

To ablate galanin neurons, I generated Gal DTA animals by mating a GAL Cre mouse line with a lox-STOP-lox DTA line. Expression of intra-cellular DTA blocks translation, causing death of Cre expressing cells. I verified the loss of galanin neurons in



the hypothalamus by performing immunostaining for galanin in adult animals. There was a marked decrease in number of galanin positive cells in several hypothalamic nuclei including the mPOA, ARC, DMH and LH (Figure 28A-I). I noted that galanin cells were not lost in the PVN, possibly due to poor expression of Cre recombinase in this region. I next monitored the body weight and weekly food intake of Gal DTA animals on regular chow for 6 months. Gal DTA animals weighed less than littermate control animals starting at 6 weeks of age and were resistant to age-associated weight gain (Figure 29A). Weekly food intake of Gal DTA animals was also consistently lower than control animals

(Figure 29B). Consistent with weighing less, body fat percentage measurements using MRI revealed that Gal DTA accumulated less fat mass compared to controls (Figure 29C). I also observed that Gal DTA animals were shorter than their wildtype littermates (Figure 29D), suggesting a growth defect. Taken together, these data demonstrate that loss of galanin neurons leads to a lean phenotype, which was not observed in galanin null animals.



Loss of GABA transmission in a subset of galanin neurons contributes to leanness

The loss of galanin neurons but not galanin peptide results in leanness, suggesting that other properties of galanin neurons besides the galanin peptide might mediate this phenotype. I next investigated whether galanin neurons also use the inhibitory neurotransmitter GABA by crossing a galanin tdTomato reporter line with a Gad67 GFP

reporter line. Examination of brain slices in these animals showed that a subset of galanin neurons in various hypothalamic nuclei colocalized with GFP (Figure 30A-D), suggesting that they are GABAergic. I then generated animals with conditional knockout of Vgat, an integral membrane protein involved in packaging of GABA into synaptic vesicles, in galanin neurons. Gal Vgat fl/fl animals maintained on a high fat diet (60% fat) consistently weighed less than littermate control animals starting from 8 weeks of age (Figure 30E). Consistent with weighing less, Gal Vgat fl/fl animals accumulated less fat mass when body composition was measured by MRI (Figure 30G).

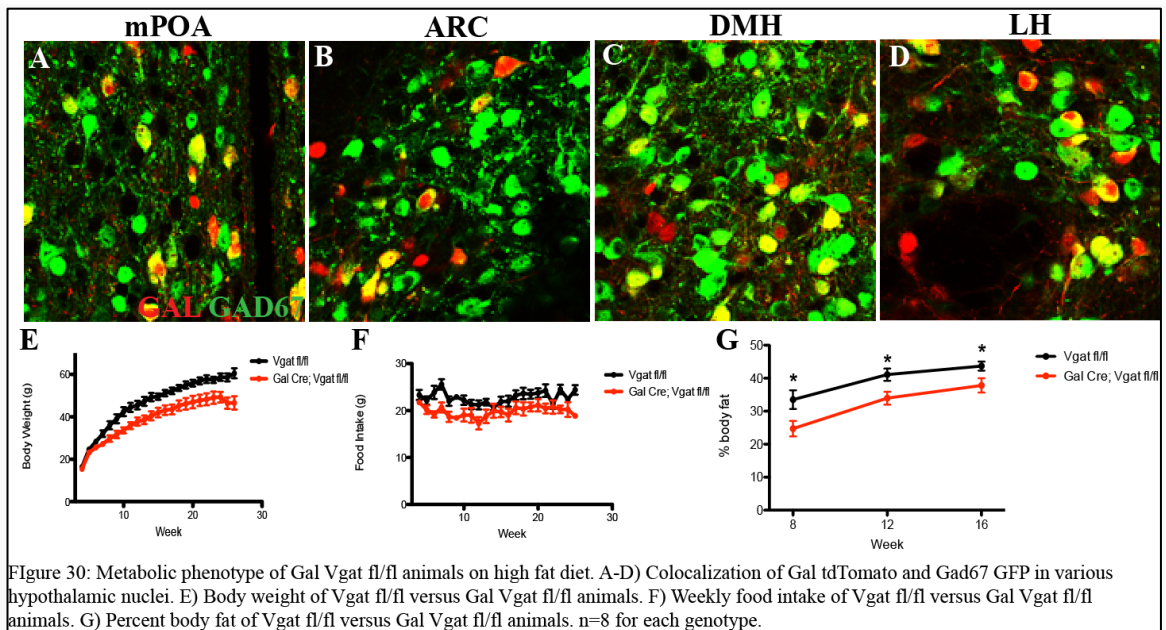


Figure 30: Metabolic phenotype of Gal Vgat fl/fl animals on high fat diet. A-D) Colocalization of Gal tdTomato and Gad67 GFP in various hypothalamic nuclei. E) Body weight of Vgat fl/fl versus Gal Vgat fl/fl animals. F) Weekly food intake of Vgat fl/fl versus Gal Vgat fl/fl animals. G) Percent body fat of Vgat fl/fl versus Gal Vgat fl/fl animals. n=8 for each genotype.

Discussion

In this chapter, I investigate the role of galanin neurons in energy homeostasis using diphtheria toxin alpha chain mediated cell ablation. Loss of galanin immunoreactivity was observed in the mPOA, ARC, DMH and LH. Although not all galanin neurons were ablated, Gal DTA animals weighed less than control animals and consistently consumed less food. These animals also accumulated less age-associated body fat. This result is

surprising since galanin knockout animals do not exhibit changes in body weight and food intake (Hohmann et al., 2003; Wynick et al., 1998). Taken together, these data suggest that other aspects of galanin neurons, besides the galanin neuropeptide, might play a role in energy balance.

I further determined that a subset of galanin neurons use the inhibitory neurotransmitter GABA for synaptic transmission and proceeded to disrupt GABA signaling in this subset of neurons. Animals with impaired GABA signaling in galanin neurons were leaner than controls when maintained on a 60% high fat diet and also accumulated less body fat as measured by MRI, suggesting that GABA signaling from galanin neurons plays a role in energy balance.

The finding in chapter 3 that galanin neurons in the mPOA and DMH are selectively activated after food deprivation suggests that galanin neurons in these 2 regions might play key roles in maintaining body weight and food intake. The genetic approach employed in this chapter is unable to target galanin neurons in specific anatomical regions. Therefore, more intricate manipulation of galanin neurons is required to determine the specific roles of galanin neurons in each anatomical region in controlling energy homeostasis. For example, selective manipulation of specific galanin neurons in defined anatomical regions using optogenetics or DREADDs can potentially reveal the function of galanin neurons in each region.

Chapter 7:

Summary and Conclusion

Prior studies have provided evidence for a physiological system that maintains energy homeostasis. Numerous studies in the past decades have provided great insights into the neural substrates that regulate this system. Disruption of this physiological system can lead to obesity and metabolic syndrome. However, there is reason to believe that not all neural components of this system have been identified and that there are many unidentified and/or under-studied neural populations awaiting discovery. Furthermore, metabolism and daily cycles of circadian rhythms appear to be coupled and misalignment can result in metabolic disorders but this aspect has received less attention. Here, I developed a novel method to identify functionally activated neurons in the central nervous system using phosphorylated ribosome capture. I used this new method to identify new neural populations as well as uncover novel functions for previously well-studied populations.

In this dissertation, I describe a novel method using phosphorylated ribosomal subunit S6 as a molecular tag for functionally activated neurons in the central nervous system. I showed that it is possible to isolate mRNA transcripts using commercial antibodies against pS6 and I further confirmed the fidelity of this method by successfully identifying known cell types that become activated upon physiological stimuli such as salt challenge (OXT, AVP) and food deprivation (NPY, AGRP). The method is also sensitive enough to detect cell type specific markers of cells that become inhibited following a physiological stimulus such as the anorexigenic peptide POMC following an

overnight fast.

A lesser studied gene marker, galanin, was identified following overnight fast, which I confirmed with immunostaining for both pS6 and cfos. Although galanin can stimulate food intake when administered to rodents, genetic manipulation of the galanin gene did not reveal any crucial role for galanin in energy balance. Using diphtheria toxin alpha chain mediated cell ablation, I generated animals with significant loss of galanin neurons in the hypothalamus and found these animals to be lean, implicating galanin neurons itself as important for metabolic homeostasis. I further determined that GABA signaling from a subset of galanin contributes to this lean phenotype. However, galanin is expressed in many neurons in various nuclei of the hypothalamus. Genetic manipulation of galanin neurons does not provide insights into how each subpopulation of galanin neurons control energy balance. Interestingly, only galanin neurons in the mPOA and DMH are activated after overnight fast and these populations do not express the active leptin receptor. Additional experiments that can manipulate a specific population of galanin neurons, such as optogenetics or DREADDs, are required to further dissect the specific contribution of each population to energy homeostasis. Nevertheless, the lean phenotype observed after loss of galanin neurons is the first example of the role of galanin neurons in regulating energy balance.

I also employed phosphorylated ribosome capture to identify molecular markers of cell types that are involved in coordinating meal pattern behavior. PDYN neurons in the DMH become activated, in a ghrelin independent manner, when animals were entrained on a scheduled feeding protocol where food was only available for 3 hours during the light phase. The activation of PDYN neurons is rhythmic, peaking in the middle of the

food window. Pharmacological blockage of the endogenous receptor of PDYN revealed that PDYN activation acts as a 'stop' signal to restrain bouts of voracious feeding, especially when animals are entrained to eat a whole day's worth of calories within a short time window.

Besides PDYN, the activation of AgRP neurons also exhibited a rhythmic pattern during scheduled feeding, with activation peaking at the start of the feeding window. Diphtheria toxin mediated loss of AgRP neurons impaired the ability of animals to adapt to a feeding window in the light phase, a period when rodents do not normally consume food. This impairment was not observed when the food window remained in the dark phase, when rodents are active and eat most of their food. Taken together, these data revealed the importance of AgRP neurons in coordinating behavior to adapt to changes in food availability, especially when food availability is decoupled from light-dependent rhythms.

I also investigated the role of MCH neurons, which were inhibited during scheduled feeding, in meal pattern behavior. Diphtheria toxin induced adult ablation of MCH neurons resulted in viable animals. Animals with complete loss of MCH neurons acclimated to scheduled feeding faster than animals with intact MCH neurons, demonstrating MCH neurons are part of the neural circuitry that regulates adaption to scheduled feeding.

Using phosphorylated ribosome capture, I identified molecular markers for cell types that regulated adaption to scheduled feeding. This data now provide defined neuronal populations where the intracellular mechanisms of meal pattern behavior can be studied. As mentioned in chapter 4, there is reason to believe novel, yet undiscovered genes and

their gene products regulate meal pattern behavior as animals with genetic knockout of known clock components can still be entrained by food.

Phosphorylated ribosome capture is a novel and powerful tool that supplements current efforts in neuroscience to map function organization of the mammalian brain. Since this method utilizes an endogenous biochemical tag on ribosomal subunit S6, it can potentially be applied to model organisms that are less amenable to genetic manipulation as long as S6 is phosphorylated.

Future Directions

In this dissertation, I have shown that S6 phosphorylation can be used as a mark for biochemical activation of neurons and this post-translation tag correlates well with the immediate early gene *cfos*. However, electrophysiological evidence is still the gold standard in neuroscience to definitively demonstrate neural activity. Thus, it would be of great interest to activate a discrete neuronal population using optogenetics or pharmacogenetics and determine the level of pS6 induction in those cells after activation. This set of experiments would provide greater understanding on how the electrical activity of neurons correlates with S6 phosphorylation.

The findings that the activity of cells expressing the neuropeptides PDYN, AgRP and MCH contribute to the food entrainment phenotype observed in a scheduled feeding paradigm provide molecular entry points to further study the components of the food entrainable oscillator and the mechanisms that entrain and maintain meal pattern behavior. Mutants deficient in canonical clock genes do exhibit food anticipatory activity, suggesting that the molecular components that regulate this behavior differ from that of

the light entrainable oscillator. Transcriptional profiling of AgRP or PDYN neurons using BAC-TRAP(Heiman et al., 2008) at different time points after entrainment to scheduled feeding can provide greater molecular information of the components that cycle with food schedule, potentially revealing novel circadian components.

As mentioned in Chapter 4, disrupting metabolic signaling pathways such as the gut hormone ghrelin or the adipocyte derived hormone leptin do affect food anticipatory activity but cannot completely abolish this behavior, strongly suggesting that other physiological pathways must also play a role. It is highly plausible that the ability to anticipate food availability is a trait highly selected for by evolution since consumption of nutrients is one of the most fundamental survival necessities, thus it makes sense that information from several physiological systems is processed to drive this anticipatory activity. Therefore, interfering with one system is insufficient to abolish food anticipatory activity. Examples of other signaling molecules that could play a role in food anticipatory activity include blood glucose, insulin and glucocorticoid. The involvement of additional systems that contribute to food anticipatory activity can possibly be discerned from the transcriptional profiling experiment as mentioned above since intracellular pathways that process these peripheral signals could exhibit rhythmicity that closely track with the imposed food schedule.

References:

- Acosta-Galvan, G., Yi, C.-X., van der Vliet, J., Jhamandas, J.H., Panula, P., Angeles-Castellanos, M., Del Carmen Basualdo, M., Escobar, C., and Buijs, R.M. (2011). Interaction between hypothalamic dorsomedial nucleus and the suprachiasmatic nucleus determines intensity of food anticipatory behavior. *Proc Natl Acad Sci USA* *108*, 5813–5818.
- Ahima, R.S., Prabakaran, D., and Flier, J.S. (1998). Postnatal leptin surge and regulation of circadian rhythm of leptin by feeding. Implications for energy homeostasis and neuroendocrine function. *J Clin Invest* *101*, 1020–1027.
- Akhtar, R.A., Reddy, A.B., Maywood, E.S., Clayton, J.D., King, V.M., Smith, A.G., Gant, T.W., Hastings, M.H., and Kyriacou, C.P. (2002). Circadian cycling of the mouse liver transcriptome, as revealed by cDNA microarray, is driven by the suprachiasmatic nucleus. *Curr Biol* *12*, 540–550.
- Alivisatos, A.P., Chun, M., Church, G.M., Greenspan, R.J., Roukes, M.L., and Yuste, R. (2012). The brain activity map project and the challenge of functional connectomics. *Neuron* *74*, 970–974.
- Alon, T., and Friedman, J.M. (2006). Late-onset leanness in mice with targeted ablation of melanin concentrating hormone neurons. *J Neurosci* *26*, 389–397.
- Alon, T., Zhou, L., Pérez, C.A., Garfield, A.S., Friedman, J.M., and Heisler, L.K. (2009). Transgenic mice expressing green fluorescent protein under the control of the corticotropin-releasing hormone promoter. *Endocrinology* *150*, 5626–5632.
- ANAND, B.K., and Brobeck, J.R. (1951). Hypothalamic Control of Food Intake in Rats and Cats. *Yale J Biol Med* *24*, 123–140.
- Aponte, Y., Atasoy, D., and Sternson, S.M. (2011). AGRP neurons are sufficient to orchestrate feeding behavior rapidly and without training. *Nat Neurosci* *14*, 351–355.
- Atasoy, D., Betley, J.N., Su, H.H., and Sternson, S.M. (2012). Deconstruction of a neural circuit for hunger. *Nature* *488*, 172–177.
- Balsalobre, A., Damiola, F., and Schibler, U. (1998). A serum shock induces circadian gene expression in mammalian tissue culture cells. *Cell* *93*, 929–937.
- Balthasar, N., Coppari, R., McMinn, J., Liu, S.M., Lee, C.E., Tang, V., Kenny, C.D., McGovern, R.A., Chua, S.C., Elmquist, J.K., et al. (2004). Leptin receptor signaling in POMC neurons is required for normal body weight homeostasis. *Neuron* *42*, 983–991.

- Baskin, D.G., Breininger, J.F., and Schwartz, M.W. (1999). Leptin receptor mRNA identifies a subpopulation of neuropeptide Y neurons activated by fasting in rat hypothalamus. *Diabetes* 48, 828–833.
- Betley, J.N., Cao, Z.F.H., Ritola, K.D., and Sternson, S.M. (2013). Parallel, redundant circuit organization for homeostatic control of feeding behavior. *Cell* 155, 1337–1350.
- Billington, C.J., and Levine, A.S. (1992). Hypothalamic neuropeptide Y regulation of feeding and energy metabolism. *Curr. Opin. Neurobiol.* 2, 847–851.
- Bjørbaek, C., Uotani, S., da Silva, B., and Flier, J.S. (1997). Divergent signaling capacities of the long and short isoforms of the leptin receptor. *J Biol Chem* 272, 32686–32695.
- Blum, I.D., Patterson, Z., Khazall, R., Lamont, E.W., Sleeman, M.W., Horvath, T.L., and Abizaid, A. (2009). Reduced anticipatory locomotor responses to scheduled meals in ghrelin receptor deficient mice. *Neuroscience* 164, 351–359.
- Bouchard, C., Tremblay, A., Després, J.P., Nadeau, A., Lupien, P.J., Thériault, G., Dussault, J., Moorjani, S., Pinault, S., and Fournier, G. (1990). The response to long-term overfeeding in identical twins. *N. Engl. J. Med.* 322, 1477–1482.
- Bray, G.A., FISLER, J., and York, D.A. (1990). Neuroendocrine Control of the Development of Obesity - Understanding Gained From Studies of Experimental Animal-Models. *Front Neuroendocrinol* 11, 128–181.
- Brobeck, J.R. (1946). Mechanism of the Development of Obesity in Animals with Hypothalamic Lesions. *Physiol. Rev.* 26, 541–559.
- Brobeck, J.R., Tepperman, J., and Long, C.N. (1943). Experimental Hypothalamic Hyperphagia in the Albino Rat. *Yale J Biol Med* 15, 831–853.
- Brown, M.R., Mortrud, M., Crum, R., and Sawchenko, P. (1988). Role of somatostatin in the regulation of vasopressin secretion. *Brain Res* 452, 212–218.
- Bruchas, M.R., Yang, T., Schreiber, S., Defino, M., Kwan, S.C., Li, S., and Chavkin, C. (2007). Long-acting kappa opioid antagonists disrupt receptor signaling and produce noncompetitive effects by activating c-Jun N-terminal kinase. *J Biol Chem* 282, 29803–29811.
- Buhr, E.D., and Takahashi, J.S. (2013). Molecular components of the Mammalian circadian clock. *Handb Exp Pharmacol* 3–27.
- Campfield, L.A., Smith, F.J., Guisez, Y., Devos, R., and Burn, P. (1995). Recombinant mouse OB protein: evidence for a peripheral signal linking adiposity and central neural networks. *Science* 269, 546–549.
- Cao, R., Anderson, F.E., Jung, Y.-J., Dziema, H., and Obrietan, K. (2011). Circadian

regulation of mammalian target of rapamycin signaling in the mouse suprachiasmatic nucleus. *Neuroscience* *181*, 79–88.

Cao, R., Lee, B., Cho, H.-Y., Saklayen, S., and Obrietan, K. (2008). Photic regulation of the mTOR signaling pathway in the suprachiasmatic circadian clock. *Mol. Cell. Neurosci.* *38*, 312–324.

Cao, R., Li, A., Cho, H.-Y., Lee, B., and Obrietan, K. (2010). Mammalian target of rapamycin signaling modulates photic entrainment of the suprachiasmatic circadian clock. *J Neurosci* *30*, 6302–6314.

Carroll, I., Thomas, J.B., Dykstra, L.A., Granger, A.L., Allen, R.M., Howard, J.L., Pollard, G.T., Aceto, M.D., and Harris, L.S. (2004). Pharmacological properties of JD1c: a novel kappa-opioid receptor antagonist. *European Journal of Pharmacology* *501*, 111–119.

Chen, H., Charlat, O., Tartaglia, L.A., Woolf, E.A., Weng, X., Ellis, S.J., Lakey, N.D., Culpepper, J., Moore, K.J., Breitbart, R.E., et al. (1996). Evidence that the diabetes gene encodes the leptin receptor: identification of a mutation in the leptin receptor gene in db/db mice. *Cell* *84*, 491–495.

Cheung, C.C., Clifton, D.K., and Steiner, R.A. (1997). Proopiomelanocortin neurons are direct targets for leptin in the hypothalamus. *Endocrinology* *138*, 4489–4492.

Clark, J.T., Kalra, P.S., Crowley, W.R., and Kalra, S.P. (1984). Neuropeptide Y and human pancreatic polypeptide stimulate feeding behavior in rats. *Endocrinology* *115*, 427–429.

Coleman, D.L. (1973). Effects of parabiosis of obese with diabetes and normal mice. *Diabetologia* *9*, 294–298.

Coleman, D.L., and Hummel, K.P. (1969). Effects of parabiosis of normal with genetically diabetic mice. *Am. J. Physiol.* *217*, 1298–1304.

Coleman, D.L. (2010). A historical perspective on leptin.

Cone, R.D., Lu, D., Koppula, S., Vage, D.I., Klungland, H., Boston, B., Chen, W., Orth, D.N., Pouton, C., and Kesterson, R.A. (1996). The melanocortin receptors: agonists, antagonists, and the hormonal control of pigmentation. *Recent Prog Horm Res* *51*, 287–317–discussion318.

Cowley, M.A., Pronchuk, N., Fan, W., Dinulescu, D.M., Colmers, W.F., and Cone, R.D. (1999). Integration of NPY, AGRP, and melanocortin signals in the hypothalamic paraventricular nucleus: evidence of a cellular basis for the adipostat. *Neuron* *24*, 155–163.

Cowley, M.A., Smart, J.L., Rubinstein, M., Cerdán, M.G., Diano, S., Horvath, T.L., Cone, R.D., and Low, M.J. (2001). Leptin activates anorexigenic POMC neurons through

a neural network in the arcuate nucleus. *Nature* *411*, 480–484.

Crawley, J.N., Austin, M.C., Fiske, S.M., Martin, B., Consolo, S., Berthold, M., Langel, U., Fisone, G., and Bartfai, T. (1990). Activity of centrally administered galanin fragments on stimulation of feeding behavior and on galanin receptor binding in the rat hypothalamus. *J Neurosci* *10*, 3695–3700.

Croizier, S., Franchi-Bernard, G., Colard, C., Poncet, F., La Roche, A., and Risold, P.-Y. (2010). A comparative analysis shows morphofunctional differences between the rat and mouse melanin-concentrating hormone systems. *PLoS ONE* *5*, e15471.

Damiola, F., Le Minh, N., Preitner, N., Kornmann, B., Fleury-Olela, F., and Schibler, U. (2000). Restricted feeding uncouples circadian oscillators in peripheral tissues from the central pacemaker in the suprachiasmatic nucleus. *Genes Dev* *14*, 2950–2961.

de Luca, C., Kowalski, T.J., Zhang, Y., Elmquist, J.K., Lee, C., Kilimann, M.W., Ludwig, T., Liu, S.M., and Chua, S.C. (2005). Complete rescue of obesity, diabetes, and infertility in db/db mice by neuron-specific LEPR-B transgenes. *J Clin Invest* *115*, 3484–3493.

de Mateos-Verchere, J.G., Leprince, J., Tonon, M.C., Vaudry, H., and Costentin, J. (2001). The octadecaneuropeptide [diazepam-binding inhibitor (33-50)] exerts potent anorexigenic effects in rodents. *European Journal of Pharmacology* *414*, 225–231.

Dielenberg, R.A., Hunt, G.E., and McGregor, I.S. (2001). “When a rat smells a cat”: the distribution of Fos immunoreactivity in rat brain following exposure to a predatory odor. *Neuroscience* *104*, 1085–1097.

Dietrich, M.O., Bober, J., Ferreira, J.G., Tellez, L.A., Mineur, Y.S., Souza, D.O., Gao, X.-B., Picciotto, M.R., Araújo, I., Liu, Z.-W., et al. (2012). AgRP neurons regulate development of dopamine neuronal plasticity and nonfood-associated behaviors. *Nat Neurosci* *15*, 1108–1110.

Dietrich, M.O., Liu, Z.-W., and Horvath, T.L. (2013). Mitochondrial dynamics controlled by mitofusins regulate *Agrp* neuronal activity and diet-induced obesity. *Cell* *155*, 188–199.

Drazen, D.L., Vahl, T.P., D'Alessio, D.A., Seeley, R.J., and Woods, S.C. (2006). Effects of a fixed meal pattern on ghrelin secretion: evidence for a learned response independent of nutrient status. *Endocrinology* *147*, 23–30.

Ellingsen, T., Bener, A., and Gehani, A.A. (2007). Study of shift work and risk of coronary events. *J R Soc Promot Health* *127*, 265–267.

Elliott-Hunt, C.R., Marsh, B., Bacon, A., Pope, R., Vanderplank, P., and Wynick, D. (2004). Galanin acts as a neuroprotective factor to the hippocampus. *Proc Natl Acad Sci USA* *101*, 5105–5110.

- Elmqvist, J.K., Coppari, R., Balthasar, N., Ichinose, M., and Lowell, B.B. (2005). Identifying hypothalamic pathways controlling food intake, body weight, and glucose homeostasis. *J Comp Neurol* 493, 63–71.
- Farooqi, I.S., Yeo, G.S., Keogh, J.M., Aminian, S., Jebb, S.A., Butler, G., Cheetham, T., and O'Rahilly, S. (2000). Dominant and recessive inheritance of morbid obesity associated with melanocortin 4 receptor deficiency. *J Clin Invest* 106, 271–279.
- Farooqi, I.S., Keogh, J.M., Yeo, G.S.H., Lank, E.J., Cheetham, T., and O'Rahilly, S. (2003). Clinical spectrum of obesity and mutations in the melanocortin 4 receptor gene. *N. Engl. J. Med.* 348, 1085–1095.
- Fei, H., Okano, H.J., Li, C., Lee, G.H., Zhao, C., Darnell, R., and Friedman, J.M. (1997). Anatomic localization of alternatively spliced leptin receptors (Ob-R) in mouse brain and other tissues. *Proc Natl Acad Sci USA* 94, 7001–7005.
- Flavell, S.W., and Greenberg, M.E. (2008). Signaling mechanisms linking neuronal activity to gene expression and plasticity of the nervous system. *Annu Rev Neurosci* 31, 563–590.
- Flegal, K.M., Carroll, M.D., Ogden, C.L., and Curtin, L.R. (2010). Prevalence and trends in obesity among US adults, 1999-2008. *Jama* 303, 235–241.
- Flier, J.S. (2004). Obesity wars: molecular progress confronts an expanding epidemic. *Cell* 116, 337–350.
- Fuller, P.M., Lu, J., and Saper, C.B. (2008). Differential rescue of light- and food-entrainable circadian rhythms. *Science* 320, 1074–1077.
- Gai, W.P., Geffen, L.B., and Blessing, W.W. (1990). Galanin immunoreactive neurons in the human hypothalamus: colocalization with vasopressin-containing neurons. *J Comp Neurol* 298, 265–280.
- Gavrila, A.M., Robinson, B., Hoy, J., Stewart, J., Bhargava, A., and Amir, S. (2008). Double-stranded RNA-mediated suppression of *Period2* expression in the suprachiasmatic nucleus disrupts circadian locomotor activity in rats. *Neuroscience* 154, 409–414.
- Gong, S., Zheng, C., Doughty, M.L., Losos, K., Didkovsky, N., Schambra, U.B., Nowak, N.J., Joyner, A., Leblanc, G., Hatten, M.E., et al. (2003). A gene expression atlas of the central nervous system based on bacterial artificial chromosomes. *Nature* 425, 917–925.
- Gooley, J.J., Schomer, A., and Saper, C.B. (2006). The dorsomedial hypothalamic nucleus is critical for the expression of food-entrainable circadian rhythms. *Nat Neurosci* 9, 398–407.
- Groos, G., and Hendriks, J. (1982). Circadian rhythms in electrical discharge of rat suprachiasmatic neurones recorded in vitro. *Neurosci Lett* 34, 283–288.

- Gropp, E., Shanabrough, M., Borok, E., Xu, A.W., Janoschek, R., Buch, T., Plum, L., Balthasar, N., Hampel, B., Waisman, A., et al. (2005). Agouti-related peptide-expressing neurons are mandatory for feeding. *Nat Neurosci* 8, 1289–1291.
- Grundy, S.M. (2000). Metabolic complications of obesity. *Endocrine* 13, 155–165.
- Guan, X.M., Yu, H., Palyha, O.C., McKee, K.K., Feighner, S.D., Sirinathsinghji, D.J., Smith, R.G., Van der Ploeg, L.H., and Howard, A.D. (1997). Distribution of mRNA encoding the growth hormone secretagogue receptor in brain and peripheral tissues. *Brain Res Mol Brain Res* 48, 23–29.
- Guilding, C., and Piggins, H.D. (2007). Challenging the omnipotence of the suprachiasmatic timekeeper: are circadian oscillators present throughout the mammalian brain? *Eur J Neurosci* 25, 3195–3216.
- Guilding, C., Hughes, A.T.L., Brown, T.M., Namvar, S., and Piggins, H.D. (2009). A riot of rhythms: neuronal and glial circadian oscillators in the mediobasal hypothalamus. *Mol Brain* 2, 28.
- Hahn, S., Fekete, C., Mizuno, T.M., Windsor, J., Yan, H., Boozer, C.N., Lee, C., Elmquist, J.K., Lechan, R.M., Mobbs, C.V., et al. (2002). VGF is required for obesity induced by diet, gold thioglucose treatment, and agouti and is differentially regulated in pro-opiomelanocortin- and neuropeptide Y-containing arcuate neurons in response to fasting. *J Neurosci* 22, 6929–6938.
- Hahn, T.M., Breininger, J.F., Baskin, D.G., and Schwartz, M.W. (1998). Coexpression of *Agrp* and *NPY* in fasting-activated hypothalamic neurons. *Nat Neurosci* 1, 271–272.
- Halaas, J.L., Boozer, C., Blair-West, J., Fidahusein, N., Denton, D.A., and Friedman, J.M. (1997). Physiological response to long-term peripheral and central leptin infusion in lean and obese mice. *Proc Natl Acad Sci USA* 94, 8878–8883.
- Halaas, J.L., Gajiwala, K.S., Maffei, M., Cohen, S.L., Chait, B.T., Rabinowitz, D., Lallone, R.L., Burley, S.K., and Friedman, J.M. (1995). Weight-reducing effects of the plasma protein encoded by the obese gene. *Science* 269, 543–546.
- Hara, R., Wan, K., Wakamatsu, H., Aida, R., Moriya, T., Akiyama, M., and Shibata, S. (2001). Restricted feeding entrains liver clock without participation of the suprachiasmatic nucleus. *Genes Cells* 6, 269–278.
- Hastings, M.H., Reddy, A.B., and Maywood, E.S. (2003). A clockwork web: circadian timing in brain and periphery, in health and disease. *Nat. Rev. Neurosci.* 4, 649–661.
- Heiman, M., Schaefer, A., Gong, S., Peterson, J.D., Day, M., Ramsey, K.E., Suárez-Fariñas, M., Schwarz, C., Stephan, D.A., Surmeier, D.J., et al. (2008). A translational profiling approach for the molecular characterization of CNS cell types. *Cell* 135, 738–748.

Hetherington, A.W. (1944). Non-production of hypothalamic obesity in the rat by lesions rostral or dorsal to the ventro-medial hypothalamic nuclei. *J Comp Neurol* 80, 33–45.

Hetherington, A.W., and Ranson, S.W. (1942). The relation of various hypothalamic lesions to adiposity in the rat. *J Comp Neurol* 76, 475–499.

Hohmann, J.G., Krasnow, S.M., Teklemichael, D.N., Clifton, D.K., Wynick, D., and Steiner, R.A. (2003). Neuroendocrine profiles in galanin-overexpressing and knockout mice. *Neuroendocrinology* 77, 354–366.

Huszar, D., Lynch, C.A., Fairchild-Huntress, V., Dunmore, J.H., Fang, Q., Berkemeier, L.R., Gu, W., Kesterson, R.A., Boston, B.A., Cone, R.D., et al. (1997). Targeted disruption of the melanocortin-4 receptor results in obesity in mice. *Cell* 88, 131–141.

Isogai, Y., Si, S., Pont-Lezica, L., Tan, T., Kapoor, V., Murthy, V.N., and Dulac, C. (2011). Molecular organization of vomeronasal chemoreception. *Nature* 478, 241–245.

Ivanova, E.A., Bechtold, D.A., Dupré, S.M., Brennand, J., Barrett, P., Luckman, S.M., and Loudon, A.S.I. (2008). Altered metabolism in the melatonin-related receptor (GPR50) knockout mouse. *Am. J. Physiol. Endocrinol. Metab.* 294, E176–E182.

Jego, S., Glasgow, S.D., Herrera, C.G., Ekstrand, M., Reed, S.J., Boyce, R., Friedman, J., Burdakov, D., and Adamantidis, A.R. (2013). Optogenetic identification of a rapid eye movement sleep modulatory circuit in the hypothalamus. *Nat Neurosci* 16, 1637–1643.

Joly-Amado, A., Denis, R.G.P., Castel, J., Lacombe, A., Cansell, C., Rouch, C., Kassis, N., Dairou, J., Cani, P.D., Ventura-Clapier, R., et al. (2012). Hypothalamic AgRP-neurons control peripheral substrate utilization and nutrient partitioning. *Embo J.* 31, 4276–4288.

Karlsson, B., Knutsson, A., and Lindahl, B. (2001). Is there an association between shift work and having a metabolic syndrome? Results from a population based study of 27,485 people. *Occup Environ Med* 58, 747–752.

Kaushik, S., Rodriguez-Navarro, J.A., Arias, E., Kiffin, R., Sahu, S., Schwartz, G.J., Cuervo, A.M., and Singh, R. (2011). Autophagy in hypothalamic AgRP neurons regulates food intake and energy balance. *Cell Metab* 14, 173–183.

Kawasaki, M., Yamaguchi, K., Saito, J., Ozaki, Y., Mera, T., Hashimoto, H., Fujihara, H., Okimoto, N., Ohnishi, H., Nakamura, T., et al. (2005). Expression of immediate early genes and vasopressin heteronuclear RNA in the paraventricular and supraoptic nuclei of rats after acute osmotic stimulus. *J Neuroendocrinol* 17, 227–237.

Kawauchi, H., Kawazoe, I., Tsubokawa, M., Kishida, M., and Baker, B.I. (1983). Characterization of melanin-concentrating hormone in chum salmon pituitaries. *Nature* 305, 321–323.

KENNEDY, G.C. (1953). The role of depot fat in the hypothalamic control of food intake

in the rat. *Proc. R. Soc. Lond., B, Biol. Sci.* *140*, 578–596.

Kita, Y., Shiozawa, M., Jin, W., Majewski, R.R., Besharse, J.C., Greene, A.S., and Jacob, H.J. (2002). Implications of circadian gene expression in kidney, liver and the effects of fasting on pharmacogenomic studies. *Pharmacogenetics* *12*, 55–65.

Knight, Z.A., Hannan, K.S., Greenberg, M.L., and Friedman, J.M. (2010). Hyperleptinemia is required for the development of leptin resistance. *PLoS ONE* *5*, e11376.

Knight, Z.A., Tan, K., Birsoy, K., Schmidt, S., Garrison, J.L., Wysocki, R.W., Emiliano, A., Ekstrand, M.I., and Friedman, J.M. (2012). Molecular profiling of activated neurons by phosphorylated ribosome capture. *Cell* *151*, 1126–1137.

Koch, C., and Crick, F. (2001). Neural basis of consciousness.

Koch, C., and Reid, R.C. (2012). Neuroscience: Observatories of the mind. *Nature* *483*, 397–398.

Koike, K., Sakamoto, Y., Kiyama, H., Masuhara, K., Miyake, A., and Inoue, M. (1997). Cytokine-induced neutrophil chemoattractant gene expression in the rat hypothalamus by osmotic stimulation. *Brain Res Mol Brain Res* *52*, 326–329.

Kokkotou, E.G., Tritos, N.A., Mastaitis, J.W., Sliker, L., and Maratos-Flier, E. (2001). Melanin-concentrating hormone receptor is a target of leptin action in the mouse brain. *Endocrinology* *142*, 680–686.

Kokkotou, E., Jeon, J.Y., Wang, X., Marino, F.E., Carlson, M., Trombly, D.J., and Maratos-Flier, E. (2005). Mice with MCH ablation resist diet-induced obesity through strain-specific mechanisms. *Am J Physiol Regul Integr Comp Physiol* *289*, R117–R124.

Kopelman, P.G. (2000). Obesity as a medical problem. *Nature* *404*, 635–643.

Kowalski, T.J., Liu, S.M., Leibel, R.L., and Chua, S.C. (2001). Transgenic complementation of leptin-receptor deficiency. I. Rescue of the obesity/diabetes phenotype of LEPR-null mice expressing a LEPR-B transgene. *Diabetes* *50*, 425–435.

Kramer, R.H., Mourot, A., and Adesnik, H. (2013). Optogenetic pharmacology for control of native neuronal signaling proteins. *Nat Neurosci* *16*, 816–823.

Krieger, D.T., Hauser, H., and Krey, L.C. (1977). Suprachiasmatic nuclear lesions do not abolish food-shifted circadian adrenal and temperature rhythmicity. *Science* *197*, 398–399.

Kyrkouli, S.E., Stanley, B.G., and Leibowitz, S.F. (1986). Galanin: stimulation of feeding induced by medial hypothalamic injection of this novel peptide. *European Journal of Pharmacology* *122*, 159–160.

- Kyrkouli, S.E., Stanley, B.G., Seirafi, R.D., and Leibowitz, S.F. (1990). Stimulation of feeding by galanin: anatomical localization and behavioral specificity of this peptide's effects in the brain. *Peptides* *11*, 995–1001.
- Landry, G.J., Simon, M.M., Webb, I.C., and Mistlberger, R.E. (2006). Persistence of a behavioral food-anticipatory circadian rhythm following dorsomedial hypothalamic ablation in rats. *Am J Physiol Regul Integr Comp Physiol* *290*, R1527–R1534.
- Laposky, A.D., Bass, J., Kohsaka, A., and Turek, F.W. (2008). Sleep and circadian rhythms: key components in the regulation of energy metabolism. *FEBS Lett.* *582*, 142–151.
- Lee, G.H., Proenca, R., Montez, J.M., Carroll, K.M., Darvishzadeh, J.G., Lee, J.I., and Friedman, J.M. (1996). Abnormal splicing of the leptin receptor in diabetic mice. *Nature* *379*, 632–635.
- Leibel, R.L., Rosenbaum, M., and Hirsch, J. (1995). Changes in energy expenditure resulting from altered body weight. *N. Engl. J. Med.* *332*, 621–628.
- Lein, E.S., Hawrylycz, M.J., Ao, N., Ayres, M., Bensinger, A., Bernard, A., Boe, A.F., Boguski, M.S., Brockway, K.S., Byrnes, E.J., et al. (2007). Genome-wide atlas of gene expression in the adult mouse brain. *Nature* *445*, 168–176.
- LeSauter, J., Hoque, N., Weintraub, M., Pfaff, D.W., and Silver, R. (2009). Stomach ghrelin-secreting cells as food-entrainable circadian clocks. *Proc Natl Acad Sci USA* *106*, 13582–13587.
- Lew, E.A. (1985). Mortality and weight: insured lives and the American Cancer Society studies. *Ann. Intern. Med.* *103*, 1024–1029.
- Lichtman, J.W., and Denk, W. (2011). The big and the small: challenges of imaging the brain's circuits. *Science* *334*, 618–623.
- Lin, D., Boyle, M.P., Dollar, P., Lee, H., Lein, E.S., Perona, P., and Anderson, D.J. (2011). Functional identification of an aggression locus in the mouse hypothalamus. *Nature* *470*, 221–226.
- Liu, H.-X., and Hökfelt, T. (2002). The participation of galanin in pain processing at the spinal level. *Trends Pharmacol Sci* *23*, 468–474.
- Lowrey, P.L., and Takahashi, J.S. (2004). Mammalian circadian biology: elucidating genome-wide levels of temporal organization. *Annu Rev Genomics Hum Genet* *5*, 407–441.
- Luquet, S., Perez, F.A., Hnasko, T.S., and Palmiter, R.D. (2005). NPY/AgRP neurons are essential for feeding in adult mice but can be ablated in neonates. *Science* *310*, 683–685.
- Luquet, S., Phillips, C.T., and Palmiter, R.D. (2007). NPY/AgRP neurons are not

essential for feeding responses to glucoprivation. *Peptides* 28, 214–225.

Maes, H.H., Neale, M.C., and Eaves, L.J. (1997). Genetic and environmental factors in relative body weight and human adiposity. *Behav. Genet.* 27, 325–351.

Maffei, M., Halaas, J., Ravussin, E., Pratley, R.E., Lee, G.H., Zhang, Y., Fei, H., Kim, S., Lallone, R., and Ranganathan, S. (1995). Leptin levels in human and rodent: measurement of plasma leptin and ob RNA in obese and weight-reduced subjects. *Nature Medicine* 1, 1155–1161.

Mahoney, S.-A., Hosking, R., Farrant, S., Holmes, F.E., Jacoby, A.S., Shine, J., Iismaa, T.P., Scott, M.K., Schmidt, R., and Wynick, D. (2003). The second galanin receptor GalR2 plays a key role in neurite outgrowth from adult sensory neurons. *J Neurosci* 23, 416–421.

Masland, R.H. (2004). Neuronal cell types. *Curr Biol* 14, R497–R500.

McCarthy, J.J., Andrews, J.L., McDearmon, E.L., Campbell, K.S., Barber, B.K., Miller, B.H., Walker, J.R., Hogenesch, J.B., Takahashi, J.S., and Esser, K.A. (2007). Identification of the circadian transcriptome in adult mouse skeletal muscle. *Physiol. Genomics* 31, 86–95.

McCowen, K.C., Chow, J.C., and Smith, R.J. (1998). Leptin signaling in the hypothalamus of normal rats in vivo. *Endocrinology* 139, 4442–4447.

McMinn, J.E., Liu, S.M., Liu, H., Dragatsis, I., Dietrich, P., Ludwig, T., Boozer, C.N., and Chua, S.C. (2005). Neuronal deletion of *Lepr* elicits diabetes in mice without affecting cold tolerance or fertility. *Am. J. Physiol. Endocrinol. Metab.* 289, E403–E411.

Meikle, L., Talos, D.M., Onda, H., Pollizzi, K., Rotenberg, A., Sahin, M., Jensen, F.E., and Kwiatkowski, D.J. (2007). A mouse model of tuberous sclerosis: neuronal loss of *Tsc1* causes dysplastic and ectopic neurons, reduced myelination, seizure activity, and limited survival. *J Neurosci* 27, 5546–5558.

Merkestein, M., van Gestel, M.A., van der Zwaal, E.M., Brans, M.A., Luijendijk, M.C., van Rozen, A.J., Hendriks, J., Garner, K.M., Boender, A.J., Pandit, R., et al. (2014). GHS-R1a signaling in the DMH and VMH contributes to food anticipatory activity. *Int J Obes (Lond)* 38, 610–618.

Meyuhas, O. (2008). Physiological roles of ribosomal protein S6: one of its kind. *Int Rev Cell Mol Biol* 268, 1–37.

Mieda, M., Williams, S.C., Richardson, J.A., Tanaka, K., and Yanagisawa, M. (2006). The dorsomedial hypothalamic nucleus as a putative food-entrainable circadian pacemaker. *Proc Natl Acad Sci USA* 103, 12150–12155.

Mistlberger, R.E. (1994). Circadian food-anticipatory activity: formal models and physiological mechanisms. *Neurosci Biobehav Rev* 18, 171–195.

- Mistlberger, R.E., and Antle, M.C. (1999). Neonatal monosodium glutamate alters circadian organization of feeding, food anticipatory activity and photic masking in the rat. *Brain Res* 842, 73–83.
- Mistlberger, R.E., and Marchant, E.G. (1999). Enhanced food-anticipatory circadian rhythms in the genetically obese Zucker rat. *Physiol Behav* 66, 329–335.
- Mistlberger, R.E. (2011). Neurobiology of food anticipatory circadian rhythms. *Physiol Behav* 104, 535–545.
- Miyata, S., Tsujioka, H., Itoh, M., Matsunaga, W., Kuramoto, H., and Kiyohara, T. (2001). Time course of Fos and Fras expression in the hypothalamic supraoptic neurons during chronic osmotic stimulation. *Brain Res Mol Brain Res* 90, 39–47.
- Morgan, J.I., and Curran, T. (1991). Stimulus-transcription coupling in the nervous system: involvement of the inducible proto-oncogenes fos and jun. *Annu Rev Neurosci* 14, 421–451.
- Moriya, T., Aida, R., Kudo, T., Akiyama, M., Doi, M., Hayasaka, N., Nakahata, N., Mistlberger, R., Okamura, H., and Shibata, S. (2009). The dorsomedial hypothalamic nucleus is not necessary for food-anticipatory circadian rhythms of behavior, temperature or clock gene expression in mice. *Eur J Neurosci* 29, 1447–1460.
- Morton, G.J., Cummings, D.E., Baskin, D.G., Barsh, G.S., and Schwartz, M.W. (2006). Central nervous system control of food intake and body weight. *Nature* 443, 289–295.
- Mountjoy, K.G., Mortrud, M.T., Low, M.J., Simerly, R.B., and Cone, R.D. (1994). Localization of the melanocortin-4 receptor (MC4-R) in neuroendocrine and autonomic control circuits in the brain. *Mol. Endocrinol.* 8, 1298–1308.
- NEEL, J.V. (1962). Diabetes mellitus: a "thrifty" genotype rendered detrimental by "progress"? *Am. J. Hum. Genet.* 14, 353–362.
- NEEL, J.V. (1999a). Diabetes mellitus: a "thrifty" genotype rendered detrimental by "progress?" 1962.
- NEEL, J.V. (1999b). The "thrifty genotype" in 1998. *Nutr. Rev.* 57, S2–S9.
- Nelson, S.B., Sugino, K., and Hempel, C.M. (2006). The problem of neuronal cell types: a physiological genomics approach. *Trends Neurosci* 29, 339–345.
- Ollmann, M.M., Wilson, B.D., Yang, Y.K., Kerns, J.A., Chen, Y., Gantz, I., and Barsh, G.S. (1997). Antagonism of central melanocortin receptors in vitro and in vivo by agouti-related protein. *Science* 278, 135–138.
- Packer, A.M., Roska, B., and Häusser, M. (2013). Targeting neurons and photons for optogenetics. *Nat Neurosci* 16, 805–815.

- Panda, S., Antoch, M.P., Miller, B.H., Su, A.I., Schook, A.B., Straume, M., Schultz, P.G., Kay, S.A., Takahashi, J.S., and Hogenesch, J.B. (2002). Coordinated transcription of key pathways in the mouse by the circadian clock. *Cell* 109, 307–320.
- Parker, J.A., and Bloom, S.R. (2012). Hypothalamic neuropeptides and the regulation of appetite. *Neuropharmacology* 63, 18–30.
- Pelleymounter, M.A., Cullen, M.J., Baker, M.B., Hecht, R., Winters, D., Boone, T., and Collins, F. (1995). Effects of the obese gene product on body weight regulation in ob/ob mice. *Science* 269, 540–543.
- Penny, M.L., Bruno, S.B., Cornelius, J., Higgs, K.A.N., and Cunningham, J.T. (2005). The effects of osmotic stimulation and water availability on c-Fos and FosB staining in the supraoptic and paraventricular nuclei of the hypothalamus. *Exp. Neurol.* 194, 191–202.
- Pittendrigh, C.S. (1993). Temporal organization: reflections of a Darwinian clock-watcher. *Annu. Rev. Physiol.* 55, 16–54.
- Porter, J.P., and Potratz, K.R. (2004). Effect of intracerebroventricular angiotensin II on body weight and food intake in adult rats. *Am J Physiol Regul Integr Comp Physiol* 287, R422–R428.
- Ralph, M.R., Foster, R.G., Davis, F.C., and Menaker, M. (1990). Transplanted suprachiasmatic nucleus determines circadian period. *Science* 247, 975–978.
- Ramsköld, D., Luo, S., Wang, Y.-C., Li, R., Deng, Q., Faridani, O.R., Daniels, G.A., Khrebtkova, I., Loring, J.F., Laurent, L.C., et al. (2012). Full-length mRNA-Seq from single-cell levels of RNA and individual circulating tumor cells. *Nat. Biotechnol.* 30, 777–782.
- Ravelli, G.P., Stein, Z.A., and Susser, M.W. (1976). Obesity in young men after famine exposure in utero and early infancy. *N. Engl. J. Med.* 295, 349–353.
- Reaux-Le Goazigo, A., Bodineau, L., De Mota, N., Jeandel, L., Chartrel, N., Knauf, C., Raad, C., Valet, P., and Llorens-Cortes, C. (2011). Apelin and the proopiomelanocortin system: a new regulatory pathway of hypothalamic α -MSH release. *Am. J. Physiol. Endocrinol. Metab.* 301, E955–E966.
- Reddy, A.B., Karp, N.A., Maywood, E.S., Sage, E.A., Deery, M., O'Neill, J.S., Wong, G.K.Y., Chesham, J., Odell, M., Lilley, K.S., et al. (2006). Circadian orchestration of the hepatic proteome. *Curr Biol* 16, 1107–1115.
- Reppert, S.M., and Weaver, D.R. (2002). Coordination of circadian timing in mammals. *Nature* 418, 935–941.
- Ribeiro, A.C., Ceccarini, G., Dupré, C., Friedman, J.M., Pfaff, D.W., and Mark, A.L. (2011). Contrasting effects of leptin on food anticipatory and total locomotor activity.

PLoS ONE 6, e23364.

Ridaura, V.K., Faith, J.J., Rey, F.E., Cheng, J., Duncan, A.E., Kau, A.L., Griffin, N.W., Lombard, V., Henrissat, B., Bain, J.R., et al. (2013). Gut microbiota from twins discordant for obesity modulate metabolism in mice. *Science* 341, 1241214.

Ring, L.E., and Zeltser, L.M. (2010). Disruption of hypothalamic leptin signaling in mice leads to early-onset obesity, but physiological adaptations in mature animals stabilize adiposity levels. *J Clin Invest* 120, 2931–2941.

Rosenwasser, A.M., Boulos, Z., and Terman, M. (1981). Circadian organization of food intake and meal patterns in the rat. *Physiol Behav* 27, 33–39.

Rossi, M., Choi, S.J., O'Shea, D., Miyoshi, T., Ghatei, M.A., and Bloom, S.R. (1997). Melanin-concentrating hormone acutely stimulates feeding, but chronic administration has no effect on body weight. *Endocrinology* 138, 351–355.

Ruvinsky, I., Sharon, N., Lerer, T., Cohen, H., Stolovich-Rain, M., Nir, T., Dor, Y., Zisman, P., and Meyuhas, O. (2005). Ribosomal protein S6 phosphorylation is a determinant of cell size and glucose homeostasis. *Genes Dev* 19, 2199–2211.

Sanz, E., Yang, L., Su, T., Morris, D.R., McKnight, G.S., and Amieux, P.S. (2009). Cell-type-specific isolation of ribosome-associated mRNA from complex tissues. *Proc Natl Acad Sci USA* 106, 13939–13944.

Schwartz, M.W., Baskin, D.G., Bukowski, T.R., Kuijper, J.L., Foster, D., Lasser, G., Prunkard, D.E., Porte, D., Woods, S.C., Seeley, R.J., et al. (1996). Specificity of leptin action on elevated blood glucose levels and hypothalamic neuropeptide Y gene expression in ob/ob mice. *Diabetes* 45, 531–535.

Schwartz, M.W., Sipols, A.J., Grubin, C.E., and Baskin, D.G. (1993). Differential effect of fasting on hypothalamic expression of genes encoding neuropeptide Y, galanin, and glutamic acid decarboxylase. *Brain Res. Bull.* 31, 361–367.

Seidell, J.C. (1995). The impact of obesity on health status: some implications for health care costs. *Int J Obes Relat Metab Disord* 19 Suppl 6, S13–S16.

Sherman, T.G., Civelli, O., Douglass, J., Herbert, E., and Watson, S.J. (1986). Coordinate expression of hypothalamic pro-dynorphin and pro-vasopressin mRNAs with osmotic stimulation. *Neuroendocrinology* 44, 222–228.

Shimada, M., Tritos, N.A., Lowell, B.B., Flier, J.S., and Maratos-Flier, E. (1998). Mice lacking melanin-concentrating hormone are hypophagic and lean. *Nature* 396, 670–674.

Siebert, S., Scherf, B.G., Del Punta, K., Didkovsky, N., Heintz, N., and Roska, B. (2009). Genetic address book for retinal cell types. *Nat Neurosci* 12, 1197–1204.

Sims, E.A., Danforth, E., Horton, E.S., Bray, G.A., Glennon, J.A., and Salans, L.B.

(1973). Endocrine and metabolic effects of experimental obesity in man. *Recent Prog Horm Res* 29, 457–496.

Spanswick, D., Smith, M.A., Groppi, V.E., Logan, S.D., and Ashford, M. (1997). Leptin inhibits hypothalamic neurons by activation of ATP-sensitive potassium channels. *Nature* 390, 521–525.

Stephan, F.K., Swann, J.M., and Sisk, C.L. (1979). Anticipation of 24-hr feeding schedules in rats with lesions of the suprachiasmatic nucleus. *Behav. Neural Biol.* 25, 346–363.

Stephan, F.K. (2002). The “other” circadian system: food as a Zeitgeber. *J. Biol. Rhythms* 17, 284–292.

Stevens, C.F. (1998). Neuronal diversity: too many cell types for comfort? *Curr Biol* 8, R708–R710.

Stokkan, K.A., Yamazaki, S., Tei, H., Sakaki, Y., and Menaker, M. (2001). Entrainment of the circadian clock in the liver by feeding. *Science* 291, 490–493.

Storch, K.-F., and Weitz, C.J. (2009). Daily rhythms of food-anticipatory behavioral activity do not require the known circadian clock. *Proc Natl Acad Sci USA* 106, 6808–6813.

Storch, K.-F., Lipan, O., Leykin, I., Viswanathan, N., Davis, F.C., Wong, W.H., and Weitz, C.J. (2002). Extensive and divergent circadian gene expression in liver and heart. *Nature* 417, 78–83.

Stunkard, A.J., Harris, J.R., Pedersen, N.L., and McClearn, G.E. (1990). The body-mass index of twins who have been reared apart. *N. Engl. J. Med.* 322, 1483–1487.

Szentirmai, E., Kapás, L., Sun, Y., Smith, R.G., and Krueger, J.M. (2010). Restricted feeding-induced sleep, activity, and body temperature changes in normal and preproghrelin-deficient mice. *Am J Physiol Regul Integr Comp Physiol* 298, R467–R477.

Tamamaki, N., Yanagawa, Y., Tomioka, R., Miyazaki, J.-I., Obata, K., and Kaneko, T. (2003). Green fluorescent protein expression and colocalization with calretinin, parvalbumin, and somatostatin in the GAD67-GFP knock-in mouse. *J Comp Neurol* 467, 60–79.

Tartaglia, L.A., Dembski, M., Weng, X., Deng, N., Culpepper, J., Devos, R., Richards, G.J., Campfield, L.A., Clark, F.T., Deeds, J., et al. (1995). Identification and expression cloning of a leptin receptor, OB-R. *Cell* 83, 1263–1271.

Thornton, S.M., and Fitzsimons, J.T. (1995). The effects of centrally administered porcine relaxin on drinking behaviour in male and female rats. *J Neuroendocrinol* 7, 165–169.

Turek, F.W., Joshu, C., Kohsaka, A., Lin, E., Ivanova, G., McDearmon, E., Laposky, A., Losee-Olson, S., Easton, A., Jensen, D.R., et al. (2005). Obesity and metabolic syndrome in circadian Clock mutant mice. *Science* *308*, 1043–1045.

Ueda, H.R., Chen, W., Adachi, A., Wakamatsu, H., Hayashi, S., Takasugi, T., Nagano, M., Nakahama, K.-I., Suzuki, Y., Sugano, S., et al. (2002). A transcription factor response element for gene expression during circadian night. *Nature* *418*, 534–539.

Urban, D.J., and Roth, B.L. (2014). DREADDs (Designer Receptors Exclusively Activated by Designer Drugs): Chemogenetic Tools with Therapeutic Utility. *Annu. Rev. Pharmacol. Toxicol.*

Vaisse, C., Clement, K., Guy-Grand, B., and Froguel, P. (1998). A frameshift mutation in human MC4R is associated with a dominant form of obesity. *Nat Genet* *20*, 113–114.

Vaisse, C., Halaas, J.L., Horvath, C.M., Darnell, J.E., Stoffel, M., and Friedman, J.M. (1996). Leptin activation of Stat3 in the hypothalamus of wild-type and ob/ob mice but not db/db mice. *Nat Genet* *14*, 95–97.

Valjent, E., Bertran-Gonzalez, J., Bowling, H., Lopez, S., Santini, E., Matamales, M., Bonito-Oliva, A., Hervé, D., Hoeffler, C., Klann, E., et al. (2011). Haloperidol regulates the state of phosphorylation of ribosomal protein S6 via activation of PKA and phosphorylation of DARPP-32. *Neuropsychopharmacology* *36*, 2561–2570.

van de Wall, E., Leshan, R., Xu, A.W., Balthasar, N., Coppari, R., Liu, S.M., Jo, Y.H., MacKenzie, R.G., Allison, D.B., Dun, N.J., et al. (2008). Collective and individual functions of leptin receptor modulated neurons controlling metabolism and ingestion. *Endocrinology* *149*, 1773–1785.

van den Top, M., Lee, K., Whyment, A.D., Blanks, A.M., and Spanswick, D. (2004). Orexigen-sensitive NPY/AgRP pacemaker neurons in the hypothalamic arcuate nucleus. *Nat Neurosci* *7*, 493–494.

Verhagen, L.A.W., Egecioglu, E., Luijendijk, M.C.M., Hillebrand, J.J.G., Adan, R.A.H., and Dickson, S.L. (2011). Acute and chronic suppression of the central ghrelin signaling system reveals a role in food anticipatory activity. *Eur Neuropsychopharmacol* *21*, 384–392.

Verwey, M., Khoja, Z., Stewart, J., and Amir, S. (2008). Region-specific modulation of PER2 expression in the limbic forebrain and hypothalamus by nighttime restricted feeding in rats. *Neurosci Lett* *440*, 54–58.

Villanueva, E.C., Münzberg, H., Cota, D., Leshan, R.L., Kopp, K., Ishida-Takahashi, R., Jones, J.C., Fingar, D.C., Seeley, R.J., and Myers, M.G. (2009). Complex regulation of mammalian target of rapamycin complex 1 in the basomedial hypothalamus by leptin and nutritional status. *Endocrinology* *150*, 4541–4551.

Vong, L., Ye, C., Yang, Z., Choi, B., Chua, S., Jr., and Lowell, B.B. (2011). Leptin

Action on GABAergic Neurons Prevents Obesity and Reduces Inhibitory Tone to POMC Neurons. *Neuron* 71, 142–154.

Wakamatsu, H., Yoshinobu, Y., Aida, R., Moriya, T., Akiyama, M., and Shibata, S. (2001). Restricted-feeding-induced anticipatory activity rhythm is associated with a phase-shift of the expression of mPer1 and mPer2 mRNA in the cerebral cortex and hippocampus but not in the suprachiasmatic nucleus of mice. *Eur J Neurosci* 13, 1190–1196.

Weigle, D.S. (1994). Appetite and the regulation of body composition. *Faseb J* 8, 302–310.

Whiddon, B.B., and Palmiter, R.D. (2013). Ablation of neurons expressing melanin-concentrating hormone (MCH) in adult mice improves glucose tolerance independent of MCH signaling. *J Neurosci* 33, 2009–2016.

Willesen, M.G., Kristensen, P., and Rømer, J. (1999). Co-localization of growth hormone secretagogue receptor and NPY mRNA in the arcuate nucleus of the rat. *Neuroendocrinology* 70, 306–316.

Willett, W.C., Dietz, W.H., and Colditz, G.A. (1999). Guidelines for healthy weight. *N. Engl. J. Med.* 341, 427–434.

Willett, W.C., Manson, J.E., Stampfer, M.J., Colditz, G.A., Rosner, B., Speizer, F.E., and Hennekens, C.H. (1995). Weight, weight change, and coronary heart disease in women. Risk within the “normal” weight range. *Jama* 273, 461–465.

Willie, J.T., Sinton, C.M., Maratos-Flier, E., and Yanagisawa, M. (2008). Abnormal response of melanin-concentrating hormone deficient mice to fasting: hyperactivity and rapid eye movement sleep suppression. *Neuroscience* 156, 819–829.

Wrenn, C.C., Turchi, J.N., Schlosser, S., Dreiling, J.L., Stephenson, D.A., and Crawley, J.N. (2006). Performance of galanin transgenic mice in the 5-choice serial reaction time attentional task. *Pharmacol Biochem Behav* 83, 428–440.

Wu, Q., Clark, M.S., and Palmiter, R.D. (2012). Deciphering a neuronal circuit that mediates appetite. *Nature* 483, 594–597.

Wynick, D., Small, C.J., Bloom, S.R., and Pachnis, V. (1998). Targeted disruption of the murine galanin gene. *Ann. N. Y. Acad. Sci.* 863, 22–47.

Xu, X.J., Hökfelt, T., Bartfai, T., and Wiesenfeld-Hallin, Z. (2000). Galanin and spinal nociceptive mechanisms: recent advances and therapeutic implications. *Neuropeptides* 34, 137–147.

Yamazaki, S., Numano, R., Abe, M., Hida, A., Takahashi, R., Ueda, M., Block, G.D., Sakaki, Y., Menaker, M., and Tei, H. (2000). Resetting central and peripheral circadian oscillators in transgenic rats. *Science* 288, 682–685.

Yaswen, L., Diehl, N., Brennan, M.B., and Hochgeschwender, U. (1999). Obesity in the mouse model of pro-opiomelanocortin deficiency responds to peripheral melanocortin. *Nature Medicine* 5, 1066–1070.

Yizhar, O., Fenno, L.E., Davidson, T.J., Mogri, M., and Deisseroth, K. (2011). Optogenetics in neural systems. *Neuron* 71, 9–34.

Zeng, L.-H., Rensing, N.R., and Wong, M. (2009). The mammalian target of rapamycin signaling pathway mediates epileptogenesis in a model of temporal lobe epilepsy. *J Neurosci* 29, 6964–6972.

Zhang, F., Aravanis, A.M., Adamantidis, A., de Lecea, L., and Deisseroth, K. (2007). Circuit-breakers: optical technologies for probing neural signals and systems. *Nat. Rev. Neurosci.* 8, 577–581.

Zhang, Y., Proenca, R., Maffei, M., Barone, M., Leopold, L., and Friedman, J.M. (1994). Positional cloning of the mouse obese gene and its human homologue. *Nature* 372, 425–432.

Zhou, D., Shen, Z., Strack, A.M., Marsh, D.J., and Shearman, L.P. (2005). Enhanced running wheel activity of both Mch1r- and Pmch-deficient mice. *Regul. Pept.* 124, 53–63.

Zigman, J.M., Jones, J.E., Lee, C.E., Saper, C.B., and Elmquist, J.K. (2006). Expression of ghrelin receptor mRNA in the rat and the mouse brain. *J Comp Neurol* 494, 528–548.

Zvonic, S., Ptitsyn, A.A., Conrad, S.A., Scott, L.K., Floyd, Z.E., Kilroy, G., Wu, X., Goh, B.C., Mynatt, R.L., and Gimble, J.M. (2006). Characterization of peripheral circadian clocks in adipose tissues. *Diabetes* 55, 962–970.